

Distribution Agreement

In presenting this thesis or dissertation as a partial fulfillment of the requirements for an advanced degree from Emory University, I hereby grant to Emory University and its agents the non-exclusive license to archive, make accessible, and display my thesis or dissertation in whole or in part in all forms of media, now or hereafter known, including display on the world wide web. I understand that I may select some access restrictions as part of the online submission of this thesis or dissertation. I retain all ownership rights to the copyright of the thesis or dissertation. I also retain the right to use in future works (such as articles or books) all or part of this thesis or dissertation.

Signature:

Si'Ana A. Coggins

Date

Host dNTPase SAMHD1, Lentiviral Accessory Protein Vpx/Vpr, and the Evolutionarily Honed
Reverse Transcriptases of SAMHD1 Non-Counteracting Lentiviruses

By

Si'Ana A. Coggins
Doctor of Philosophy

Graduate Division of Biological and Biomedical Science
Biochemistry, Cell, and Developmental Biology

Baek Kim, Ph.D.
Advisor

Graeme Conn, Ph.D.
Committee Member

David Lynn, Ph.D.
Committee Member

Gregory Melikian, Ph.D.
Committee Member

Daniel Reines, Ph.D.
Committee Member

Accepted:

Lisa A. Tedesco, Ph.D.
Dean of the James T. Laney School of Graduate Studies

Date

Host dNTPase SAMHD1, Lentiviral Accessory Protein Vpx/Vpr, and the Evolutionarily Honed Reverse
Transcriptases of SAMHD1 Non-Counteracting Lentiviruses

By

Si'Ana A. Coggins

B.S., University of Arizona, 2015

Advisor: Baek Kim, Ph.D.

An abstract of

A dissertation submitted to the Faculty of the
James T. Laney School of Graduate Studies of Emory University
in partial fulfillment of the requirements for the degree of
Doctor of Philosophy
in Biochemistry, Cell, and Developmental Biology

2020

Abstract

Host dNTPase SAMHD1, Lentiviral Accessory Protein Vpx/Vpr, and the Evolutionarily Honed Reverse Transcriptases of SAMHD1 Non-Counteracting Lentiviruses

By Si'Ana A. Coggins

Since its devastating appearance in 1981, human immunodeficiency virus (HIV) has remained a major global health concern. With approximately 37.9 million people infected worldwide, the need to understand and adequately treat HIV infections is ever-present. HIV-1 and HIV-2 are the result of two independent cross-species transmission events, with the originating viruses being simian immunodeficiency virus (SIV) from chimpanzees and sooty mangabeys respectively. During the course of viral pathogenesis, HIV/SIV infects dividing (i.e. CD4⁺ T cells) and nondividing (i.e. macrophages and microglia) CD4⁺ cells within the host immune system. With no necessity to support DNA replication, nondividing myeloid cells express high levels of SAM domain- and HD domain-containing protein 1 (SAMHD1), an enzyme that hydrolyzes dNTPs into 2'-deoxynucleoside (dNs) and actively depletes intracellular dNTP pools in nondividing cells. While sharing a target cell tropism, HIV-1 and HIV-2 display distinct replication kinetics in nondividing macrophages: contrary to HIV-1 infection, which is restricted in macrophages, HIV-2 and some SIVs readily replicate in this target cell type. This is because HIV-2 and some SIVs target host SAMHD1 for proteasomal degradation using their viral protein R (Vpr) or viral protein X (Vpx) proteins. Virus-induced degradation of SAMHD1 elevates intracellular dNTP concentrations and enables efficient viral replication in macrophages. Unlike HIV-2, HIV-1 cannot counteract SAMHD1 and thus replicates under low dNTP conditions in nondividing myeloid cells.

Previous studies have shown that reverse transcriptase (RT) proteins from lentiviruses without the ability to counteract SAMHD1 (i.e. HIV-1) reach maximum velocity at lower dNTP concentrations and are able to incorporate dNTP substrates faster than RTs from SAMHD1 counteracting lentiviruses (i.e. SIVmac239). The enhanced kinetics of HIV-1 RT enable complete proviral DNA synthesis in restrictive dNTP concentrations. This dissertation builds upon previous knowledge by showing that RTs from SAMHD1 non-counteracting lentiviruses circumvent SAMHD1 restriction by executing a faster polymerase conformational change during dNTP incorporation. Further, RTs from SIVmac239 infections devoid of Vpx display enhanced enzyme kinetics when compared to RTs from wild type infections—suggesting that intracellular dNTP environments and the lentiviral ability to counteract host SAMHD1 can influence RT kinetics and evolution during the infection of a single host.

Host dNTPase SAMHD1, Lentiviral Accessory Protein Vpx/Vpr, and the Evolutionarily Honed Reverse
Transcriptases of SAMHD1 Non-Counteracting Lentiviruses

By

Si'Ana A. Coggins

B.S., University of Arizona, 2015

Advisor: Baek Kim, Ph.D.

A dissertation submitted to the Faculty of the
James T. Laney School of Graduate Studies of Emory University
in partial fulfillment of the requirements for the degree of
Doctor of Philosophy
in Biochemistry, Cell, and Developmental Biology

2020

Acknowledgements

I'd like to start by thanking Dr. Baek Kim for welcoming me into his lab and schooling me in both the technical and professional intricacies of science. Thank you for teaching me the art of scientific storytelling, challenging me to think like reviewer #3, and encouraging my independence as a scientist. You have taught me how to ask the right questions to address gaps in the field and have served as a constant reminder of what a true passion for science looks like.

Thank you to all the Kim lab members (past and present) who have provided invaluable insight, feedback, and training throughout the years. Specifically, I would like to first thank Dr. Tatsuya Maehigashi for sharing his wealth of knowledge and providing hands-on protein purification and enzymology training that was central to my work in the lab. Next, I'd like to thank Emily Hammond for teaching me how to safely use the almighty KinTek machine—I am grateful for the positivity you brought to training and to the lab in general. Lastly, I'd like to thank Dr. Michele Daly for her encouragement and career guidance that persisted even after she moved on from the lab. I am appreciative of you all for your patience and approachability during the time we've worked together.

I would like to emphatically thank my committee members Drs. Graeme Conn, David Lynn, Gregory Melikian, and Daniel Reines for their time, support, advocacy, questions, and suggestions. Thank you for challenging me to think deeply about my research and offering much needed guidance throughout my time at Emory.

Graduate school has taught me the urgency of balance. While professional support throughout this process was imperative, I would not have made it to the end without the incredible support from my friends, family, and boyfriend Sterling Mitchell. Briefly, to my friends, thank you for the innumerable moments of levity and laughter that provided much needed mental breaks from science throughout the years. To my parents, thank you for not only stoking and encouraging my thirst for knowledge but also embracing my flower-child spirit—you both have taught me the power of self-motivation and the freedom in personal evolution. To Nickness, thank you for being my lifelong best friend. I am so grateful to you for continually fostering an environment of nonjudgement, love, and growth, and just being an incredible 'big' sister (we both know I got stuck though haha). Lastly, Sterling, I don't even know how to begin to express my gratitude for you. You have uplifted me when I was hanging on by a single grey hair, you have pushed me when procrastination and indifference have tempted me, and you have inspired me not only to remain steadfast in my goals, but also to continue setting new ones. Thank you for being my partner in growth and the anchor that always keeps me grounded. I love you so much.

And finally, I would like to express my humble gratitude for my ancestors and all the brothers and sisters who have painstakingly paved the way for me, both personally and professionally. This would not have been possible without your unwavering bravery, fortitude, vision, resilience, and dedication to create a better world for future generations. Your aspirations are mine and I can only hope to be to others a fraction of what you have been to me.

Table of Contents

Chapter 1: Introduction	1
1.1 HIV/AIDS.....	1
A. Global Impact.....	1
B. Origins.....	2
1.2 Viral Genome and Replication Cycle.....	6
A. Viral Genome Organization.....	6
B. Viral Components.....	8
C. Viral Replication Cycle.....	15
D. Disease Progression to AIDS.....	25
E. HIV/SIV Target Cells.....	29
i. Viral Tropism.....	29
ii. Intracellular dNTP Pools and SAMHD1.....	31
1.3 Reverse Transcriptase.....	33
A. Structural Features and Drug-Induced Viral Mutagenesis.....	36
B. DNA Polymerase Reaction Pathway and Kinetics.....	39
C. Differences Between RTs from SAMHD1 Counteracting and Non-Counteracting Lentiviruses.....	40
1.4 Dissertation Direction.....	43
Chapter 2: Evolutionarily Improved Pre-Catalytic Conformational Change of SAMHD1 Non- Counteracting Lentiviral Reverse Transcriptase Proteins	44
2.1 Abstract.....	45
2.2 Introduction.....	46
2.3 Experimental Procedures.....	49
2.4 Results and Discussion.....	53
2.5 References.....	68

Chapter 3: Enhanced Enzyme Kinetics of Reverse Transcriptase Variants Cloned from Animals

Infected with SIVmac239 Lacking Viral Protein X.....	75
3.1 Abstract.....	76
3.2 Introduction.....	77
3.3 Experimental Procedures.....	80
3.4 Results.....	84
3.5 Discussion.....	98
3.6 References.....	103
Chapter 4: General Discussion.....	109
References.....	117

List of Figures and Tables

Chapter 1

Figure 1.1 —Phylogenetic tree of HIV-1, HIV-2, and SIVs.....	5
Figure 1.2 —HIV/SIV genomic organization.....	7
Figure 1.3 —HIV replication cycle.....	16
Figure 1.4 —Process of HIV/SIV reverse transcription.....	21
Figure 1.5 —AIDS disease progression.....	28
Figure 1.6 —HIV-1 reverse transcriptase structure and reaction pathway.....	34
Figure 1.7 —Implications of SAMHD1 restriction on HIV/SIV infection in nondividing cells and evolution of reverse transcriptase.....	42

Chapter 2

Figure 2.1 —SAMHD1 degradation capability of primate lentiviruses.....	56
Figure 2.2 —Determination of active site concentrations of SIVgor and SIVcpz reverse transcriptase proteins by burst kinetic analysis.....	59
Figure 2.3 —Comparison of pre-steady state kinetic values among six lentiviral RT proteins.....	61
Figure 2.4 —Phosphorothioate elemental effect of six lentiviral RT proteins.....	63
Figure 2.5 — Model for anti-SAMHD1 strategies employed by SAMHD1 non-counteracting and counteracting lentiviruses in non-dividing myeloid cells.....	64
Table 2.1 —Pre-steady state kinetic values of six primate lentiviral RT proteins with dTTP.....	61
Table 2.2 —Pre-steady state kinetic values of six primate lentiviral RT proteins with dTTP α S.....	63
Supplemental Figure 2.1 — Purity of the six lentiviral reverse transcriptase enzymes used in pre-steady state studies.....	67
Supplemental Figure 2.2 —Representative active site titration curves.....	67

Chapter 3

Figure 3.1 —Summary of amino acid mutations found in Vpx (+) and Vpx (-) RT variants.....	87
Figure 3.2 —Steady state kinetic measurement of Vpx (+) and Vpx (-) RT variants.....	88

Figure 3.3 —Steady state kinetic activity of Vpx (-) 2G7 and 2N0 RT variants compared to that of wild type SIVmac239 RT.....	93
Figure 3.4 —Active site determination for wild type SIVmac239 RT and Vpx (-) 2G7 and 2N0 RT variants.....	95
Figure 3.5 — Pre-steady state kinetic activity of Vpx (-) 2G7, 2N0 RT, and 1M6 RT variants compared to that of wild type SIVmac239 RT.....	97
Figure 3.6 —Location of mutated residues in 2G7, 2N0, and 1M6 Vpx (-) RT variants.....	102
Table 3.1 —Redundant amino acid mutations found in Vpx (+) and Vpx (-) RTs.....	86
Table 3.2 —Melting temperatures (T _m) of various Vpx (+) and Vpx (-) RTs compared to that of wild type SIVmac239 RT.....	90
Table 3.3 —Amino acid mutations present in Vpx (-) clones 2G7, 2N0, and 1M6.....	90
Table 3.4 —Steady state dTTP incorporation by WT SIVmac239 RT and Vpx (-) RTs 2G7 and 2N0 from RNA and DNA templates.....	92
Table 3.5 —Pre- steady state dTTP incorporation by wild type SIVmac239 RT and Vpx (-) RT variants 2G7, 2N0, and 1M6 from DNA template.....	96

Chapter 4

Figure 4.1 —Summary of thesis work.....	115
--	-----

List of Abbreviations

3TC	Lamivudine
ABC	Abacavir
AGS	Aicardi–Goutières Syndrome
AIDS	Acquired immunodeficiency syndrome
APOBEC3G	Apolipoprotein B mRNA editing enzyme, catalytic polypeptide-like 3G
AZT	Zidovudine
CA	Capsid protein
CCR3	C-C chemokine receptor type 3
CCR5	C-C chemokine receptor type 5
CD4	Cluster of differentiation 4
CDC	Centers for Disease Control and Prevention
cPPT	Central polypurine tract
CRF	Circulating recombinant forms
CTL	Cytotoxic T lymphocyte
CXCR4	C-X-C chemokine receptor type 4
DC	Dendritic cell
dNs	2'-deoxynucleoside
DNA	Deoxyribonucleic acid
dNTP	Deoxyribonucleoside triphosphate
dsDNA	Double-stranded DNA
EFV	Efavirenz
Env	Envelope
ER	Endoplasmic reticulum
ESCRT	Endosomal sorting complexes required for transport
FDA	Food and drugs administration
FeLV	Feline leukemia virus
FTC	Emtricitabine
Gag	Group specific antigen
Gp120/41	Glycoprotein120/41
HAART	Highly active antiretroviral therapy
HD	Histidine-aspartic domain
HAND	HIV-associated neurocognitive disorders
HIV-1	Human immunodeficiency virus type 1
HIV-2	Human immunodeficiency virus type 2
HTLV	Human T-cell leukemia virus
IN	Integrase
k_{cat}	Turnover number; the number of times each enzyme active site converts substrate to product per unit time
K_{conf}	Rate of polymerase conformational change; together with K_{chem} makes k_{pol}
K_{chem}	Rate of dNTP incorporation chemistry reaction; together with K_{conf} makes k_{pol}
K_D	Equilibrium binding affinity of T/P to RT enzyme
K_d	Equilibrium binding affinity of dNTP substrate to RT enzyme
K_m	Substrate concentration needed to achieve half-maximum enzyme velocity (V_{max})
k_{pol}	Rate of substrate incorporation
k_{ss}	Steady-state rate constant
KS	Kaposi's sarcoma
LAV	Lymphadenopathy-associated virus
LTR	Long terminal repeat
MA	Matrix protein
MuLV	Murine leukemia virus

MHC-I	Major histocompatibility complex I
MHC-II	Major histocompatibility complex II
NC	Nucleocapsid
Nef	Negative regulatory factor
NLS	Nuclear localization sequence
NNRTI	Non-nucleoside reverse transcriptase inhibitor
NRTI	Nucleoside reverse transcriptase inhibitor
NVP	Nevirapine
ORF	Open reading frame
PBS	Primer binding site
PIC	Pre-integration complex
Pol	Polymerase
Pol II	RNA polymerase II
PPT	Polypurine tract
PR	Protease
Rev	Regulator of expression of virion proteins
RNR	Ribonucleotide reductase
RRE	Rev response element
RT	Reverse transcriptase
RTC	Reverse transcription complex
SAM domain	Sterile α motif domain
SAMHD1	SAM domain- and HD domain-containing protein 1
SIV	Simian immunodeficiency virus
SIVagm	African green monkey SIV
SIVcpz	Chimpanzee SIV
SIVgor	Gorilla SIV
SIVmac	Macaque SIV
SIVmnd	Mandrill SIV
SIVmus	Mustached monkey SIV
SIVrcm	Red capped mangabey SIV
SIVsm(m)	Sooty mangabey SIV
ssDNA	single-stranded DNA
ssRNA	single-stranded RNA
TDF	Tenofovir disoproxil fumarate
T/P	Template/ primer
TAR	Transactivation response element
Tat	Transactivator of transcription
TK	Thymidine kinase
Vif	Viral infectivity factor
V_{max}	Maximum enzyme velocity
Vpr	Viral protein R
Vpx	Viral protein X
Vpx (+)	SIVmac239 virus encoding Vpx; wild type SIVmac239 virus
Vpx (-)	SIVmac239 virus lacking Vpx (101-base pair deletion)
Vpu	Viral protein U
UNAIDS	Joint United Nations Program on HIV/AIDS
WHO	World Health Organization
WT	Wild type

Chapter 1: Introduction

1.1 HIV/AIDS

In June 1981, UCLA Medical Center observed advanced and unexplained immunodeficiency in four young, previously healthy, homosexual men^[1, 2]. Soon after, clustered outbreaks of opportunistic infections such as *Pneumocystis carinii* pneumonia, cytomegalovirus, and Kaposi's sarcoma rapidly arose within the United States. While initial cases appeared to be concentrated to the gay and Haitian communities, individuals requiring frequent blood transfusions, and intravenous drug users, the epidemic quickly spread across the world, indiscriminate of sexual orientation, ethnicity, socioeconomic standing, and previous health history^[3-5]. Both the scientific and medical communities alike presumed the disease likely spread horizontally in humans through blood or fluid contact and noted a similarity amongst all the reported cases: a stark decrease in T cell populations^[6, 7]. By September 1982, the Centers for Disease Control and Prevention (CDC) reported 593 cases of this novel disease termed acquired immunodeficiency syndrome (AIDS), of which 243 concluded in the patient's death^[8]. In 1983, the laboratories of Drs. Robert Gallo at the National Cancer Institute in Bethesda, MD and Luc Montagnier at the Pasteur Institute in Paris, France independently isolated the causative agent of AIDS, a novel pathogen belonging to a group of reverse transcribing RNA viruses named *Retroviridae* family. While the two labs settled on different names for the infecting virus, Dr. Gallo's "human T-cell leukemia virus III (HTLV-III)"^[9] and Dr. Montagnier's "lymphadenopathy-associated virus (LAV)"^[10] were, in fact, what we know today as human immunodeficiency virus type 1 (HIV-1).

A. Global Impact

Within a year of its discovery, the isolation and propagation of HIV-1 from AIDS patient samples was well documented and reproducible^[11, 12]. Serological tests, developed to identify positive cases^[13, 14], were instrumental in executing the mass community testing that ultimately confirmed the link between HIV and AIDS. Molecular cloning^[15-17] and sequencing^[18, 19] of HIV-1 in 1984 enabled segmentation of the virus into its various components and development of patient viral load tests, unleashing the opportunity for further scientific and treatment exploration. These initial studies were crucial to the identification of a

second variant in 1986, HIV type 2 (HIV-2), which was isolated from AIDS patients in West Africa^[20]. While morphologically and biologically similar to HIV-1, HIV-2 bore more sequence similarity and serological resemblance to simian immunodeficiency virus (SIV), a virus initially discovered in macaque animal populations that was known to induce host immunodeficiency in a manner similar to AIDS^[21, 22].

By the year-end of 2018 there were 1,040,352 individuals living with diagnosed HIV infections in the United States—that is 374.6 diagnosed infections for every 100,000 people^[23]. UNAIDS estimated that by the end of 2018, 37.9 million people globally were living with HIV, 20.6 million of whom live in eastern and southern Africa, a sub-portion of sub-Saharan Africa. The advent of antiretroviral therapy (ART) and highly active antiretroviral therapy (HAART) throughout the years has drastically improved the prognosis of HIV/AIDS, however, adherence and access remain the two most prominent hurdles to minimizing viral re-emergence in treated individuals and preventing viral spread to the uninfected global community. While new infections are down from 2.9 million newly infected people during the peak of the pandemic in 1997 to 1.7 million in 2018, 770,000 people died from AIDS-related illnesses in 2018 while only 62% of the global population had access to and were on ART^[24]. In addition to its enduring prevalence, HIV still disproportionately impacts various groups including the LBGQTQ and Black/African American communities within the United States. Globally, HIV remains a public health concern and current efforts aim not only to improve the reach of HIV testing and treatment^[25] but also to continue advancing scientific knowledge of the virus: where it comes from, what biochemical, immunological, and evolutionary dynamics exist between it and the human body, and how these findings can help expand HIV treatment options as well as aid in the investigation of other viruses.

B. Origins

In 1985, the isolation of a simian retrovirus from sick rhesus macaques at the New England Regional Primate Research Center (NERPRC) sprouted the first branch on the HIV/SIV phylogenetic tree^[26, 27]. Scientists observed that this simian virus, now commonly known as SIVmac, caused immunodeficiency in its primate host—indicated by cytopathic effects to CD4⁺ T cell populations—and was antigenically similar to HIV-1^[28]. Subsequently, healthy African green monkeys (SIVagm)^[29] and

sooty mangabeys (SIVsm)^[30] were found to be naturally infected by HIV-related viruses that did not cause the disease symptoms seen in HIV-1 and SIVmac infections. Upon the isolation of HIV-2 in 1986, sequence analysis revealed HIV-2 was more closely related to SIVmac than HIV-1, sharing 75% and 40% genome sequence homology respectively^[21, 22, 31].

To better understand the origin and evolution of HIVs and SIVs, isolates have been taken from over 45 species of nonhuman primates—including mandrills (SIVmnd)^[32] and red-capped mangabeys (SIVrcm)^[33]—to observe phylogenetic relationships through viral genome sequence comparisons^[34]. Various studies have analyzed a combination of five key categories of data to assess the probability of SIV zoonotic transmission into humans: (i) viral genome organization, (ii) phylogenetic relatedness, (iii) prevalence of the virus in the natural host, (iv) geographic coincidence, and (v) plausible routes of transmission^[35]. The culmination of these studies revealed that HIV-1, HIV-2, and all known SIVs originated from a single viral lineage within the *Lentiviridae* genus, a genus comprised of viruses that cause chronic and progressive disease states that are characterized by long viral incubation periods^[36]. As such, HIV/AIDS has been found to be the result of at least eleven independent zoonotic transmission events of SIV into human populations spanning back to the early 20th century^[37, 38]. While the nature of the SIV zoonoses remains unknown, it is likely the virus was transferred to humans through exposure to infected primate bodily fluids during the hunting of bushmeat^[39].

The aforementioned viral surveillance and sequencing projects were instrumental in comparing the viral genomes of various isolates originating from naturally infected wild primates in sub-Saharan Africa and captive primates across the world. Interestingly, the vast majority of recovered SIV strains do not induce immunodeficiency in their natural hosts, rather, they are endemic to the originating primate species and only possess pathogenic potential following cross-species transmission events into a new host organism^[40]. Unlike other SIVs, SIVmac was initially identified due to the AIDS-like disease state observed in virtually all infected macaque animals. Retrospective phylogenetic analysis revealed that a cross-species transmission event of SIVsm to rhesus macaques in the 1970s resulted in the establishment of the SIVmac viral strain^[41, 42], with ancestral SIV strains existing only a few hundred years ago^[37] (Figure 1.1). It was

the transfer of SIVsm to humans in two independent transmission events that resulted in the establishment of HIV-2 groups A and B in the 1930s^[37].

While HIV-2 can be traced back to the SIVsm/SIVmac lineage^[42] with extreme clarity, the origins of HIV-1 are more complicated. HIV-1 is characterized by high genetic variation and has been transmitted to humans in multiple transmission events resulting in strains that can be grouped by their genetic similarity: groups M (main), O (outlier), N (non-M and non-O), and P (pending the identification of further human cases). While HIV-1 groups M and N are most closely related to SIVcpz, an SIV strain originating from a common chimpanzee (*Pan troglodytes troglodytes*) in Cameroon^[35, 43, 44], HIV-1 groups O and P are more closely related to SIVgor from western gorillas (*Gorilla gorilla gorilla*) also in Cameroon^[45-47]. Studies show that despite distinct geographical clustering of various chimpanzee colonies within the west Central African region, there is evidence of multiple SIVcpz coinfection and recombination events within single chimpanzee and gorilla hosts, adding to the genetic diversity of this group and its resulting HIV-1 strains^[48, 49].

HIV-1 group M viruses are responsible for more than 90% of HIV infections worldwide^[50] and are so genetically diverse they are subclassified into eleven distinct clades that are denoted as subtypes A-K^[51]. Like SIVcpz, group M viruses frequently establish coinfections in human hosts, thus increasing genetic diversity and promoting the further division of subtypes A-K into circulating recombinant forms (CRFs). With a total number of 100,000 estimated cases globally^[52], HIV-1 group O accounts for roughly 1-5% of HIV infections^[53, 54] and is primarily isolated to west Central Africa^[55]. Unlike HIV-1 group M viruses, group N and the newly discovered group P viruses^[46] are extremely rare^[56]. By 2010, group N viruses accounted for only 0.1% of HIV infections in Cameroon with only 13 total cases identified worldwide^[57]. Similarly, in 2011, group P only represented 0.006% of HIV-1 infections^[58], leading some to hypothesize that this group is less adapted to humans and less pathogenic than other HIV-1 strains^[59].



Figure 1.1 Phylogenetic tree of HIV-1, HIV-2, and SIVs. An unrooted phylogenetic comparison based on HIV/SIV Gag polyprotein amino acid sequences was generated using the neighbor-joining method. This figure was created by Yosuke Sakai^[60] and is distributed under a [CC BY 4.0](https://creativecommons.org/licenses/by/4.0/) license.

1.2 Viral Genome and Replication Cycle

During lentiviral pathogenesis, HIV-1, HIV-2, and SIV hijack host cell machinery and utilize virally encoded proteins in order to successfully replicate viral genetic material, produce viral proteins, assemble progeny virions, and propagate viral infection.

A. Viral Genome Organization

HIV-1, HIV-2, and SIV are positive sense, single-stranded RNA viruses (i.e. (+)ssRNA viruses) that contain two copies of a viral RNA (vRNA) genome that is roughly 10,000 nucleotides long. HIV/SIV genomes are flanked by long terminal repeat (LTR) sequences that are approximately 640 base pairs in length, contain several regulatory sites that are essential for viral replication, and can be segmented into the U3, R, and U5 regions that are characteristic of all retroviruses^[61]. Key elements of the HIV/SIV LTR include (i) the transactivation response (TAR) element (nt +1 to +60) which forms a 5' stem-loop structure that can be bound by viral and cellular proteins to regulate the transcription of viral genes^[62], (ii) a core promoter (nt -78 to -1), (iii) an enhancer element (nt -104 to -81), and (iv) a modulatory region (nt -454 to -78) that contains the negative regulatory element (NRE) (nt -340 to -185) (location of LTR regions reviewed in^[63]). Interestingly, deletion of the NRE results in a 2-3 fold increase in viral gene expression^[64], indicating that this region might be involved in the negative regulation of viral replication, hence its name. Extensive studies have demonstrated that numerous cellular proteins interact with the genomic and proviral HIV/SIV LTR in a sequence-specific manner to enact a variety of functional roles throughout the viral lifecycle^[65].

Viral proteins originate from the nine open reading frames (ORFs) between the LTRs: three of these genes—*gag*, *pol*, and *env*—encode for structural proteins essential for viral replication and common to all retroviruses^[61], while the remaining six are either regulatory or accessory proteins. Since HIV-1, HIV-2, and SIV share a common single ancestor, it is expected that they display similar genome organization. However, a stark difference in accessory proteins was demarked by the discovery of *vpu* exclusively in the HIV-1 lineages, and the presence of *vpx* in HIV-2 and some SIV strains including SIV_{sm}, SIV_{mac}, SIV_{rcm} and SIV_{mnd2} (Figure 1.2). This distinction lies at the foundation of this thesis.

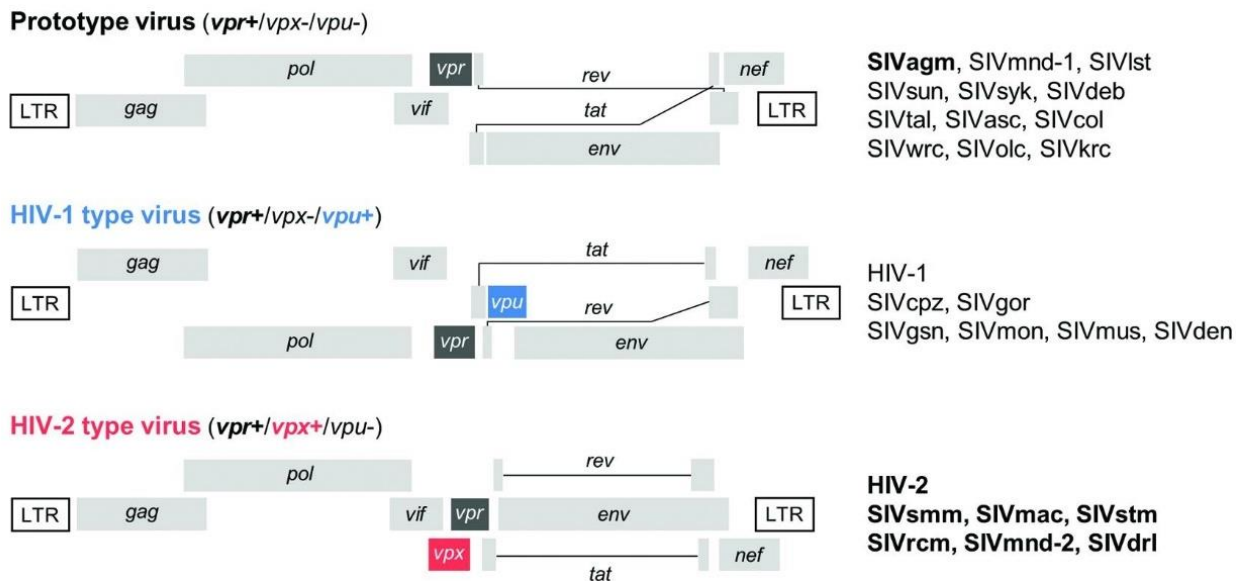


Figure 1.2 HIV/SIV genomic organization. Three types of HIV/SIV retroviral genomes are schematically illustrated. Representative viral strains are listed to the right of the genome. This figure was created by Yosuke Sakai^[60] and is distributed under a [CC BY 4.0](https://creativecommons.org/licenses/by/4.0/) license.

B. Viral Components

While protein weight and nomenclature may differ between HIV-1, HIV-2, and SIV viruses (e.g. capsid protein is called p24 in HIV-1 versus p28 in SIV), functional properties are retained amongst these lentiviruses. The gene products of the HIV-1 genome are discussed below.

Gag

The *gag* gene encodes for a precursor polyprotein, known as Gag (or Pr55^{gag} for HIV-1), that is cleaved during viral pathogenesis into four structural proteins called matrix (MA, p17), capsid (CA, p24), nucleocapsid (NC, p7) and p6 as well as two spacer peptides termed p1 and p2. Sequential proteolytic processing of Gag is regulated by p1 and p2^[66], while the resulting functional proteins are required for the formation of retroviral virion structures, recruitment of viral components to the plasma membrane, and budding of newly assembled virions. Additionally, Pr55^{gag} itself is recruited to the plasma membrane during viral assembly for packaging into immature virions^[67].

As a 17 kDa proteolytic product of Gag, MA constitutes the N-terminal domain of the polyprotein prior to cleavage. MA is cotranslationally myristoylated at the N-terminus, a post-translational modification that is necessary for virus production^[68] as it promotes the targeting of this structural protein to lipid rafts at the plasma membrane^[69]. Functional trimeric MA^[70] lines the inner surface of the viral membrane in a mature virion and is responsible for recruiting envelope glycoproteins^[71], Gag, Gag-Pol^[72], and possibly genomic vRNA^[73] to the site of viral assembly. Finally, early in the viral replication lifecycle, MA is a component of the pre-integration complex (PIC). While it is rumored the nuclear localization sequence (NLS) of MA may aid in viral nuclear import during the infection of nondividing cells, recent studies fail to fully support this hypothesis (reviewed in^[74]).

In a mature virion, the canonical capsid core is comprised of approximately 1,500 CA monomers^[75] (24 kDa) assembled predominantly into hexamers and pentamers^[76]. This cone-like protein shell encloses the dimeric (+)ssRNA genome, numerous NC proteins, auxiliary/accessory proteins, and viral enzymes^[77, 78], protecting its contents from detection by the host immune system^[79, 80]. Interestingly, studies within the 21st century have implicated CA as a potential determinant of retroviral infectivity in nondividing cells^[81].

NC is a small (7 kDa), basic protein that utilizes its zinc fingers to non-specifically bind the phospho-backbone of nucleic acids, yet specifically interacts with a packaging signal at the 5' end of genomic vRNA (Ψ)^[82] to recruit the viral genome to sites of viral assembly^[83]. Ultimately encapsulating the genomic material in mature virions, NC anneals tRNA^{Lys3} to vRNA, promotes efficient minus-strand transfer, and facilitates the remodeling of nucleic acid structures during reverse transcription (reviewed in^[84]). Lastly, NC is a component of the PIC.

Originating from the C-terminal of Gag, p6 aids in virion assembly and maturation through its recruitment of accessory protein Vpr^[85] (or Vpx for HIV-2 and some SIVs) and facilitation of viral budding^[86, 87] through its highly conserved PTAP motif that interacts with the cellular endosomal sorting complex required for transport (ESCRT) machinery^[88]. Recent studies have demonstrated that p6 is phosphorylated at many residues including a highly conserved serine at position 40 (S40)^[89], illuminating a mechanism to its function as a membrane-associated docking site for numerous cellular binding partners^[90].

Pol

All Pol proteins are generated by the processing of the Gag-Pol precursor polyprotein (Pr160^{gagpol})—a fused translation product that is produced at a frequency of 5-10%^[91] of all Gag translation events and results from a -1 ribosomal frameshift event at the palindromic region between *gag* and *pol*^[92]. Once cleaved, Pol produces the viral enzyme components: protease (PR), reverse transcriptase (RT), and integrase (IN).

Encoded by the *pol* gene, viral aspartic protease PR catalyzes the sequential cleavage of the Gag and Gag-Pol polyproteins to drive viral maturation following viral assembly and budding from the plasma membrane^[93]. Once liberated from Pr160^{gagpol} in a two-step proteolytic cleavage process called precursor autoprocessing^[94], PR forms tightly associated dimers ($K_d < 5\text{nM}$) and cleaves at least ten sites of Gag and Gag-Pol to generate mature viral proteins^[95]. Proteolytic processing of the Gag and Gag-Pol polyproteins is essential for viral maturation, making functional PR not only required for production of infectious progeny virions^[96] but also a major antiviral drug target (reviewed in^[97]).

RT is a viral RNA- and DNA- dependent DNA polymerase that is responsible for converting the (+)ssRNA genome into a double-stranded proviral DNA during the course of viral pathogenesis. This heterodimeric enzyme is generated by two PR cleavage reactions: the first cleavage creates the RT catalytic subunit (p66 in HIV-1/SIV and p68 in HIV-2) from the Gag-Pol polyprotein, while the second reaction further processes half of these proteolytic products by cutting a 15 kDa fragment from the larger RT subunit to generate the structural subunit (p51 in HIV-1/SIV and p54 in HIV-2) of RT^[98, 99]. In addition to DNA polymerization, RT is capable of performing strand transfer and strand displacement functions while also harboring an RNaseH domain that is responsible for degrading viral RNA during proviral DNA synthesis^[100]. Overall, functional RT possesses five enzymatic functions, all of which will be discussed in further detail in Section 1.3.

IN (32 kDa) is formed from the C-terminal end of Pr160^{gagpol} and is an essential member of the PIC. Made up of an N-terminal zinc-binding domain, central catalytic domain, and a nonspecific C-terminal DNA-binding domain. IN is tasked with inserting the proviral dsDNA genome into the host genome following translocation of the PIC to the nucleus. IN begins performing this function by first locating a CAGT sequence in the proviral DNA 3'-LTRs in order to cleave off the terminal GT dinucleotide and generate vDNA 3'-OH overhangs^[101]. The catalytic core then facilitates a nucleophilic attack of a phosphodiester bond within the host genome, resulting in the successful insertion of viral DNA into the host genome^[102]. Interestingly, IN possesses an NLS that may aid in the infection of nondividing cells^[103], however its role in PIC nuclear import is unclear^[104]. Since it holds the least resemblance to any human protein, IN is also an attract anti-HIV drug target^[105, 106].

Env

Env (gp160) is a heavily glycosylated polyprotein that trimerizes in the endoplasmic reticulum (ER) prior to being cleaved by cellular furin-like proteases to generate surface (SU, gp120 in HIV-1 and gp105 in HIV-2) and transmembrane (TM, gp41 in HIV-1 and gp36 in HIV-2) proteins^[107, 108]. Env proteins gp120 and gp41 remain associated through weak noncovalent interactions and are trafficked, via the Golgi secretory pathway, to the plasma membrane where the trimerized proteins anchor themselves and form

spike structures on the cell surface (reviewed in^[109]). Env spike structures interact with CD4—a cell receptor unique to immune cells—to gain entry into target cells during the initial stages of viral infection. While gp120 is rapidly recycled through endocytosis^[110], resulting in the incorporation of roughly ten spikes per virion^[111] (53), the human immune system generates large numbers of broadly neutralizing antibodies against the surface-exposed residues of Env protein, thus creating immense selective pressure that drives viral immune evasion and the constant evolution of Env^[112]. Interestingly, Joshi et al. recently identified an Env variant that displays > 300% increased viral infectivity in the presence of HIV-1-positive plasma, revealing an intriguing virus-host interaction in which host defenses alleviate a viral defect^[113]. In HIV-1, the *env* gene is translated from a bicistronic mRNA that encodes for both Env proteins (gp120 and gp41) as well as Vpu.

Vif

Vif is a 23 kDa accessory protein^[114] that counteracts host restriction factor (APOBEC3G)^[115], a cytidine deaminase that catalyzes the conversion of cytosine to uracil in ssDNA and has the potential to severely mutate nascent viral ssDNA during reverse transcription^[116]. Viral Vif targets host APOBEC3G for ubiquitination and subsequent proteasomal degradation via the Cul5-SCF pathway^[117].

Vpr

Vpr—the arginine-rich, 15 kDa accessory protein resulting from the *vpr* gene—is packaged into virions via p6^[118] and serves a multitude of functions in lentiviral HIV-1, HIV-2, and SIV. Like IN, MA, NC, and p6, Vpr is a component of the PIC. While it does not possess a classical NLS, Vpr appears to participate in PIC nuclear entry by utilizing a cluster of six arginine residues at its C-terminus^[119] to support MA binding to karyopherin α , a cell receptor for nuclear-targeted proteins^[120]. HIV-1 Vpr is required for efficient replication in macrophage populations^[121] and is known to prevent the progression of the cell cycle from G2 to M phase (G2 arrest) in CD4⁺ cells irrespective of cellular proliferative state^[122], leading Jacquot et al. to conclude that both properties may be dependent on the nuclear localization of HIV-1 Vpr^[123]. Unlike HIV-1 Vpr, HIV-2/SIVsm Vpr does not participate in PIC nuclear import but still retains the ability to induce G2 arrest^[124].

Additionally, some SIV strains (e.g. SIV_{mus1}, SIV_{deb}, SIV_{agm677}, and SIV_{agm9648}^[125]) contain Vpr proteins that are able to interact with DCAF1, a cellular substrate receptor that forms a complex with Cullin4-RING E3 ubiquitin ligase (CRL4). The Vpr-DCAF1-CRL4 complex recruits and targets host sterile alpha motif (SAM) domain and histidine-aspartate domain (HD)-containing protein 1 (SAMHD1), an enzyme that degrades cellular deoxyribonucleotide triphosphates (dNTPs) into 2'-deoxynucleosides (dNs) and triphosphates (reviewed in^[126]), for ubiquitin-mediated proteasomal degradation^[127]. In nondividing cells, like macrophages, deoxynucleotide triphosphohydrolase (dNTPase) SAMHD1 depletes intracellular dNTPs, restricts viral reverse transcription, and delays replication kinetics^[128] during HIV-1 infections. Therefore, in some SIVs, virus induced degradation of SAMHD1 by Vpr elevates macrophage cellular dNTP pools and promotes complete and efficient reverse transcription of the viral genome. Recently, Zhou et al. showed that HIV-1 Vpr degrades host helicase-like transcription factor (HTLF), a protein involved in DNA repair and genome maintenance, in a manner similar to SAMHD1^[129].

Vpx

The *vpx* gene, found exclusively in the HIV-2/SIV_{sm} lineage (Figure 1.2), is the suggested gene duplication product of *vpr*^[130]. Once translated, Vpx is a 14 kDa viral accessory protein that is composed of a three-helix bundle that is stabilized by a zinc finger motif. Interestingly, this protein is expressed at strain-dependent levels^[60], however ~150 molecules are packaged into a budding virion. Like HIV-1 Vpr, Vpx is packaged into virions by p6^[131] and is required for nuclear import^[124]. HIV-2/SIV_{sm} Vpx hijacks the same cellular ubiquitination pathway used by some Vpr proteins^[132-134], in order to counteract host restriction factor SAMHD1^[135], elevate intracellular dNTPs, and successfully replicate within the restrictive dNTP pools found in macrophages^[136]. Crystal structures have shown that both Vpr and Vpx directly interact with SAMHD1 in the Vpr/Vpx-DCAF1-CRL4-SAMHD1 complex. This interaction has driven the evolution of the interface between SAMHD1 and Vpr/Vpx, spurring a virus-host arms race^[137]. The focus of this dissertation involves virus induced SAMHD1 degradation and its effects on viral protein evolution.

Vpu

Translated from a bicistronic mRNA containing Env^[138], Vpu is a viral accessory protein that is exclusive to the HIV-1/SIVcpz lineage (Figure 1.2). Vpu targets newly synthesized CD4 in the endoplasmic reticulum (ER) and induces rapid degradation^[139] of the receptor in a process that is dependent upon the phosphorylation of its S52 and S56 residues^[140]. Antagonization of CD4 disrupts the formation of gp160-CD4 complexes^[141] and protects against host detection via antibodies involved in antibody-dependent cell-mediated cytotoxicity (ADCC)^[142]. In addition to downregulating CD4, Vpu also counteracts host restriction factor tetherin (i.e. BST-2), a protein that dimerizes at the cell surface and prevents viral release in the absence of Vpu^[143, 144]. HIV-1 Vpu—an integral membrane protein that is comprised of a plasma membrane-anchored N-terminal region, a transmembrane region, and a cytoplasmic C-terminal region—uses its transmembrane domain to interact with the transmembrane domain of tetherin, inducing the degradation of the host restriction factor via a lysosomal pathway^[145]. Recent studies have shown that Vpu from SIV originating from greater spot-nose monkeys (SIVgsn71), uses different residues to counteract BST-2, instead requiring two AxxxxxxW motifs to properly induce the degradation of the host restriction factor^[146]. Ultimately, the counteraction of host CD4 and tetherin proteins by viral Vpu protects HIV-1 infected cells from antibody-mediated cell lysis and enhances the efficiency of virion production^[147].

Tat

The *tat* gene is comprised of two exons that surround and partially overlap the *env* gene^[148, 149] within the HIV/SIV genome. Once properly spliced and translated, Tat is an 86 amino acid long protein that is essential for efficient HIV replication^[150, 151]. As a *trans*-activator, Tat binds the vRNA TAR element and cellular kinase CDK9^[152] to induce phosphorylation of the RNA Polymerase II carboxyl terminal domain (CTD) and facilitate the production of full-length viral transcripts^[153-155]. Since the *tat* gene is located near the viral promoter, generation of incomplete transcripts often produces mRNA encoding the Tat protein. Therefore, the protein exists in a feedback loop that inevitably results in its high expression in both productively and latently infected cells. Studies have shown that HIV-1-infected cells secrete the majority of the Tat produced during their lifespan through a nontraditional mechanism involving phospholipids at the cellular plasma membrane^[156]. Since extracellular Tat remains biologically active and

can be endocytosed by uninfected cells, recent studies have associated the viral protein with the dysregulation of intracellular processes in HIV-1-associated neurocognitive disorders (HAND)^[157].

Rev

Rev is a 16 kDa protein that conducts the nuclear export of intron-containing vRNA transcripts to the cytoplasm for translation^[72]. Studies demonstrate that vRNA transcripts are fully spliced and fail to be trafficked to the cytoplasm in the absence of Rev^[158], making this protein essential for viral replication^[159]. Rev binds a roughly 350-nucleotide region within an intron of the viral genome (nt 7362-7596) called the Rev response element (RRE). The RRE is characterized by several hairpin structures^[160] which Rev binds with a stoichiometric ratio of 4 Rev proteins to 1 RRE^[161, 162]. Current studies seek to employ a gRNA-directed CRISPR/Cas9 system to selectively remove integrated viral DNA from host genomes by targeting conserved *tat* and *rev* sequences^[163].

Nef

Nef (27 kDa) is translated from a multiply spliced mRNA (like Tat and Rev) and is myristoylated (like MA)^[164]. As a master regulator, Nef modulates the cell surface expression of various receptors^[165], downregulating both CD4 (reviewed in^[166]) and major histocompatibility complex class I (MHC-I)^[167] thus protecting infected cells from superinfection^[168] and against killing by cytotoxic T cells^[169]. SIV Nef has also been found to downregulate BST-2 expression in infected rhesus macaque and sooty mangabey animals, counteracting tetherin restriction, much like HIV-1 Vpu, to achieve successful viral budding^[170]. Recent studies seek to explore Nef as a potential therapeutic target after discovering the viral protein induces expression of C-C motif chemokine ligand 2 (CCL2), a leukocyte chemoattractant whose dysregulation is suspected to result in a variety of neurological diseases^[171].

C. Viral Replication Cycle

The HIV/SIV replication cycle (Figure 1.3) is one that can be divided into two phases: the early stage (which includes viral entry, uncoating, reverse transcription, and integration) and the late stage (which is comprised of transcription and translation of viral gene products, followed by virion assembly, budding, and maturation). The viral replication cycle of HIV-1 will be discussed in this section. For the scope of this dissertation, distinct emphasis will be placed on the process of reverse transcription.

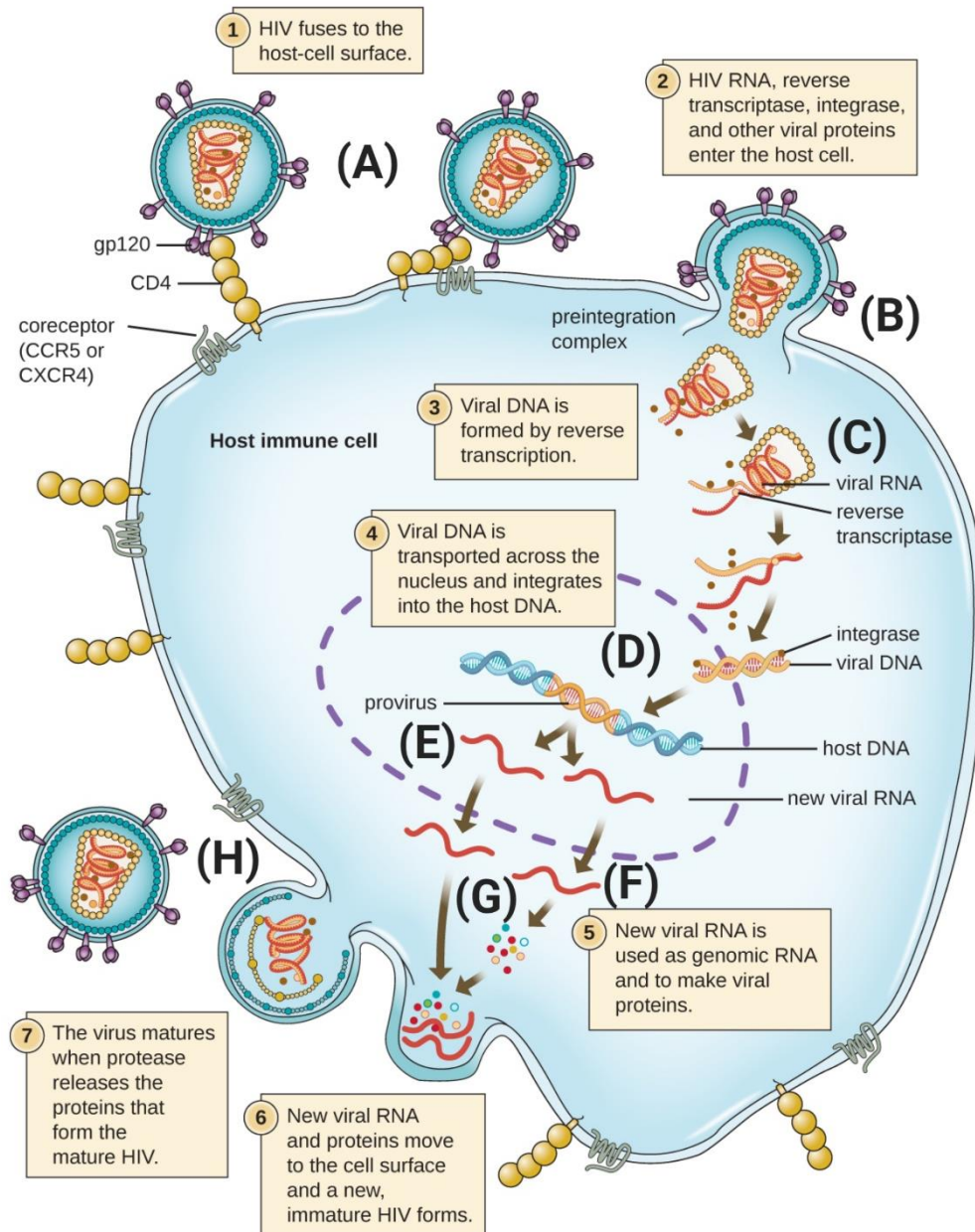


Figure 1.3 HIV replication cycle. (A) To initiate infection of a target host cell, HIV first binds CD4 and a coreceptor at the cell surface. The outer layer of the HIV virion fuses with the host cell, depositing the viral capsid into the cytoplasm. (B) Capsid uncoating then empties the viral contents into the cytoplasm. (C) RT converts the (+)ssRNA genome into proviral DNA which is transported to the nucleus where (D) IN inserts the viral dsDNA into the host genome. (E) Host RNA Pol II transcribes viral proteins from the integrated DNA segment, generating full-length mRNAs that are shuttled out of the nucleus by Rev so they can either be packaged into a progeny virion or (F) spliced by cellular enzymes. Cellular ribosomes translate viral

mRNAs into proteins, **(G)** which are then assembled at the cell surface. **(H)** Host ESCRT proteins are recruited by viral p6 to facilitate virion budding. Once the virion is release, PR cleaves Gag and Gag-Pol polyproteins to create a mature viral particle. This figure was produced by OpenStax under a [CC BY 4.0](#) license and is adapted from NIAID, NIH.

Entry

The viral replication cycle begins with entry of a mature virion into a target immune cell (Figure 1.3A). Mature lentiviral virions are enveloped in host cell plasma membrane that is decorated with glycosylated viral Env trimeric spikes. Binding of the SU glycoprotein (gp120) to host surface receptor CD4^[172, 173] induces a conformational change of the gp120/CD4 complex, exposing an Env co-receptor binding site^[174, 175] that accommodates binding to host C-X-C motif receptor 4 (CXCR4)^[176] or C-C motif receptor 5 (CCR5)^[177] which are G protein-coupled chemokine receptors with seven transmembrane (7TM) domains that facilitate the transduction of extracellular signal to intracellular signaling cascades. Following co-receptor binding, gp41 undergoes a conformational change in which its hydrophobic N-terminal fusion peptide (FP) translocates and inserts into the plasma membrane before forming a six-helical bundle known as the postfusion conformation^[178]. This series of sequential conformational changes promotes fusion of the viral envelope with the host cell plasma membrane—in a process that is dependent on virus-induced, surface exposed phosphatidylserine^[179]—thereby allowing entry of the viral capsid into the cytoplasm.

Uncoating

Once inside the host cell, the viral capsid, which is roughly 119 nm in length with a maximum diameter of 60 nm^[75], disassembles to allow nuclear import of the PIC through the nuclear pore which permits entry of macromolecules with diameters of approximately 39 nm^[180] (Figure 1.3B). The temporal and mechanistic details of uncoating remain unclear^[181-185].

Reverse Transcription

The process of reverse transcription occurs within the reverse transcriptase complex (RTC)^[186], a complex that converts the (+)ssRNA viral genome into proviral dsDNA that can be processed and integrated into the host genome (reviewed in^[187]) (Figure 1.3C, Figure 1.4). Using a tRNA^{Lys3} primer that is packaged into the virion during viral assembly and annealed to the 5'-primer binding site (PBS) on the vRNA genome through complementary sequences^[188] (Figure 1.4A), reverse transcriptase begins processive RNA-dependent DNA polymerization that continues through the U5 and R sequences of the 5'-LTR until reaching the end of the viral genome^[189]. This initial stage of polymerization is called minus-strand strong

stop DNA synthesis, as it generates a complementary (-)ssDNA prior to synthesis that halts at the end of the vRNA strand (Figure 1.4B). During minus-strand synthesis, RT utilizes its p66 C-terminal RNaseH domain to degrade the vRNA genome. This liberates the nascent DNA nucleotides from their previous base pair interactions and enables the newly synthesized 5'-R sequence to complementarily bind to the vRNA 3'-R sequence in the first strand transfer event (Figure 1.4C). Subsequent elongation of minus-strand DNA proceeds towards the 5'-PBS at end of the viral genome, all while viral RT actively degrades its vRNA template. While HIV/SIV virions harbor two copies of genomic RNA, these RNAs are often nicked. To circumvent damaged nucleic acid regions, minus-strand synthesis can be transferred to the second vRNA template in a process called template switching^[190].

Two purine-rich regions of vRNA called the central polypurine tract (cPPT) and the 3'-polypurine tract (3'PPT) are resistant to RNaseH degradation and remain annealed to the minus-strand during elongation^[191] (Figure 1.4D). These resilient PPT regions serve as primers for plus-strand DNA-dependent DNA synthesis that uses the newly synthesized DNA as a template for polymerization. Unlike 3'PPT, cPPT is not essential for HIV-1 replication; however, generation and use of the cPPT enhances plus-strand DNA synthesis and aids in efficient viral replication^[192]. Once tRNA^{Lys3} is copied at the end plus-strand strong stop DNA synthesis, generating a 3'-PBS sequence, the tRNA is finally degraded by the RNaseH domain of RT^[193] (Figure 1.4E). The tRNA^{Lys3}-derived 3'-PBS sequence on strong stop plus-strand DNA complementarily binds to the 5'PBS sequence in the minus-strand DNA, facilitating a second strand transfer event (Figure 1.4F). Proviral DNA synthesis is completed via the DNA-dependent DNA polymerization and strand displacement activities of RT, ultimately yielding a linear double-stranded vDNA that can undergo integration into host genomes (Figure 1.4G).

NC aids in reverse transcription by lowering the melting temperature of DNA which facilitates stable DNA annealing, promotes efficient strand transfer, catalyzes the rearrangement of nucleic acid into thermodynamically stable structures that favor efficient DNA polymerization by RT^[194]. Reverse transcription can lead to the generation of 2-LTR circles^[195], a circularized byproduct often found in the nucleus that is created through ligation of the two distal LTRs in viral dsDNA by cellular non-homologous

end joining (NHEJ) machinery (reviewed in^[196, 197]). While Brussel et al. reported evidence of gene expression from 2-LTRs, the biological functions of this circularized viral DNA and its subsequent transcript are still unclear^[198]. Since RT is a low fidelity enzyme that not only possesses template switching abilities but also lacks a proofreading mechanism, reverse transcription is a highly mutagenic process. Lastly, recent studies have called into question the order of events regarding viral uncoating and reverse transcription: while uncoating is often depicted as preceding reverse transcription during viral replication, it has been shown that intracellular nucleotides are packaged into budding virions, enabling endogenous reverse transcription within the virion after viral maturation^[199]. Interestingly, other studies have demonstrated that reverse transcription strand transfer events trigger viral uncoating^[181]. Reviews by Sarafianos et al.^[100] and Hu and Hughes^[187] discuss the process of reverse transcription and the various mechanisms of RT-based viral mutagenesis in great detail.

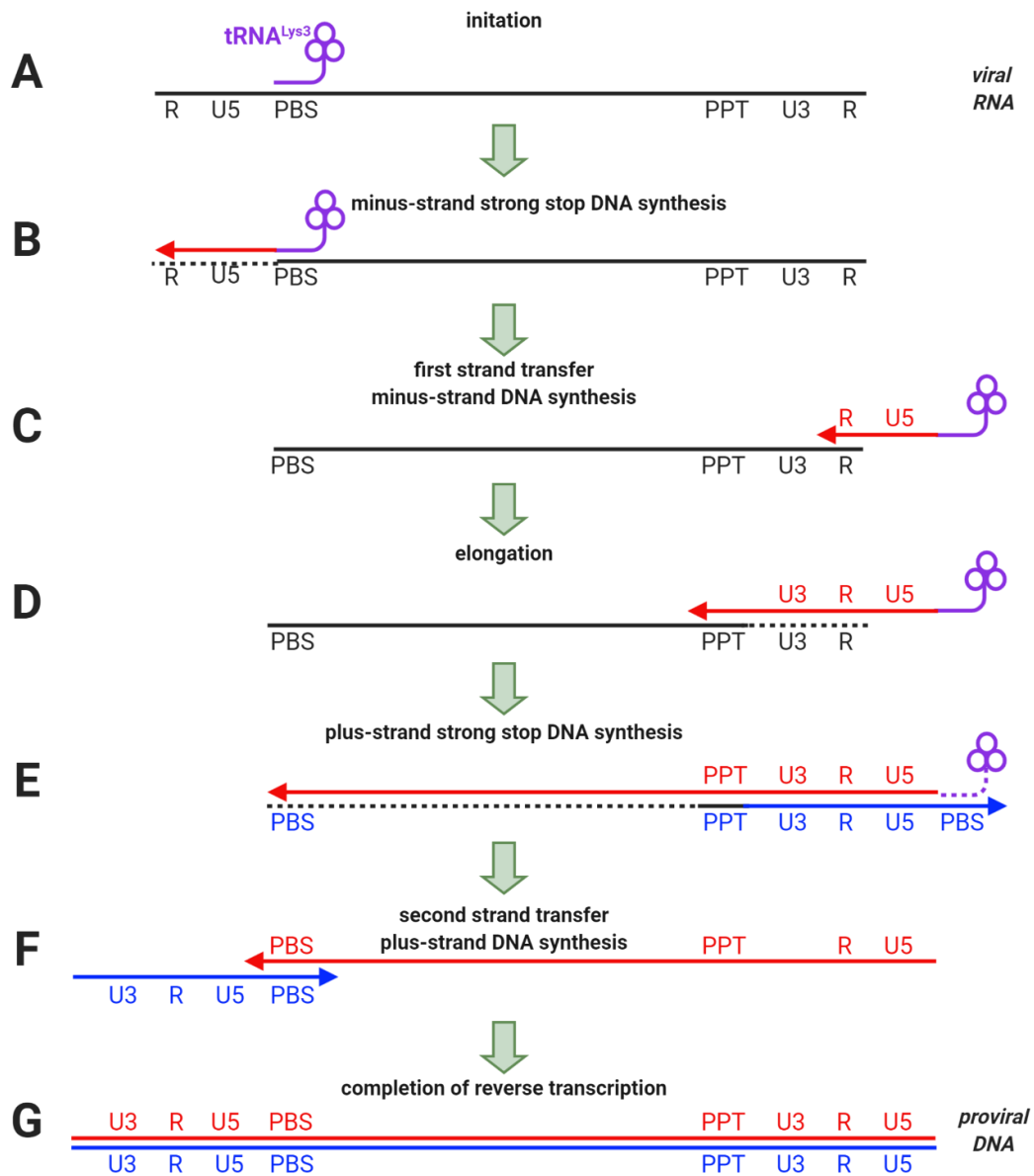


Figure 1.4 Process of HIV/SIV reverse transcription. (A) During viral assembly, cellular $tRNA^{Lys3}$ (purple) is annealed to the PBS sequence at the 5' end of the viral RNA genome (black). Using cellular dNTPs, reverse transcriptase initiates RNA-dependent DNA polymerization, (B) synthesizes minus-strand (red) DNA, and encounters the first strong stop after reaching the 5' end of the HIV/SIV genome. While polymerizing, RT degrades the viral RNA template (dashed line). (C) The first strand transfer event is facilitated by homologous R regions in the nascent DNA and 3' end of the viral genome. (D) Elongation of the minus-strand persists as RT degrades the vRNA genome, leaving behind the RNaseH resistant

polypurine tract (PPT). **(E)** Plus-strand (blue) synthesis is initiated from the PPT and continues until reaching the 3' end of the vRNA genome (second strong stop), where RT degrades tRNA^{Lys3}. **(F)** A second strand transfer event takes place in which homologous PBS sequences on the plus- and minus-strands interact, enabling DNA-dependent DNA synthesis and the elongation both strands. **(G)** Full extension of minus- and plus-strands concludes reverse transcription and generates proviral DNA. This schematic representation of lentiviral reverse transcription was adapted from original art licensed under a [CC BY 3.0](#) created by Ilina et al.^[200].

Integration

Upon the completion of reverse transcription, the proviral dsDNA is bound by IN within the PIC which then catalyzes an endonucleolytic cleavage of the conserved 3'-CA sites at the proviral DNA ends. This cleavage reaction generates CA-3'-OH ends that conduct a nucleophilic attack of the host DNA phosphodiester bond^[101], effectively inserting the proviral DNA into the host genome (Figure 1.3D). Researchers have found that viral integration is targeted to transcriptionally active regions of the genome via association of IN with lens epithelium-derived growth factor (LEDGF/p75)^[201], a host protein implicated in the regulation of gene expression that tethers the PIC to host genomic DNA^[202, 203].

Transcription and Translation

Integration of proviral DNA into the host genome enables the transcription of viral genes by host RNA polymerase II, a process greatly enhanced by viral Tat (Figure 1.3E). Proviral DNA contains a polyadenylation signal located between nucleotides 9205 and 9210 that is used to generate the 3' end of viral mRNA transcripts^[72]. This process yields full-length viral mRNAs that are bound by Rev at their RRE sequences and shuttled from the nucleus into the cytoplasm^[204]. Similarly, Hulver et al. recently reported cellular HIV-1 dependency factor Tat-specific factor 1 (Tat-SF1)^[205] binds HIV-1 RNAs at the TAR to selectively transport unspliced vRNA out of the nucleus while retaining singly spliced RNAs in the nucleus^[206]. Host splicing machinery produces singly- or multiply-spliced viral mRNAs that encode the various viral proteins (reviewed in^[207]) while unspliced, full-length viral mRNA serves two purposes: synthesis of the Gag and Gag/Pol polyproteins and packaging into virions during viral assembly. Viral mRNAs are translated into viral proteins by host ribosomes and undergo the necessary post-translational modifications by cellular machinery (reviewed in^[208]) (Figure 1.3F).

Assembly

During viral assembly (Figure 1.3G), HIV-1 Vpu promotes degradation of newly synthesized CD4 at the ER, a function that enables the trimeric Env glycoprotein to easily traffic to the surface of the infected cell without forming intracellular Env-CD4 dimers. Additionally, CD4 present at the cell surface is recycled by Nef, protecting the cell from superinfections and, once again, preventing the formation of Env-CD4 dimers. Localization of unprocessed Gag and Gag-Pol polyproteins within lipid microdomains at the cell membrane is facilitated through the N-terminal myristic acid moiety of the Gag polyprotein (MA) and Gag-Gag interactions. Once anchored at the plasma membrane, the p6 domain of Gag recruits Vpr/Vpx proteins to the site of viral assembly. Similarly, the NC domain of Gag recruits full-length viral RNA to the assembly site (reviewed in^[209]) where the two (+)ssRNA genomes dimerize at their 5'-ends forming a “kissing loop” hairpin structure that ensures both copies are encapsulated into the assembled virion^[210]. Ultimately, various viral and cellular proteins are assembled into the virion including viral Vif and Nef as well as various cellular proteins including lysyl-tRNA synthetase, tRNA^{Lys3}, ubiquitin, actin, and various actin binding proteins^[211].

Budding and Maturation

Assembled viral particles begin pinching away from the infected cell in a process called viral budding. Here, using its PTAP motif, the C-terminal domain of Gag (p6) recruits host ESCRT machinery which complexes with other cellular factors to constrict the membrane at the neck of the budding virion and sever the immature viral virion from the infected cell^[212]. Finally, precursor autoprocessing liberates PR from the Gag-Pol polyprotein, permitting complete processing of Gag and Gag-Pol into their various viral components, and completing virion maturation as CA forms a capsid around the dimerized, NC-covered (+)ssRNA genome (Figure 1.3H).

D. Disease Progression to AIDS

HIV transmission occurs through exposure to infectious virus at host mucosal surfaces—this can often be in the form of sexual contact or the exchange of bodily fluids like blood, semen, vaginal fluid, or breast milk through damaged tissues or lesions in the skin. Broadly, 70% of HIV-1 infections can be attributed to heterosexual sexual transmission^[213]. While there are many confounding risk factors for exposure and subsequent transmission, the biological markers of infection and disease progression are well characterized and reproducible.

Since macaques display AIDS-like disease progression when infected with SIV, much of our knowledge regarding HIV-1 infections has been aided through animal studies. Following exposure, founder viruses from the originating host^[214] productively infect CD4⁺ cell populations proximal to the mucosal entry site in an event that can be visualized as early as two days post infection^[215]. Within an infected host, viral spread can occur via cell-free or cell-to-cell transmission. Cell-free transmission is the most common *in vivo* infection route (described in Section 1.2C) however, this route exposes infectious particles to harsh host immune defenses. Conversely, cell-to-cell transmission occurs via virological synapses that form between the infected cell and target cell and in an infection process that is completed within roughly 6 hours^[216]. Within two weeks, the virus spreads to draining lymph nodes which disseminate the virus to the lymphoid system and throughout the body, creating a widespread infection in a period termed the eclipse phase (Figure 1.5A). During this phase, reservoirs in lymphatic tissue are established^[217, 218], and an initial interferon response generated by the host immune system.

Around 2-3 weeks post infection, the number of viral RNAs detected in the plasma rapidly increase and the acute phase of viral infection begins (Figure 1.5B). The onset of seroconversion, or the point in time where antigen-specific antibodies against an exogenous biomaterial become available in the blood, prompts the infected individual to experience fevers, swollen lymph nodes, oral ulcers, skin rashes, and flu-like symptoms^[219]. During this time, there is a sharp decrease in CD4⁺ T cell populations^[220] as 10-100 million infected CD4⁺ T cells die per day^[221], each producing about 20 progeny virions during their lifetime^[222]. Since the gut serves as one of the largest replication sites during viral pathogenesis^[223], the GI

tract experiences substantial CD4⁺ T cell depletion which persists throughout all stages of disease progression^[224, 225]. Around six weeks post infection, the adaptive immune system mounts an activated immune response using HIV-specific CD8⁺ cytotoxic T lymphocytes, follicular helper T cells, and B cells, drastically reducing viral levels^[226-228]. Assault of the virus by the immune system promotes the generation of cytotoxic T lymphocyte (CTL) mutant virus that aid in viral escape and the establishment of reservoirs that are impervious to host clearance mechanisms^[229]. CTL mutant viruses often contain numerous mutants in the Env viral protein.

Partial immune control over the virus results in a slight rebound in CD4⁺ T cell numbers and the establishment of the viremia set point ((Figure 1.5, black arrow), or the steady state level of virus going into the clinical latency phase (Figure 1.5C). High set points are often associated with elevated levels of inflammation, viral escape, and poor disease prognosis while lower set points typically coincide with minor inflammation, poorly fit virus, and better disease prognosis—with this, the virus set point during clinical latency is often used as a predictor of HIV progression and disease outcome^[230]. During viral latency, an estimated 1 billion virions are produced per day while host humoral and cellular defenses attempt to control the infection^[231]. Unrelenting evolutionary pressure from the immune system generates more viral CTL escape mutants (reviewed in^[232]), resulting in prolonged immune activation and steady virus production during the latency phase, which can persist for five to ten years depending on genetics and the strength of the individual's immune system^[233]. If adhered to, HAART can drastically suppress viral replication and virtually induce perpetual viral latency—however, viral rebound and the emergence of drug resistant mutants closely follows the discontinuance of treatment, making adherence a must^[234].

Likely due to exhaustion from prolonged immune activation^[235, 236], steadily declining CD4⁺ T cell counts are accompanied by upward creeping viral loads during the latency period. While severe bacterial infections present around <350 CD4⁺ T cells per μL (CD4⁺ cell counts are often obtained through bloodwork), the patient is said to have AIDS once CD4⁺ T cell levels drop beneath 200 cells per μL , according to the CDC^[237] (Figure 1.5D). During this time, it is possible to acquire a variety of opportunistic

infections such as *Pneumocystis* pneumonia, cytomegalovirus, and oesophageal candidiasis that are typically only found in immunosuppressed individuals.

A small group of individuals called elite controllers (ECs) maintain low viral set points and never progress towards AIDS. Rather, they experience a unique immune control over the virus, often displaying undetectable viral loads and no immune cell loss^[238]. The mechanism of viral control by ECs is of great interests to researchers as it could provide insight for therapeutic intervention. ECs have been found to contain an enrichment of a particular antigen (human leukocyte antigen-B*5701 (HLA-B*5701)^[239]) that presents at the surface of CD8⁺ cells and could potentially interact with natural killer cells^[240, 241]. Interestingly, despite harboring a Vpx protein that enables efficient reverse transcription in cells with low dNTP levels, HIV-2 has lower transmission rates and is characterized by a milder pathogenesis and slower disease progression when compared to HIV-1^[242]. In fact, the majority of HIV-2 infections never progress to AIDS^[243]. Researchers are still working to understand the underlying determinants prescribing the dampened pathogenesis of HIV-2.

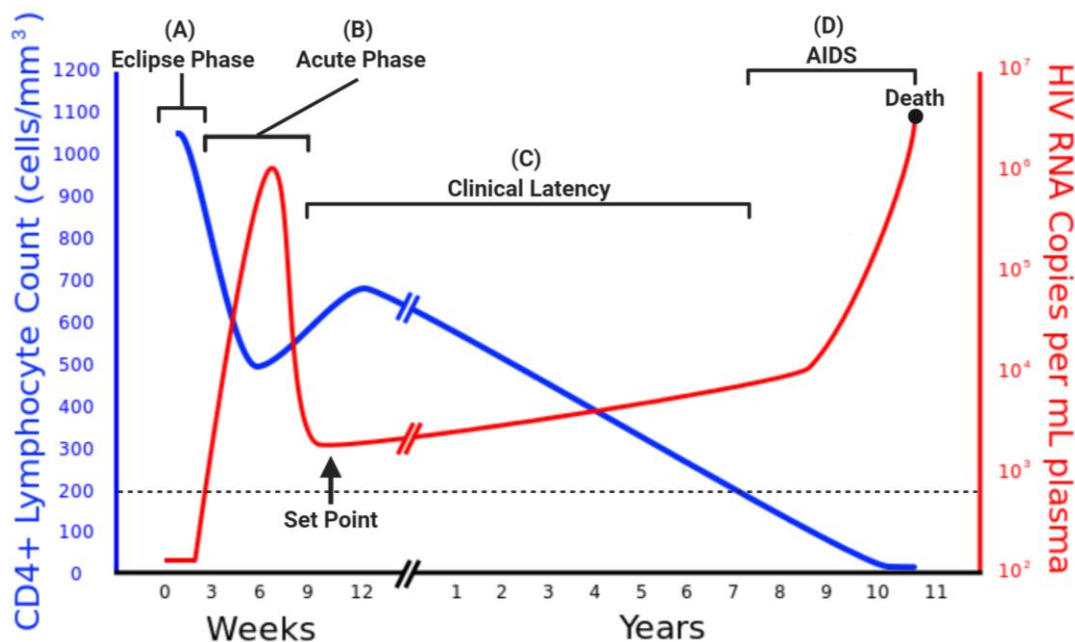


Figure 1.5 AIDS disease progression. (A) After transmission of HIV-1 (red line), a primary infection is established near the mucosal entry site as the eclipse phase begins. For the next few weeks, the virus spreads through cell-free and cell-to-cell transmission routes and quietly seeds viral reservoirs in lymphatic tissue while viral RNA remains undetectable in the blood. (B) As the infection continues to spread throughout the body, viral RNA becomes detectable in the blood stream. This signifies entry into the acute phase where rapid viral replication in CD4⁺ cells has detrimental cytopathic effects that are clinically observable in the form of plummeting CD4⁺ T cells counts (blue line). (C) Finally, 6-9 weeks post infection, the host immune system gains partial control over the virus resulting in decreased viral loads, a slight rebound in CD4⁺ T cell numbers, the establishment of a viremia set point (black arrow), and the entry into clinical latency. The host immune system can suppress viral replication for years; however, fatigue of the immune system is seen as CD4⁺ T cells continue to decline during this time. (D) Drastically reduced immune cell counts expose the immune system to opportunistic infections. Once CD4⁺ T cell counts drop below 200 cells per μL the individual is said to have AIDS. Over time, the weakened immune system becomes overwhelmed by opportunistic infections which ultimately results in death. This figure was modified from an adaptation by Sigve that was created under a CC0 1.0 license. The original copyrighted material was reproduced with permission from (Pantaleo et al., 1993^[244]), Copyright Massachusetts Medical Society.

E. HIV/SIV Target Cells

HIV/SIV lentiviral receptor CD4 is expressed at the cell surface of a variety of human cells (e.g. thymocytes, mature T lymphocytes, monocytes, macrophages, neurons, microglia, and immature dendritic cells (DCs))^[245] and tissues (e.g. brain, spleen, appendix, lymph nodes, liver, lungs, and gut)^[246], however, expression can be highly variable. For example, while the density of CD4 expression on the surface of monocyte derived macrophages (MDMs) is 20-fold lower than that of its parental monocyte, MDMs and CD4⁺ T cells have similar numbers of CD4 molecules at their cell surfaces, even though T cells have a significantly smaller surface area^[247]. In the body, CD4 receptors recognize peptide antigens presented by major histocompatibility complex II (MHC-II) molecules and subsequently initiate signaling cascades required for the proper targeting of cells containing exogenous biological material^[248]. While CD4 is required for HIV/SIV viral entry^[249] and is commonly associated with its expression in the immune system and brain^[250], viral Env amino acid sequences together with coreceptor expression and use ultimately dictate viral tropism.

i. Viral Tropism

Upon binding to CD4, Env undergoes a conformational change that exposes two regions called the V3 loop and the bridging sheet that can selectively interact with either CCR5 (R5) or CXCR4 (X4) to facilitate coreceptor binding. In vitro experiments have resulted in the identification of over 14 7TM receptors (including CCR1, CCR2b, CCR3, and CCR5) that can serve as potential coreceptors for HIV/SIV^[251]. While the identified receptors are members, or distant relatives, of the chemokine receptor family, CCR5 and CXCR4 are recognized as the primary coreceptors in HIV/SIV infections. Like CD4, coreceptor expression is highly cell-specific: memory CD4⁺ T cells primarily express large levels of CCR5 while naïve CD4⁺ T cells harbor no CCR5 on their cell surface, only CXCR4^[252]. Interestingly, macrophage coreceptor expression is dependent upon cytokine secretions as these monocytic cells display upregulation of CXCR4 when stimulated with macrophage colony stimulating factor (M-CSF) and an upregulation of CCR5 when treated with granulocyte macrophage colony-stimulating factor (GM-CSF)^[253].

Studies observing the genetic diversity of *env* within single host infections have found that productive clinical infections often result from successful infection by 1-5 founder virions that often have a preference for CCR5⁺ cells^[254]. Initial investigations noticed that HIV favors CCR5-mediated entry during the early stages of infections and evolves to utilize the CXCR4 coreceptor during the course of infection^[255, 256]. Researchers observed differential viral pathogenesis and believed CCR5 coreceptor entry was associated with non-syncytium inducing (NSI) infection of macrophages—a target cell type that supported slow viral replication—while CXCR4 usage was thought to permit rapid viral replication in T cells, resulting in a syncytium inducing (SI) phenotype^[257]. Differences in coreceptor usage and their perceived correlation with cell permissivity (i.e. which target cells supported productive infection by the viral variants) spurred the development of new nomenclature: viruses that used CCR5 for macrophage-specific cell entry were called M-tropic viruses and those which used CXCR4 coreceptors were termed T-tropic viruses^[258].

Our understanding of viral tropism has since evolved to recognize that there are, in fact, three viral tropisms during HIV infection: (i) R5 M-tropic variants capable of entering macrophages and possibly other cells expressing low levels of CD4, (ii) R5 T-tropic variants that have adapted to enter memory CD4⁺ T cells, and (iii) X4 T-tropic viruses that are capable of gaining entry into naïve CD4⁺ T cells. Since MDMs are highly variable in their HIV-1 infectivity^[259] and are hardly identified outside of the central nervous system (reviewed in^[260]), founder viruses are assumed to be R5 T-tropic variants that replicate in memory CD4⁺ T cells and grow to represent the majority of blood-derived HIV-1 virions found in productive infections^[261]. However, viral tropism is highly clade dependent within the M group of HIV-1 viruses: for example, clade A viruses remain R5 even in the late stages of infection, clade B viruses hardly transition to X4 tropism during pathogenesis, and clade C viruses utilize dual tropism throughout pathogenesis (reviewed in^[50]).

Recent studies aim to elucidate the role of Env V3 and bridging sheet sequences in the determination of HIV-1 coreceptor use and cellular tropism^[262]. Additionally, many groups are working to locate and characterize the cellular populations involved in viral latency and reservoir establishment

(reviewed in^[263]). While much is still unknown, it is thought that M-tropic and R5 T-tropic viral variants seed these reservoirs during the early stages of viral infection, thus creating monocytic and resting memory CD4⁺ T cell populations^[264-266] that can potentially be therapeutically activated and targeted to reverse viral latency^[267, 268].

ii. Intracellular dNTP Pools and SAMHD1

In addition to the variable surface expression of CD4 and its CCR5/CXCR4 coreceptors, the intracellular dNTP environment is another factor that contributes to HIV/SIV cellular permissivity. Steady state intracellular dNTP pools are carefully maintained by various cellular enzymes that either synthesize or degrade dNTP molecules. The protein expression and enzymatic activity of cellular dNTP biosynthesis machinery, which includes enzymes such as thymidine kinase (TK)^[269, 270] and ribonucleotide reductase (RNR)^[271-273], are highly dependent upon the cell cycle: upregulation of these two proteins is observed in late G1 in preparation for DNA replication in S phase^[274, 275]. Conversely, SAMHD1 (reviewed in^[126])—a negative regulator of intracellular dNTP pools that catalyzes water-mediated cleavage of dNTP molecules^[276, 277]—maintains consistent protein expression throughout the cell cycle. Instead, the dNTPase activity of SAMHD1 is thought to be controlled through phosphorylation of its T592 residue (pSAMHD1) by the cyclin A2/CDK complex during S phase^[278] and subsequent dephosphorylation by PP2A with a B55alpha subunit (PP2A-55α)^[279] during mitotic exit. While many groups have found that phosphorylation of T592 destabilizes the active SAMHD1 tetramer and results in the loss of dNTPase activity^[280, 281], conflicting reports illustrate that pSAMHD1 and phosphomimetic mutants T592D and T592E display dNTPase activity that is comparable to wildtype SAMHD1^[282, 283].

The dual mechanism involved in steady state intracellular dNTP pool maintenance—the balance of dNTP synthesis and degradation—is responsible for creating the divergent intracellular environments found in nondividing and dividing HIV/SIV target cells. As discussed above, cellular biosynthesis machinery is regulated with respect to the cell cycle, as they provide dNTP substrates for use by cellular polymerases responsible for DNA replication during S phase. Since nondividing cells, like macrophages, do not undergo cell division or participate in active DNA replication, they have no necessity to support dNTP biosynthesis.

Similarly, while SAMHD1 protein expression is not regulated by the cell cycle, its relative expression levels can drastically vary depending on cell type. SAMHD1 expression is elevated in nondividing macrophages, DCs, and resting CD4⁺ T cells; this is in stark contrast to the relatively low SAMHD1 expression seen in activated/dividing CD4⁺ T cells^[284, 285], which can be attributed to *samhd1* promoter methylation^[286] and impaired mRNA translation by miR-181^[287, 288] in this target cell type. As a result, dNTP concentrations in nondividing MDMs (20-40 nM) are 100-250 fold lower than those found in activated CD4⁺ T cells (2-5 μ M)^[289].

The low dNTP pools found in macrophages and resting CD4⁺ T cells, which results from diminished dNTP biosynthesis and the dNTPase activity of SAMHD1, have been shown to restrict HIV-1 replication^[128, 290]. This viral restriction is alleviated in HIV-2 and some SIV infections by the deployment of SAMHD1-counteracting Vpr or Vpx proteins^[22, 291]. In a process that is independent of viral uncoating^[292], Vpx and some Vpr accessory proteins recruit DCAF1 to facilitate the formation of the Vpr/Vpx-DCAF1-CRL4-E3 ubiquitin ligase complex which can target host dNTPase SAMHD1 for proteasomal degradation. Viral counteraction of SAMHD1 results in a transient 10-fold increase in macrophage and resting CD4⁺ T cell dNTP concentrations^[293-295], elevating intracellular dNTPs above the substrate concentration needed to obtain half maximal activity (K_m) of HIV-1 RT^[128] and promoting complete proviral DNA synthesis in these otherwise restrictive cell types. Interestingly, in addition to the dNTPase-dependent depletion of nondividing HIV/SIV target cell dNTP pools, many studies have suggested that SAMHD1 possesses antiviral activity that is independent of its dNTPase activity and is regulated by phosphorylation of T592^[296, 297]. The direct interaction of Vpr/Vpx and antiviral restriction factor SAMHD1 in the pro-degradation complex has resulted in their co-evolution as they engage in a host-virus evolutionary arms race^[137, 298, 299]—Vpr/Vpx adapting to better target the dNTPase for proteasomal degradation to support permissive infection in restricted cell types, and SAMHD1 adapting to evade viral counteraction while striving to maintain the enzymatic functions required for proper intracellular dNTP regulation.

1.3 Reverse Transcriptase

We have recently surpassed the 50 year mark since the discovery of reverse transcriptase by Dr. David Baltimore at Massachusetts Institute of Technology^[300] and Drs. Howard Temin and Satoshi Mizutani at the University of Wisconsin^[301] in June 1970. The protein was identified from rous sarcoma virus (RSV) virions and was unique since it functioned opposite of the central dogma (i.e. DNA → RNA → Protein) as it converts RNA into DNA. Here, we will discuss the structure and function of the HIV/SIV reverse transcriptase protein (Figure 1.6).

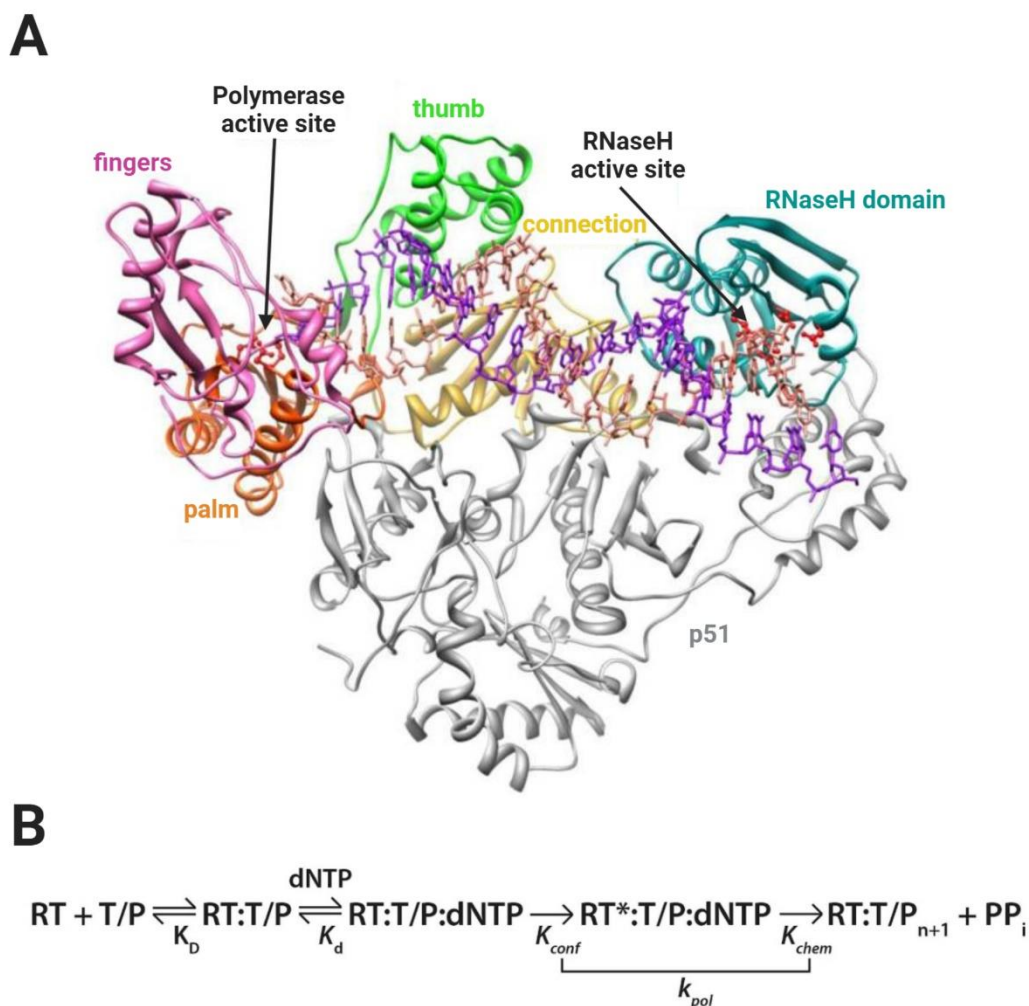


Figure 1.6 HIV-1 reverse transcriptase structure and reaction pathway. (A) The crystal structure of heterodimeric HIV-1 RT bound with nucleic acid is shown (PBD: 1RTD). The p66 subunit contains the polymerase and RNaseH active sites while p51 (grey) serves a structural role during polymerization. The p66 subunit can be further divided into the fingers (pink), palm (orange), thumb (green), connection (yellow), and RNaseH (cyan) subdomains. This figure was adapted from original art licensed under a [CC BY 3.0](#) created by Ilina et al.^[200]. (B) As a DNA polymerase, RT adheres to the well-known DNA polymerase reaction pathway. Reverse transcription begins by RT binding to a template-primer (T/P) to form the binary complex, a steady state event characterized by K_D . A dNTP molecule can then bind to the polymerase active site to form the ternary complex in a reversible association characterized by K_d . Upon formation of the ternary complex, RT undergoes a conformational change ($\text{RT} \rightarrow \text{RT}^* = K_{conf}$) and catalyzes

the formation of a phosphodiester bond between the incoming nucleotide and the 3'-OH of the primer (K_{chem}). The sum of K_{conf} and K_{chem} yield pre-steady state k_{pol} . A pyrophosphate (PP_i) byproduct is produced during the incorporation reaction and is released in the final step of the DNA polymerase reaction pathway.

A. Structural Features and Drug-Induced Viral Mutagenesis

HIV-1 reverse transcriptase is processed from the Gag-Pol polyprotein through sequential cleavage reactions that are performed by the viral protease. The cleavage process first results in p66 monomers which dimerize to form p66/p66 homodimers^[302]. PR then executes a final proteolytic cleavage that excises the C-terminal RNaseH domain from one p66 subunit, consequently generating a p15 fragment and p66/p51 heterodimeric RT, the viral DNA polymerase of HIV which assumes a right-handed polymerase structure (Figure 1.6A). The larger of the two subunits (p66 in HIV-1/SIV, p68 in HIV-2) contain the polymerase and RNaseH active sites while the smaller subunit (p51 in HIV-1/SIV, p54 in HIV-2) is catalytically inactive and plays a structural role during polymerization. Structure certainly confers function in the p66 subunit as the two enzymatic functions of RT are separated into two spatially distinct domains: the polymerase domain and RNaseH domains. The polymerase domain can be further divided into the fingers (residues 1-85, 118-155), palm (residues 86-117, 156-236), thumb (residues 237-318), and connection (residues 319-426) subdomains^[303, 304]. While p51 contains the same polymerase subdomains as p66, their relative spatial locations are different in this truncated subunit.

During polymerization, the p66 thumb subdomain orients the template-primer (T/P) such that the 3'-OH functional group of the primer sits within in the priming site (P) of the polymerase active site. This requires crucial interactions between both the template and primer strands as well as a β 12- β 13 hairpin structure within the thumb domain called the “primer grip”^[305, 306]. Once positioned correctly within the nucleic acid binding cleft—composed of all p66 subdomains and the p51 thumb and connection subdomains—the bound T/P interacts with both the polymerase and RNaseH active sites, which are separated by 17-18 base pairs. The polymerase active site contains three catalytic aspartic acid residues from the β 9- β 10 loop within the palm subdomain of p66 (D110, D185, D186), which orchestrate two Mg^{2+} ions within the active site^[307]. Residues D185 and D186 belong to the canonical YXDD motif that is conserved across the *Retroviridae* family in which X is methionine in HIV-1 RT and valine, alanine, or leucine in other viral RTs^[308]. Similarly, metal ions (likely Mg^{2+}) are oriented by conserved residues D442, E478, D498 and D549 within the RNaseH active site. Once the RT primer grip (p66 thumb) correctly orients

the T/P, forming the binary complex, a dNTP molecule is able to bind within the nucleotide binding site (N) to form the ternary complex. This binding event requires residues R72 and K65 which facilitate binding of the β - and γ -phosphates respectively in the incoming nucleotide^[309]. While residues Q151 and Y115 differentially interact with the 3'-OH group of the nucleotide bound to the N site, Y115 prevents the incorporation of 2'-OH containing nucleotides thereby effectively acting as a steric gate that deciphers between deoxy- and ribonucleotide substrates^[310, 311]. Once the ternary complex is formed, RT undergoes a conformational change in which the p66 finger subdomain closes down over the dNTP in the N site, aligning the α -phosphate of the nucleotide substrate with the 3'-OH of the P site primer and the polymerase active site^[312, 313] (i.e. "closed" RT conformation). RT then catalyzes a quick chemical reaction, in which a phosphodiester bond is formed between the 3'-OH of the primer and the incoming nucleotide, resulting in the formation of a pyrophosphate byproduct. Following nucleotide incorporation, the p66 fingers open to allow release of the pyrophosphate (i.e. "open" conformation) and, during processive polymerization, the nucleic acid translocates to free the N site for binding by the next dNTP substrate.

Since RT is a DNA- and RNA-dependent DNA polymerase, HIV-1 research is rich with studies that have characterized its differential activities when bound to RNA/DNA heteroduplex and DNA/DNA homoduplex nucleic acids. Interestingly, not only is the distance between polymerase and RNaseH active sites different between the two T/Ps (17 nucleotides for homoduplex and 18 nucleotides for heteroduplex), but RT also binds RNA/DNA with a lower off-rate constant (k_{off}) than DNA/DNA^[191, 314, 315]. Pre-steady state kinetic analysis revealed that while dNTP binding is enhanced when using a DNA template ($K_{d(DNA)}=4\mu\text{M}$; $K_{d(RNA)}=14\mu\text{M}$), the rate of dNTP incorporation (k_{pol}) increases two-fold when polymerizing from an RNA template^[313]. Finally, steady state reactions reveal that the concentration of substrate required to reach half maximal RT polymerization activity (K_m) is 3-21 fold lower when using an RNA template, resulting in an elevated catalytic efficiency during polymerization from a heteroduplex template^[316, 317]. Additionally, while p66/p51 and p66/p66 bind homoduplex DNA with the same affinity^[318], RT heterodimers are more stable and slightly more efficient at incorporating dNTPs during DNA synthesis, potentially providing

reason for why evolution has preserved further processing of the p66 homodimer despite there currently being no known functions for the p15 cleavage product^[319-321].

Because RT is essential to viral replication, it has been a key target for antiviral drug development. Anti-RT drugs come in two varieties: nucleoside RT inhibitors (NRTIs) and non-nucleoside RT inhibitors (NNRTIs). As nucleoside analogs, NRTIs, which typically lack 3'-OH groups, are incorporated into the nascent DNA and function as chain terminators. Their incorporation oftentimes leads to the formation of “dead end complexes” or ternary complexes trapped in the “closed” conformation with the NRTI stably bound to the translocated primer (P site). Conversely, NNRTIs bind a hydrophobic pocket that is adjacent to the p66 polymerase active site called the NNIBP (residues L100, K101, K103, V106, T107, V108, V179, Y181, Y188, V189, G190, F227, W229, L234, and Y318 of p66 and E138 of p51). This binding event locks the polymerase in a conformation where the p66 thumb and finger subdomains are hyperextended, leaving RT unable to perform the chemical catalysis necessary for dNTP substrate incorporation. There is no additional NNIBP on the p51 subunit and, interestingly, this hydrophobic pocket does not exist in the absence of NNRTIs .

While some compounds have been discontinued, there are currently five FDA approved NRTIs (zidovudine-AZT, abacavir-ABC, emtricitabine-FTC, lamivudine-3TC, and tenofovir DF-TDF) and five NNRTIs (doravirin-DOR, efavirenz-EFV, etravirine-ETR, nevirapine-NVP, and rilpivirine-RPV)^[322]. Unfortunately, due to its high mutation rate, HIV-1 can generate and select for drug-resistant RT variants throughout the course of pathogenesis. NRTI-resistance mutations generally function via one of two mechanisms: excision of the drug following incorporation (e.g. combinations of M41L, D67N, K70R, L210W, K219E/Q, and most importantly T215F/Y mutations are known to reduce AZT efficacy by facilitating ATP-mediated drug excision^[323]) or exclusion of the drug from the polymerase active site (e.g. M184V/I mutations reduce incorporation of FTC and 3TC through steric hindrance^[324]). Since NNRTIs bind the NNIBP, most NNRTI-resistance mutations are found near this region (reviewed in^[100]). Due to the generation of drug-resistant RT variants, which can be integrated in transmissible virions, these antivirals are often taken in combination with one another (i.e. 3TC+AZT= combivir ; EFV+FTC+TDF= symfi ;

ABC+3TC= epzicom ; ABC+3TC+AZT= trizivir) or in conjunction with drugs targeting other viral proteins (i.e. protease, integrase, fusion, and entry inhibitors)^[322].

B. DNA Polymerase Reaction Pathway and Kinetics

As a DNA polymerase, reverse transcriptase follows the typical DNA polymerase reaction pathway (reviewed in^[325]) (Figure 1.6B) in which the enzyme first binds to a template-primer (T/P) to form the binary complex (K_D). Binding of a dNTP substrate to this binary complex (i.e. pre-steady state K_d) yields the ternary complex. Formation of the ternary complex induces an RT finger-closing conformational change ($RT \rightarrow RT^*$) to correctly orient the incoming dNTP for incorporation, in an event that is characterized by pre-steady state kinetic parameter K_{conf} . Once the dNTP is positioned correctly, RT catalyzes a quick chemical reaction that results in the formation of a phosphodiester bond between the T/P and incoming dNTP. This sub-step is characterized by pre-steady state K_{chem} . The sum of the conformational change (K_{conf}) and the chemistry step (K_{chem}) is represented by the kinetic factor k_{pol} . The last step of the pathway is the release of pyrophosphate following nucleotide incorporation and, ultimately, the release of the template-primer containing the newly incorporated nucleotides (T/P_{+1}). Release of T/P_{+1} is the rate-limiting step in steady state polymerase reactions.

Steady state reactions observe product formation in the presence of equimolar enzyme and enzyme-substrate complexes. Often used for multiple-nucleotide incorporation studies, but applicable for single-nucleotide incorporation experiments, steady state conditions characterize the maximum enzyme activity and yield kinetic parameters K_m , V_{max} , and k_{cat} . K_m describes the concentration of dNTP substrate required for the enzyme to function at half its maximum product formation velocity (V_{max}), while k_{cat} (i.e. catalytic turnover rate) represents the rate that each enzyme active site turns substrate (dNTPs) into product (T/P_{+1}). Since steady state polymerization follows Michaelis-Menten enzyme kinetics, V_{max} can be converted to k_{cat} if divided by the concentration of total enzyme in the reaction ($[E]_0$). The efficiency of steady state enzyme activity can be found through determination of its catalytic efficiency (k_{cat}/K_m). While steady state studies provide an overview of enzyme activity, pre-steady state studies enable delineation of mechanism.

Pre-steady state reactions observe the formation and consumption of enzyme-substrate intermediates. To isolate dNTP incorporation kinetics from the rate-limiting steady state T/P binding and dissociation kinetics (i.e. k_{on} and k_{off} of T/P binding to RT at the beginning of the DNA reaction pathway), pre-steady state reactions are conducted with RT pre-bound to radiolabeled T/P and are quenched prior to (i) T/P dissociation from the RT:T/P₊₁ complex and (ii) subsequent formation of new binary complexes. Since these reactions permit only a single round of polymerization, they are conducted for short durations of time ranging from 0.001-3 seconds depending on the enzyme in question. Pre-steady state studies yield kinetic parameters K_d (the equilibrium dissociation constant for the dNTP substrate) and k_{pol} (the maximum rate of dNTP incorporation). Similar to the steady state catalytic efficiency value, the incorporation efficiency communicates the efficiency of T/P₊₁ generation. Various studies have characterized the pre-steady state kinetics of numerous polymerases including the Klenow Fragment (KF) of *E. coli* DNA polymerase I^[326], the T7 DNA polymerase^[327, 328], many human DNA polymerases^[329-331], and a variety of viral DNA polymerases^[312, 313, 332-334].

C. Differences Between RTs from SAMHD1 Counteracting and Non-Counteracting Lentiviruses

Over the years, our lab has done extensive studies on retroviral polymerases and the many factors that govern their enzymatic activity and polymerization fidelity. While lentiviruses, like HIV and SIV, replicate in both dividing and nondividing target cell types, other non-lentiviral retroviruses, such as gammaretroviral feline leukemia virus (FeLV) and murine leukemia virus (MuLV), exclusively replicate in dividing cells^[335-337]. Our lab found that MuLV RT has a dNTP binding affinity (K_d) that is 3.8-fold lower than that of HIV-1 RT^[338], suggesting that replication within the bountiful dNTP environments of dividing cells easily results in productive MuLV infection while the low dNTP pools of nondividing cells pose more of a challenge. This finding suggested that viral polymerase properties could potentially join (co)receptor expression and intracellular dNTPs on the list of cellular permissivity determinants.

Since there are kinetic differences between the RTs originating from lentiviral- and non-lentiviral retroviruses, our lab sought to determine whether there were kinetic difference between RTs originating from lentiviruses with and without the ability to counteract host restriction factor SAMHD1 (SAMHD1

counteracting and SAMHD1 non-counteracting lentiviruses respectively). To do this, we must first consider the dynamics of nondividing target cell infections by SAMHD1 counteracting viruses, like HIV-2 and some SIVs, compared to that of SAMHD1 non-counteracting viruses, like HIV-1 (Figure 1.7). When HIV-1 infects a macrophage, the SAMHD1-depleted intracellular dNTP pools slow reverse transcription and restrict HIV-1 infection in this cell type. Conversely, HIV-2 and some SIVs use viral Vpr or Vpx proteins to induce the proteasomal degradation of SAMHD1, increase intracellular dNTP pools, complete proviral DNA synthesis, and result in the permissive infection of nondividing macrophages. Since SAMHD1 non-counteracting lentiviruses are left to replicate within the low dNTP pools of the macrophage, our lab kinetically assessed RTs from various SAMHD1 counteracting and non-counteracting lentiviral strains to investigate whether differences in cellular dNTP availability has (i) served as a selective pressure that drives RT evolution in SAMHD1 non-counteracting lentiviruses and (ii) influenced the kinetic properties of HIV/SIV RT.

Interestingly, while SAMHD1 counteracting and non-counteracting lentiviral RTs displayed similar k_{cat} and K_d values, SAMHD1 non-counteracting RTs were characterized by lower steady state K_m values and faster rates of incorporation (k_{pol}) when compared to SAMHD1 counteracting lentiviral RTs^[339, 340]. This demonstrates that, in order to overcome SAMHD1 restriction in nondividing target cells, SAMHD1 non-counteracting viruses, like HIV-1, evolved over time to harbor RT proteins that could efficiently synthesize DNA in the low dNTP concentrations found macrophages. Conversely, since SAMHD1 counteracting viruses, like HIV-2 and SIVmac239, utilize their Vpr or Vpx proteins to induce proteasomal degradation of SAMHD1—increasing intracellular dNTP concentrations above the K_m of their viral RT, in otherwise restrictive host cellular environments—there is no pressure exerted on the viruses to promote evolution of their RT proteins. The unique interplay between host dNTPase SAMHD1, viral Vpr/Vpx, and intracellular dNTP concentrations ultimately drives lentiviral RT evolution, resulting in kinetic differences between RTs originating from SAMHD1 counteracting and non-counteracting lentiviruses.

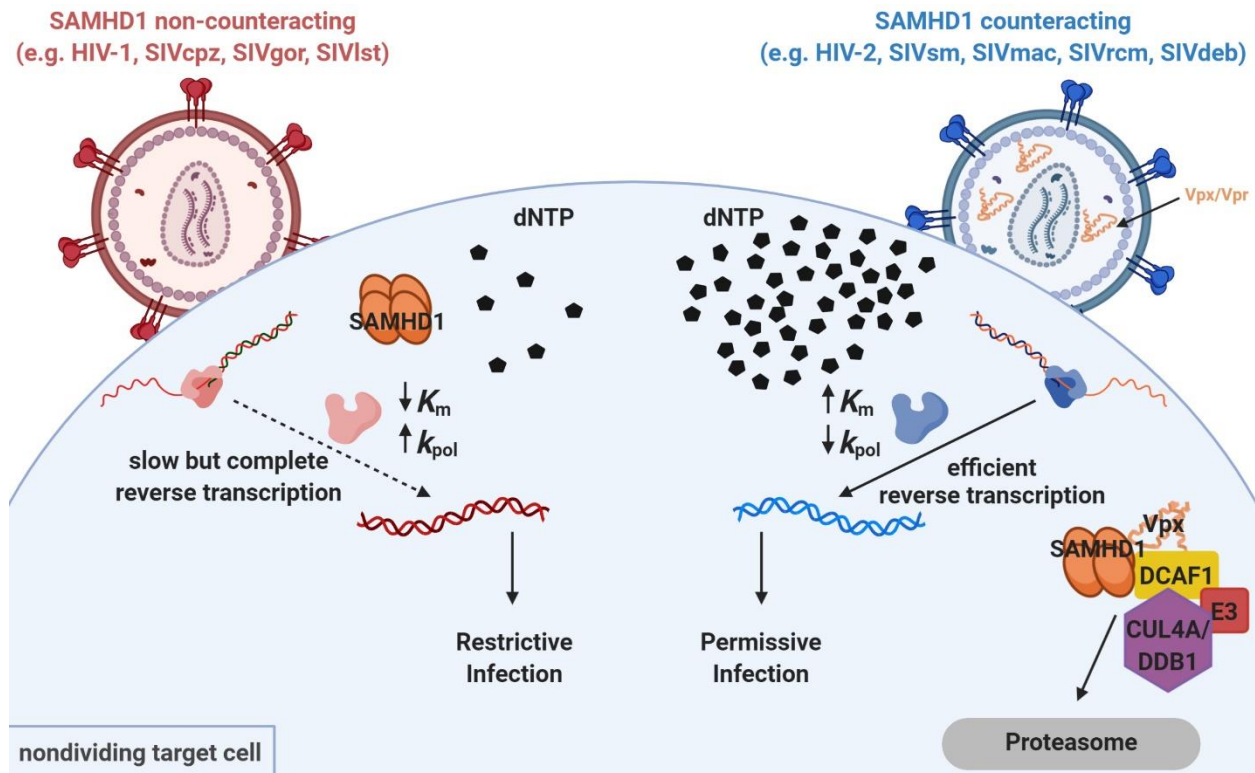


Figure 1.7 Implications of SAMHD1 restriction on HIV/SIV infection in nondividing cells and evolution of reverse transcriptase. Host dNTPase SAMHD1 degrades intracellular dNTPs in nondividing cells, resulting in slow but complete reverse transcription and a restrictive infection in nondividing target cell types (left). Conversely, viral Vpx/Vpr in SAMHD1 counteracting lentiviruses targets SAMHD1 for proteasomal degradation via the DCAF1:CRL4 complex. This increases cellular dNTP pools and promotes efficient reverse transcription in an otherwise restrictive cell type (right). RTs from SAMHD non-counteracting lentiviruses are characterized by lower K_m values and faster k_{pol} values. This figure was created with BioRender.com and adapted from original work published by St Gelais et al.^[341] under a [CC BY](#) license.

1.4 Dissertation Direction

Since virus-induced SAMHD1 counteraction appears to be correlated with lentiviral RT kinetics, this dissertation seeks to understand how SAMHD1 non-counteracting lentiviral RTs execute faster DNA polymerization (Chapter 2) and whether RT enzyme kinetics are evolutionarily enhanced in the absence of Vpx during *in vivo* SIVmac239 infections (Chapter 3). Ultimately, we conclude that SAMHD1 non-counteracting lentiviral RTs execute a faster finger-closing conformational change during dNTP incorporation, resulting in faster k_{pol} values when compared to SAMHD1 counteracting lentiviral RTs. Additionally, we observe that RTs from SIVmac239 infections devoid of Vpx (i.e. Vpx (-) virus) undergo enzymatic enhancement, displaying faster steady state and pre-steady state kinetics when compared to RTs from WT SIVmac239 infections. While Vpx (-) RTs display faster kinetics, these enzymatic improvements are not enough to overcome the SAMHD1-mediated low dNTP pools of nondividing macrophages, as both *in vitro* and *in vivo* experiments show that Vpx (-) virus is unable to infect this target cell type.

Chapter 2

Efficient Pre-catalytic Conformational Change of Reverse Transcriptases from SAMHD1 Non-counteracting Primate Lentiviruses During dNTP Incorporation

This research was originally published in *Virology*

[Efficient pre-catalytic conformational change of reverse transcriptases from SAMHD1 non-counteracting primate lentiviruses during dNTP incorporation](#)

Coggins SA, Holler JM, Kimata JT, Kim DH, Schinazi RF, and Kim B

Virology. 2019. Nov;537:36-44

Copyright © Elsevier

Si'Ana Coggins purified the enzymes, performed the kinetic experiments, analyzed the data, and wrote
and edited the paper

Jessica Holler performed the SAMHD1 degradation assays

Jason Kimata, Dong-Hyun Kim, and Raymond Schinazi conceived the experiments

Baek Kim conceived and designed the experiments and wrote the paper

Abstract

Unlike HIV-1, HIV-2 and some SIV strains replicate at high dNTP concentrations even in macrophages due to their accessory proteins, Vpx or Vpr, that target SAMHD1 dNTPase for proteasomal degradation. We previously reported that HIV-1 reverse transcriptase (RT) efficiently synthesizes DNA even at low dNTP concentrations because HIV-1 RT displays faster pre-steady state k_{pol} values than SAMHD1 counteracting lentiviral RTs. Here, since the k_{pol} step consists of two sequential sub-steps post dNTP binding, conformational change and chemistry, we investigated which of the two sub-steps RTs from SAMHD1 non-counteracting viruses accelerate in order to complete reverse transcription in the limited dNTP pools found in macrophages. Our study demonstrates that RTs of SAMHD1 non-counteracting lentiviruses have a faster conformational change rate during dNTP incorporation, supporting that these lentiviruses may have evolved to harbor RTs that can efficiently execute the conformational change step in order to circumvent SAMHD1 restriction and dNTP depletion in macrophages.

Introduction

During the course of its pathogenesis, HIV-1 infects both activated/dividing CD4⁺ T cells and terminally differentiated/nondividing myeloid cells such as macrophages and microglia^[1-4]. While activated CD4⁺ T cells support robust HIV-1 replication kinetics and undergo rapid cell death upon infection, HIV-1 replication kinetics in macrophages is greatly suppressed. HIV-1 infected myeloid cells display long cell survival, leading to the persistent production of low levels of HIV-1, particularly in the brain^[5, 6]. A series of recent studies revealed that the observed suppressed HIV-1 replication kinetics in myeloid cells is due to host SAM domain and HD domain containing protein 1 (SAMHD1) which is a dNTP triphosphohydrolase (dNTPase) that depletes the dNTP substrates of reverse transcriptases (RT) in macrophages^[7, 8]. However, some SIV strains replicate rapidly even in macrophages. The fast replication capability of these SIV strains is due to their accessory protein, viral protein X (Vpx)^[9, 10], which is a gene duplication product of another viral accessory protein, viral protein R (Vpr)^[11, 12]. Lentiviral Vpx directly binds to host SAMHD1 protein and induces the E3-ligase mediated proteasomal degradation of SAMHD1^[9, 13, 14]. Less abundant SAMHD1 leads to the elevation of cellular dNTP concentrations in macrophages and the acceleration of reverse transcription during the viral replication cycle^[15]. Several studies demonstrated that this SAMHD1 degradation capability already existed among SIV strains that encode Vpr, but not Vpx, such as the SIVagm strains^[16]. These SIV strains use their Vpr proteins to counteract their host SAMHD1 via the same proteasomal degradation pathway hijacked by Vpx^[17, 18]. Importantly, while SAMHD1 sequence variations are observed among the many primate host species, Vpr/Vpx species specificity also recognizes host-specific SAMHD1 sequences for the proteasomal degradation^[19, 20].

Due to the presence of host SAMHD1, SAMHD1 non-counteracting lentiviruses such as HIV-1 replicate in limited dNTP pools during the infection of macrophages; conversely, SAMHD1 counteracting lentiviruses such as SIVmac239 replicate under abundant dNTP conditions even in macrophages. We previously observed that SAMHD1 non-counteracting lentiviral RTs can efficiently synthesize DNA even at the low dNTP concentrations found in macrophages. This suggests that the efficient DNA synthesis capability of SAMHD1 non-counteracting lentiviral RTs enables these lentiviruses to overcome SAMHD1-

mediated viral restriction^[21]. The slower replication kinetics of HIV-1 compared to those of SAMHD1 counteracting strains such as HIV-2 and some SIVs, reveal that the potential RT-mediated mechanism to overcome low dNTP concentrations in macrophages is much less effective than Vpx/Vpr-mediated SAMHD1 degradation. However, this RT-mediated mechanism may enable HIV-1 to complete its reverse transcription step even in macrophages with limited dNTP pools. Pre-steady state kinetic analysis using a rapid quench instrument^[22, 23] can simultaneously measure K_d (dNTP binding affinity) and k_{pol} ($K_{conf} + K_{chem}$), lending insight into the molecular activities and mechanisms of various enzymes. Employing the use of pre-steady state kinetic analyses, we previously reported that while SAMHD1 non-counteracting lentiviral RTs display faster rates of incorporation (k_{pol}) when compared to SAMHD1 counteracting lentiviral RTs, these polymerases share similar K_d values^[23]. This suggests that the faster k_{pol} values of the SAMHD1 non-counteracting lentiviral RTs allow these viruses to complete proviral DNA synthesis even at the low dNTP concentrations found in macrophages.

In this study, we investigated the pre-steady state kinetics and elemental effect of RTs from various SAMHD1 counteracting and non-counteracting primate lentivirus strains in order to understand the differential relationship between RT kinetics and host SAMHD1 proteins among these lentiviruses. It was demonstrated with many DNA polymerases^[24-27], including HIV-1 RT^[28], that (i) the K_{conf} step is the slowest/rate-limiting step during the pre-steady state dNTP incorporation reaction and (ii) the K_{chem} step is very rapid, indicating that the k_{pol} value is predominantly represented by the K_{conf} step ($k_{pol} \approx K_{conf}$). This conclusion was experimentally made by the absence of the phosphorothioate elemental effect when using dNTP α S substrates which contain sulfur instead of oxygen at the α -phosphate position of dNTP. During the incorporation of dNTP α S, the sulfur atom present on the alpha-phosphate of the substrate slows only the chemistry step (K_{chem}), a phenomenon defined as an elemental effect.

In this study, we determined the elemental effect of RTs from SAMHD1 non-counteracting SIV strains, SIVcpz and SIVgor, and RTs from SAMHD1 counteracting SIV strains, SIVagm 9063-2 and SIVmne CL8. Overall, our kinetic analysis explains how the RTs of the SAMHD1 non-counteracting lentiviruses mechanistically gained faster k_{pol} rates and how these lentiviruses became capable of circumventing

SAMHD1-mediated restriction in order to complete proviral DNA synthesis even at the extremely low cellular dNTP concentrations found in nondividing macrophages.

Experimental Procedures

Cells, plasmids and chemicals: The following full-length clones of various HIV-1 and SIV strains were obtained through the AIDS Reagent Program, Division of AIDS, NIAID, National Institutes of Health: HIV-1 94UG114.1 Non-infectious Molecular Clone from Drs. Beatrice Hahn and Feng Gao, and the UNAIDS Network for HIV Isolation and Characterization (cat# 4001)^[29]; HIV-1 94CY017.41 Non-infectious Molecular Clone from Drs. Stanley A. Trask, Feng Gao, Beatrice H. Hahn, and the Aaron Diamond AIDS Research Center (cat# 6175)^[30]; pSIV_{gor}CP2139 from Drs. Jun Takehisa, Matthias H. Kraus, and Beatrice H. Hahn (cat#11722)^[31]; SIV_{CPZ}TAN2.69 from Drs. Jun Takehisa, Matthias H. Kraus and Beatrice H. Hahn (Cat #11497)^[32]. A full-length molecular clone of SIVmne CL8 was previously constructed^[33], while a full-length molecular clone of SIVagm 9063-2 was kindly provided by V. Hirsh^[34] (National Institutes of Health, Bethesda, MD). The aforementioned molecular clones were used to clone the flag tagged Vpr genes of HIV-1 Ug and HIV-1 Cy into pCDNA3.1/hygro (+) (*HindIII* and *XhoI*, ThermoFisher) while the flag tagged Vpr genes of SIVgor, SIVcpz, and SIVagm 9063-2 were synthesized into pcDNA3.1/Hygro (+) by GenScript (Piscataway, NJ). Full length molecular clones were also used to clone the RT genes of HIV-1 Cy^[21], HIV-1 Ug^[21], SIVagm 9063-2^[35], SIVgor, SIVcpz 2.69 into pET28a (*NdeI* and *XhoI* sites, Novagen) and SIVmneCL8 RT into pHis (*NdeI* and *EcoRI*). The following SAMHD1 proteins were synthesized into pLVX-IRES- mCherry with an N-terminal HA tag from NCBI Reference sequences NM_001280510.1 (chimpanzee) and NM_001279619.1 (gorilla). The hSAMHD1 gene encoded from the plasmid provided by Dr. Felipe Diaz-Griffero^[36] was cloned into pLVX-IRES-mCherry with an N-terminal HA tag. African Green Monkey SAMHD1 haplotype IV in pLPCX was gifted from Dr. Michael Emerman^[37] (Fred Hutchinson Cancer Research Center, Seattle, WA). Pigtail macaque SAMHD1 gene was amplified from pigtail macaque mRNAs and cloned into pcDNA3.1. Rhesus macaque SAMHD1 in pLenti was generously obtained from Dr. Nathaniel Landau (New York University, New York, NY). Also obtained from Dr. Nathaniel Landau were a plasmid expressing SIVmac251 proteins except Env (pSIV3 +Vpx) and pSIV3 with Vpx deletion (pSIV -Vpx)^[38, 39].

SAMHD1 degradation assay: The SAMHD1 degradation assay was conducted as previously reported^[19, 37, 40]. Briefly, using polyethylenimine, 293T cells (2×10^6 cells) were co-transfected with a plasmid expressing host specific HA-tagged SAMHD1 proteins (0.1 μ g) and a plasmid expressing either flag-tagged (SIVagm 9063-2) or HA-tagged (HIV-1 Cy, HIV-1 Ug, SIVgor, and SIVcpz) viral accessory proteins Vpx/Vpr or the entire proviral genome (SIVmne CL8) (2 μ g). The cell lysates were prepared by sonication from the transfected cells at 48 h post transfection and western blots were performed to visualize not only HA-tagged primate SAMHD1 proteins using an anti-HA antibody, but also hSAMHD1 using anti-hSAMHD1 antibody. GAPDH was used for as a loading control. Vpr and Vpx proteins were visualized using anti-flag tag and anti-HA tag antibodies. The mean relative SAMHD1 levels were calculated by densitometry analysis and normalized to the GAPDH loading control. The ratios of the normalized SAMHD1 levels with and without viral protein expression were calculated for determining the SAMHD1 degradation efficiency.

RT protein expression and purification: All six N-terminal His-tagged RTs were expressed in *E. coli* BL21 Rosetta2 DE3 (Millipore) and their p66/p66 homodimers were purified as described previously^[41] with the following changes. For HIV-1 Cy and SIVagm 9063-2 RTs, clear lysate obtained through sonication was applied to His-Bind resin (Millipore) equilibrated with a binding buffer containing 0.5M NaCl, 20mM Tris-HCl pH 7.9, and 5mM imidazole. The column was washed with 15 column volumes binding buffer prior to being eluted in 1mL fractions by a solution containing 20mM Tris-HCl pH 7.9, 0.5M NaCl, and 1M imidazole. Fractions containing the His tagged-p66/p66 were pooled and dialyzed for 16 hours in a buffer containing 50mM Tris-HCl pH 7.5, 200mM NaCl, 1mM EDTA, and 10% glycerol. The RTs then underwent an additional 3-hour dialysis in a solution containing 50mM Tris-HCl pH 7.5, 200mM NaCl, 1mM EDTA, 10% glycerol, and 1mM DTT. Purification of HIV-1 Ug, SIVmne CL8, SIVgor, and SIVcpz 2.69 RTs required different binding, elution, and dialysis/storage buffers. The clear lysate of these RTs was loaded onto a His-resin bed equilibrated with binding buffer containing 40mM Tris-HCl pH 7.5, 250mM KCl, 5 mM MgCl₂, 5mM beta-mercaptoethanol, 20mM imidazole, and 10% glycerol. The proteins were

eluted from the column using a solution containing 40mM Tris-HCl pH 7.5, 250mM KCl, 5mM MgCl₂, 240mM imidazole, and 10% glycerol before being dialyzed for 16 hours in a buffer containing 50mM Tris-HCl pH 7.5, 150mM KCl, 0.25mM EDTA, 1mM beta-mercaptoethanol, and 20% glycerol. To examine the purity of the proteins, the dialyzed RTs were run on a 4-15% SDS-PAGE gel (BioRad) (Supplemental Figure 2.1). All RTs were determined to have at least 95% purity and were flash frozen in liquid nitrogen prior to being stored at -80°C for future use.

Pre-steady state kinetic analysis: To determine the active site concentration of the six RT proteins, we first performed pre-steady-state burst experiments using an RFQ-3 rapid quench-flow apparatus (KinTek Corporation). A ³²P-labelled template:primer (T/P) was prepared by annealing a 5'-³²P-labeled 17mer primer (5'- CGCGCCGAA TTCCCGCT-3', Integrated DNA Technologies) to a 3-fold excess of 40mer RNA template (5'-AAGCUUGGCUGCAGAAUUAUUGCUAGCGGGAAUUCGGCGCG-3', Integrated DNA Technologies). In burst experiments, 100nM RT pre-bound to 300nM T/P through a 10 min incubation at 37°C was rapidly mixed with a solution containing 300uM dATP, 10mM MgCl₂, 50mM Tris-HCl, pH 7.8 and 50mM NaCl at 37°C. The reactions were quenched at the following time points with EDTA: 0, 0.005, 0.01, 0.05, 0.1, 0.5, 1, 2, and 3 seconds. Reaction products were separated on 14% polyacrylamide/8M urea gel, visualized using a PharoFX (Bio-Rad), and quantified with Image Lab Software (Bio-Rad). To determine the active site concentration of each purified RT, product formation was fit to the burst equation (Eq.1).

$$\text{Eq. 1: } [Product] = A[1 - \exp(-k_{obs} \times t)] + (k_{ss} \times t)$$

In this equation, A is the amplitude of the burst and reflects the concentration of enzyme that is in an active form, k_{obs} is the observed first-order burst rate for dNTP incorporation, and k_{ss} is the linear steady state rate constant^[23, 42, 43]. Active site titrations were performed in triplicate for each lentiviral RT.

Finally, to determine the pre-steady state kinetic activity of the six RTs, we employed single turnover experiments. For these experiments, a ³²P-labelled template:primer (T/P) was prepared by annealing a 5'-³²P-labeled 22mer primer (5'- CGCGCCGAATTCCCGC TAGCAA-3', Integrated DNA Technologies) to a 3-fold excess of 40mer RNA template (5'-

AAGCUUGGCUGCAGAAUAUUGCUAGCGGGAAUUCGGCGCG-3', Integrated DNA Technologies). In single turnover experiments, 250nM active RT enzyme pre-bound to 50nM T/P was rapidly mixed with a solution containing 10mM MgCl₂ and varying concentrations (1.6, 6.25, 12.5, 25, 50, and 100μM) of either dTTP or dTTPαS substrate in the presence of 50mM Tris-HCl, pH 7.8, and 50mM NaCl. The reactions were quenched at various time points (0, 0.01, 0.03, 0.05, 0.1, 0.5, and 2 seconds) with 3mM EDTA and visualized using the same methods as above. The amounts of product were quantified using ImageLab software and plotted as a function of time. The data were then fit to a single exponential equation (Eq. 2).

$$\text{Eq. 2: } [Product] = A(1 - e^{-k_{obs}t})$$

In which A is the amplitude of product formation, k_{obs} is the observed pre-steady state rate for dNTP incorporation, and t is time. Next, k_{obs} was plotted as a function of substrate concentration and fit to a non-linear regression curve equation (Eq. 3).

$$\text{Eq. 3: } k_{obs} = \frac{k_{pol}[dNTP]}{K_d + [dNTP]}$$

In which k_{pol} is the maximum rate of dNTP incorporation and K_d is the equilibrium dissociation constant for the dNTP substrate^[44]. Single turnover experiments were conducted in triplicate for both dTTP and dTTPαS substrates.

Elemental effect analysis: The elemental effect of each RT was determined using the following equation^[45]:

$$\text{Eq. 4: } \textit{Elemental Effect} = \frac{k_{pol}(dTTP)}{k_{pol}(dTTP\alpha S)}$$

If this value exceeds 4, it can be concluded that there is elemental effect. If this value is ≤ 4 , then there is no elemental effect present^[46, 47].

Results and Discussion

Test for SAMHD1 degradation capability of SIV strains: While SAMHD1 non-counteracting HIV-1 replicates in the SAMHD1-mediated limited dNTP pools found in macrophages, SAMHD1 counteracting lentiviruses such as HIV-2 and some SIV strains replicate under abundant dNTP conditions even in macrophages^[48, 49]. We previously reported that unlike RTs from SAMHD1 counteracting lentiviruses, HIV-1 RTs efficiently synthesize DNA even in the low dNTP concentrations found in macrophages^[21]. This led us to hypothesize that the efficient DNA synthesis capability of the SAMHD1 non-counteracting HIV-1 RTs enables these viruses to complete proviral DNA synthesis even in the SAMHD1 mediated limited dNTP concentrations found in infected macrophages. Our follow-up pre-steady state kinetic analysis reported that the efficient DNA synthesis kinetics of HIV-1 RTs is due to their performing a faster k_{pol} step than SAMHD1 counteracting lentiviral RTs^[23] - a kinetic event which occurs after the binding of dNTP substrate (K_d step) to the active site^[50].

In this study, since the k_{pol} step consists of two sequential sub-steps^[50]: 1) a conformational step followed by a 2) chemistry step^[28, 42], we investigated which of these two post dNTP binding sub-steps the RTs of the SAMHD1 non-counteracting primate lentiviruses accelerate in order to execute the faster k_{pol} step than the RTs of the SAMHD1 counteracting lentiviruses. This study aimed at mechanistically elucidating how these two groups of lentiviruses evolutionarily adapted to the largely different cellular dNTP concentrations found in their nondividing myeloid target cells. For this investigation, we employed RTs of four different SIV strains: SIVgor, SIVcpz, SIVagm 9063-2 and SIVmne CL8.

Many SIV strains from various primate species counteract the anti-viral activity of SAMHD1 by targeting the host protein for E3-ligase dependent proteasomal degradation^[9, 13, 16, 17, 51]. The mechanism of counteracting SAMHD1 via proteasomal degradation was initially found in SIV strains encoding Vpx [*i.e.* SIVsm^[10]], a protein which directly binds to SAMHD1 and recruits the host DDB1-CUL4-DCAF E3 ligase complex to induce the proteasomal degradation of SAMHD1^[9, 10, 14]. Later works demonstrated that this anti-SAMHD1 mechanism already existed even in some of SIV strains that do not encode Vpx. However, another accessory protein of these SIV strains, Vpr, is capable of inducing SAMHD1 degradation in these

primate lentiviruses. This suggests that there was a splitting of anti-SAMHD1 function during the gene duplication of Vpr that appears to have created Vpx and two populations of Vpr: one that is able to counteract SAMHD1 and one that is not^[12, 19]. Therefore, we began by testing the SAMHD1 degradation activity of the four SIV strains (SIVgor, SIVcpz, SIVagm 9063-2, and SIVmne CL8) that we here investigated for their RT enzyme kinetics.

SIVcpz and SIVgor are considered to be the origin of HIV-1^[52, 53], and like HIV-1, these two SIV strains encode Vpr, but not Vpx. Since it was previously reported that as observed with HIV-1 strains, SIVcpz Vpr does not proteasomally degrade chimpanzee SAMHD1^[16], we first verified these results and tested whether SIVgor Vpr can induce the proteasomal degradation of gorilla SAMHD1. Additionally, we tested the capability of SIVmne CL8 and SIVagm 9063-2 to degrade their host SAMHD1 proteins. Due to the host SAMHD1-lentivirus specificity^[19] including SAMHD1 sequence variations among the host species, we expressed SAMHD1 proteins from the specific host species related to each of primate lentiviruses used in this study: gorilla, chimpanzee, pig-tailed macaque, and African green monkey (haplotype IV)^[37] for the SAMHD1 degradation assay^[19, 37, 40]. The Vpr genes of SIVgor, SIVcpz and SIVagm 9063-2 were expressed in order to observe their ability to mediate the degradation of their host SAMHD1. As a control, Vpx of SIVmac251 (pSIV3) was tested. In the SAMHD1 degradation assay^[19, 37, 40], 293T cells were co-transfected with a lentiviral plasmid expressing the host SAMHD1 protein and a mammalian plasmid expressing the corresponding Vpr or Vpx protein. SAMHD1 protein levels were monitored by western blots. Vpr, Vpx, and SAMHD1 proteins expressed in this assay were tagged with either HA- or Flag-tag at their N-terminal ends. The ratios of the SAMHD1 protein levels in each of the triplicated SAMHD1 degradation assay were calculated for comparison using densitometry analysis. Since SIVmne CL8 has never been assessed for its ability to degrade SAMHD1, SIVmne CL8 Vpr or Vpx could possess or lack the ability to counteract SAMHD1. For this reason, we utilized a full-length molecular clone of SIVmne CL8, rather than a plasmid containing its Vpr or Vpx protein, to assess the SAMHD1 degradation capabilities of this virus.

First, as shown in Figure 2.1A, the level of the rhesus macaque SAMHD1 protein in the transfected 293T cells was markedly reduced when the cells were co-transfected with a SIVmac251 plasmid (pSIVmac +Vpx) that expresses all viral proteins except Env. However, this reduction was not observed when SAMHD1 was co-transfected with the same SIVmac251 plasmid containing a Vpx deletion (pSIVmac -Vpx). However, Vpr proteins of two HIV-1 strains, HIV-1 Cy (Figure 2.1B) and HIV-1 Ug (Figure 2.1C), could not degrade their host SAMHD1 proteins. In contrast, Vpr of SIVagm 9063-2 (Figure 2.1F) degraded African green monkey haplotype IV SAMHD1 protein in this assay. It was previously reported that SIVagm strains from different subspecies of African green monkeys use their Vpr proteins to degrade their host haploid type specific SAMHD1 proteins^[37]. Also, the transfection of the molecular clone of Vpx-encoding SIVmne CL8 (Figure 2.1G) also degraded pig-tail macaque SAMHD1 protein. Importantly, Vpr proteins of both SIVcpz (Figure 2.1D) and SIVgor (Figure 2.1E) could not degrade their host SAMHD1 proteins. Collectively, the results in Figure 2.1 demonstrate that, as is the case for HIV-1, SIVgor and SIVcpz do not degrade their host SAMHD1 protein, whereas SIVagm 9063-2 and SIVmne CL8 proteasomally degrade their host SAMHD1 proteins. Therefore, this data suggests that while SIVgor and SIVcpz should replicate under SAMHD1-mediated limited dNTP pools in macrophages, both SIVagm 9063-2 and SIVmne CL8 should replicate under abundant dNTP conditions even in macrophages.

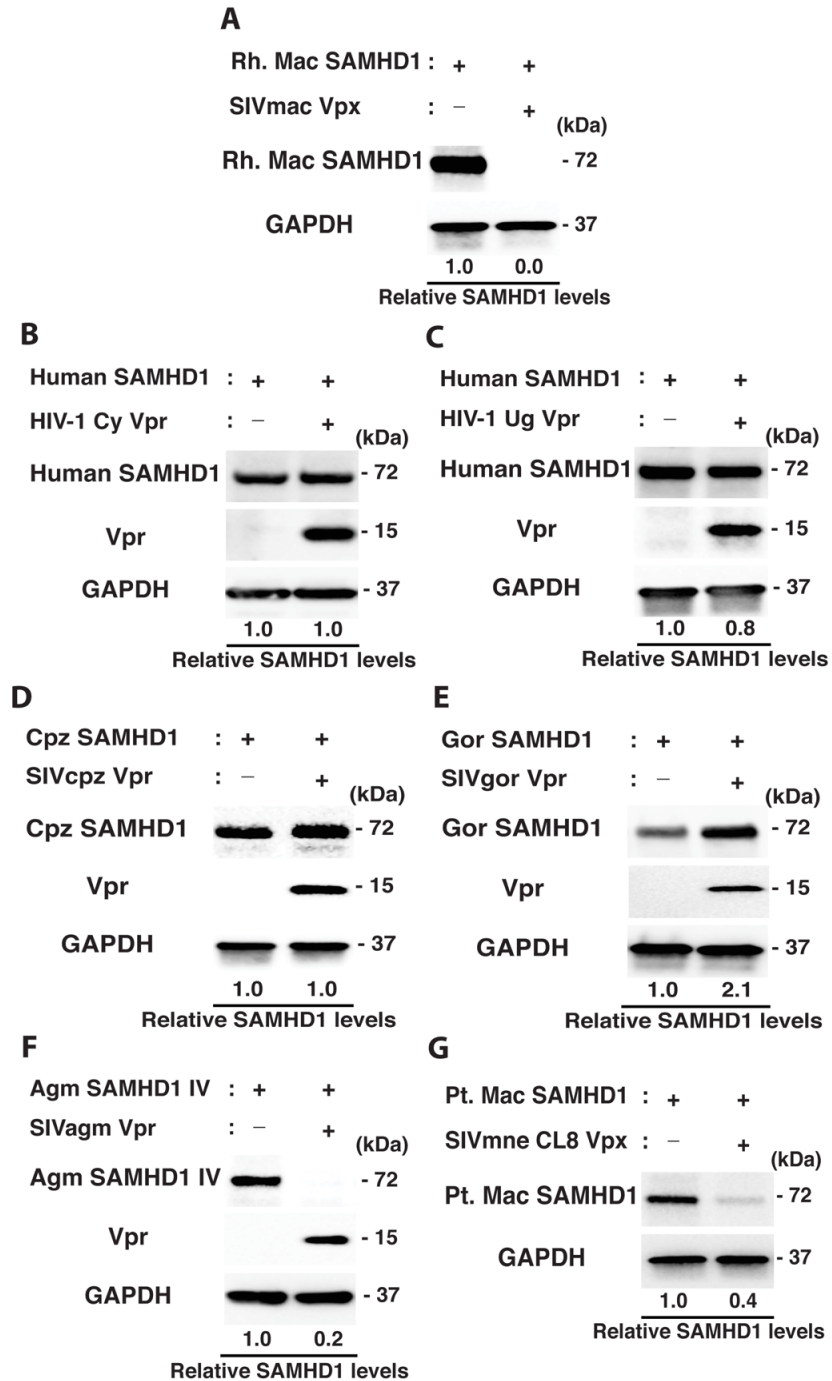


Figure 2.1: SAMHD1 degradation capability of primate lentiviruses. SAMHD1 degradation capability by lentiviral proteins was determined using the SAMHD1 degradation assay (19,37,40). In this assay, 293T cells were co-transfected with a plasmid expressing host specific HA-tagged SAMHD1 proteins (0.1 μ g) and a plasmid expressing either flag-tagged or HA-tagged viral accessory proteins (Vpx or Vpr), the entire

(SIVmne CL8), or partial viral proteins (SIVmac251) (2 μ g). The levels of SAMHD1 were determined by western blots with anti-HA antibody (A, D-G) or anti-hSAMHD1 antibody (B and C), and the expression of the viral accessory protein (Vpx or Vpr) were determined by anti-flag tag (SIVagm 9063-2) or anti-HA tag (HIV-1 Cy, HIV-1 Ug, SIVgor, and SIVcpz) antibody. GAPDH was used as a loading control. (A) Test for Rhesus macaque (Rh Mac) SAMHD1 degradation by SIVmac251 (-) and (+) Vpx. (B) Test for human SAMHD1 degradation by HIV-1 Cy Vpr protein. (C) Test for human SAMHD1 degradation by HIV-1 Ug Vpr. (D) Test for chimpanzee SAMHD1 degradation by SIVcpz Vpr. (E) Test for gorilla SAMHD1 degradation by SIVgor Vpr. (F) Test for African green monkey haploid type IV SAMHD1 (Agm SAMHD1 IV) degradation by SIVagm 9063-2 Vpr. (G) Test for pig-tail macaque (Pt Mac) SAMHD1 degradation by SIVmne CL8 full length molecular clone. pCDNA3.1-hygro, a plasmid that does not express viral proteins, was used as a negative (-) control in B-G. The molecular weight of each protein presented is marked. The data presented in this figure are representative data from two independent transfections. The mean relative SAMHD1 levels shown were calculated by densitometry analysis and normalized to the GAPDH loading control. The calculated mean \pm SD (standard deviation) values corresponding to the normalized SAMHD1 levels following challenge with Vpr/Vpx are (A) 0.024 \pm 0.025 (B) 1.042 \pm 0.485 (C) 0.766 \pm 0.101 and (D) 0.181 \pm 0.061 (E) 0.397 \pm 0.093 (F) 2.121 \pm 0.233 (G) 0.959 \pm 0.548.

Pre-steady state kinetic analysis of SIVgor and SIVcpz RTs: The enzymatic dNTP incorporation by DNA polymerases including RTs follows a series of sequential mechanistic steps that can be separately measured for their kinetic rates^[28, 42, 45, 50]. Typically, as illustrated in Figure 2.2A, first, RT binds to template:primer (T/P, K_D), forming a binary complex (RT:T/P), and this binary complex binds to a dNTP substrate (K_d , dNTP binding affinity), forming ternary complex (RT:T/P:dNTP). Next, the ternary complex will undergo the k_{pol} step, which consists of two sequential sub-steps: 1) a conformational change of the complex (RT*:T/P:dNTP, K_{conf}) followed by 2) a chemistry step (K_{chem}) to complete the phosphodiester bond formation between 3' OH of the primer and α -phosphate of the dNTP substrate. Substrate incorporation is finally followed by the slow release of PP_i product. Single round pre-steady state kinetic analysis has been extensively employed to determine the kinetic rate of these individual steps involved dNTP incorporation by DNA polymerases^[23, 28, 42, 45, 50, 54, 55].

Previous studies have shown that RTs originating from SAMHD1 non-counteracting HIV-1 strains are characterized by higher k_{pol} than RTs from various SAMHD1-counteracting SIV strains, which suggested that HIV-1 RTs might have evolved to have faster k_{pol} step in order to complete proviral DNA synthesis even in macrophages harboring SAMHD1-mediated low dNTP pools^[23]. SIVcpz and SIVgor are the closest relatives of HIV-1 and, particularly, SIVcpz is considered as the origin of HIV-1. In addition, unlike the SAMHD1-counteracting SIV strains that we previously characterized, SIVcpz and SIVgor not only lack Vpx, but their Vpr proteins do not proteasomally degrade their host SAMHD1 proteins (Figure 2.1)^[16]. Therefore, we tested whether SIVcpz and SIVgor RTs also have higher dNTP incorporation efficiency (k_{pol}/K_d) and faster k_{pol} rates, compared to the RTs of SAMHD1-counteracting SIVs (SIVagm 9063-2 and SIVmne CL8). We also employed RTs of two HIV-1 strains (HIV-1 Ug and HIV-1 Cy) as comparison controls.

In order to measure the pre-steady state kinetic values of the RT proteins, which requires a single round of incorporation, we first measured the active site concentration of each purified RT enzyme using pre-steady state burst experiments. Pre-steady state burst experiments, which are performed using an excess T/P to RT enzyme, provide a burst amplitude that defines the concentration of active RT:T/P complexes

capable of dNTP incorporation (Equation 1, Experimental Procedures) and is followed by a steady-state turnover rate as the product complex is released from the enzyme in the rate limiting step of the dNTP incorporation pathway^[28]. We observed typical burst kinetics for all six RTs and found they all possessed 20-75% active protein (Figure 2.2B-C and Supplemental Figure 2.2).

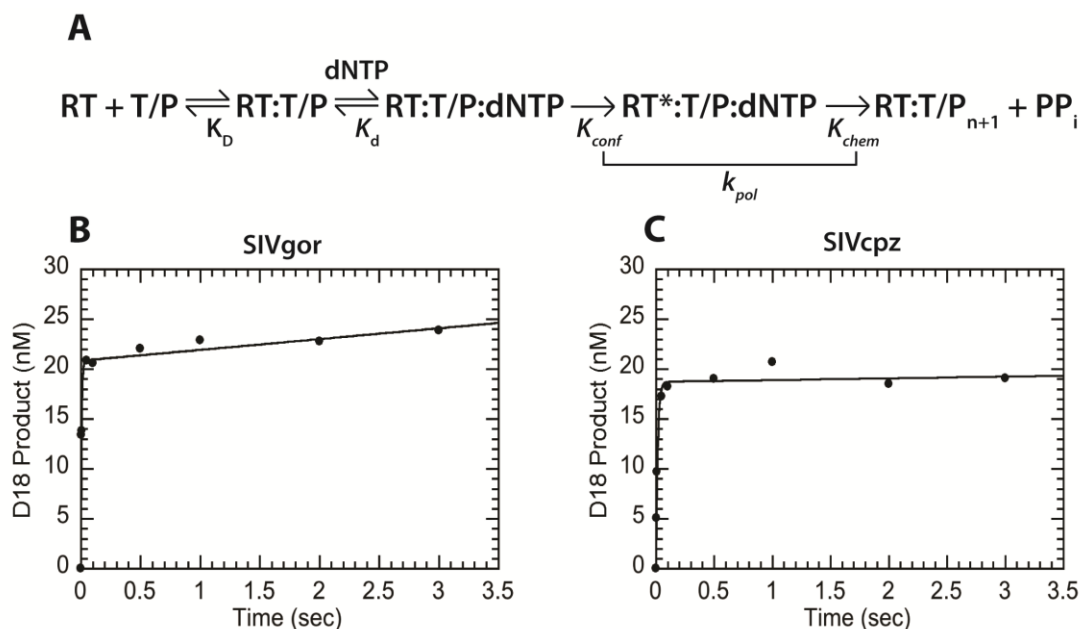


Figure 2.2: Determination of active site concentrations of SIVgor and SIVcpz reverse transcriptase proteins by burst kinetic analysis. (A) Scheme for dNTP incorporation by reverse transcriptase (RT). Free RT molecules initially bind to template:primer (T/P, K_D), forming the RT:T/P binary complex. Next, dNTP substrate binds to the binary complex, forming RT:T/P:dNTP ternary complex (K_d , dNTP binding affinity). The ternary complex then undergoes the k_{pol} step which consists of two sequential sub-steps, 1) pre-catalytic conformational change (K_{conf}) forming RT*:T/P:dNTP and 2) chemistry (K_{chem}) extending T/P to T/P_{n+1}, followed by the PP_i product release. Burst kinetic analysis of all RT proteins, including (B) SIVgor RT and (C) SIVcpz RT, determined the active site concentration of these proteins. Active site titrations were performed in excess T/P conditions to ensure all RT active sites were occupied by T/P. Substrate (dATP) was added to the reaction to allow single nucleotide incorporation events to occur for 0-3 seconds. Reaction product was quantified and fit to a burst equation to determine the active site concentration of each RT (Equation 1, Experimental Procedures). Secondary burst kinetic curves for all RTs are shown in Supplemental Figure 2.2 to display the range of active site activity for each purified enzyme. Active site concentrations were determined from triplicate experiments for all six RT proteins and the calculated activities were found to range from 20-75%.

Next, using all six RTs normalized for their active site concentrations, we employed pre-steady state single turnover experiments to determine the kinetic parameters, K_d and k_{pol} , involved in single nucleotide incorporation by these RTs. In single turnover experiments, prebound RT:T/P binary complexes, created by pre-incubating fivefold excess active RT with radiolabeled T/P, are rapidly mixed with $MgCl_2$ and various concentrations of dTTP substrate ranging from 1-100 μM for reactions ranging from 0-2 seconds. Every reaction was quenched at its designated time using EDTA. We first determined the rate of single nucleotide incorporation at each substrate concentration (Equation 2, Experimental Procedures). These rates were then plotted against substrate concentration to determine the dNTP binding affinity (K_d), maximum rate of dNTP incorporation (k_{pol}), and the dNTP incorporation efficiency (k_{pol}/K_d) for each enzyme (Equation 3, Experimental Procedures; Supplemental Figure 2.3). As summarized in Table 2.1 and Figure 2.3A, both HIV-1 Ug and HIV-1 Cy RTs displayed relatively fast k_{pol} rates of incorporation (HIV-1 Ug: $594.7\ s^{-1}$, HIV-1 Cy: $139.80\ s^{-1}$) in comparison to their SIV SAMHD1-counteracting counterparts (SIVagm 9063-2: $42.92\ s^{-1}$, SIVmneCL8: $68.17\ s^{-1}$). The relative difference in k_{pol} values between HIV-1 Ug and HIV-1 Cy was interesting to observe. This roughly four-fold difference between the two lentiviral RT k_{pol} values was retained when conducting pre-steady state kinetic analysis of a C incorporation event at a different location along the same primer-template (data not shown). This suggests that the observed difference is not an effect of primer-template sequence, rather a product of RT activity. Amino acid sequence comparisons of HIV-1 Cy and HIV-1 Ug RTs did not reveal any striking differences outside of a number of proline residue variations that might affect overall protein structure. However, of the many residue differences HIV-1 Cy and HIV-1 Ug RTs possess, any of them could play a role in overall protein dynamics during polymerization. Importantly, RTs from SIVgor and SIVcpz also displayed fast k_{pol} values similar to the HIV-1 RTs at $193.10\ s^{-1}$ and $355.70\ s^{-1}$ respectively. Consistent with previous studies, all six RTs displayed relatively similar K_d values during the incorporation of the dTTP substrate. This indicates that all RTs bind the dNTP substrate with similar affinity, whereas the RTs from the SAMHD1 non-counteracting lentiviruses displayed faster k_{pol} values than the RTs of the SAMHD1 counteracting lentiviral origins (Figure 2.3A). We were surprised to find the K_d of HIV-1 Ug RT to be relatively high in comparison to that HIV-1 Cy RT. When observing the aforementioned pre-steady state kinetics of a C incorporation event, HIV-1 Ug displayed K_d values similar to that of HIV-1 Cy, suggesting that the elevated K_d value reported here could possibly be an effect of the primer-template sequence (data not shown). In addition, the overall dNTP incorporation efficiency (k_{pol}/K_d , Figure 2.3B and Table 2.1) is 4-6 times higher in the RTs from the SAMHD1 non-counteracting lentiviruses compared to the RTs from the SAMHD1 counteracting lentiviruses. This data supports the idea that the RTs of the SAMHD1 non-counteracting lentiviruses (HIV-1, SIVgor, and SIVcpz) enable these lentiviruses to circumvent the SAMHD1 restriction

and to complete the proviral DNA synthesis even in the limited dNTP pools found in nondividing myeloid cells.

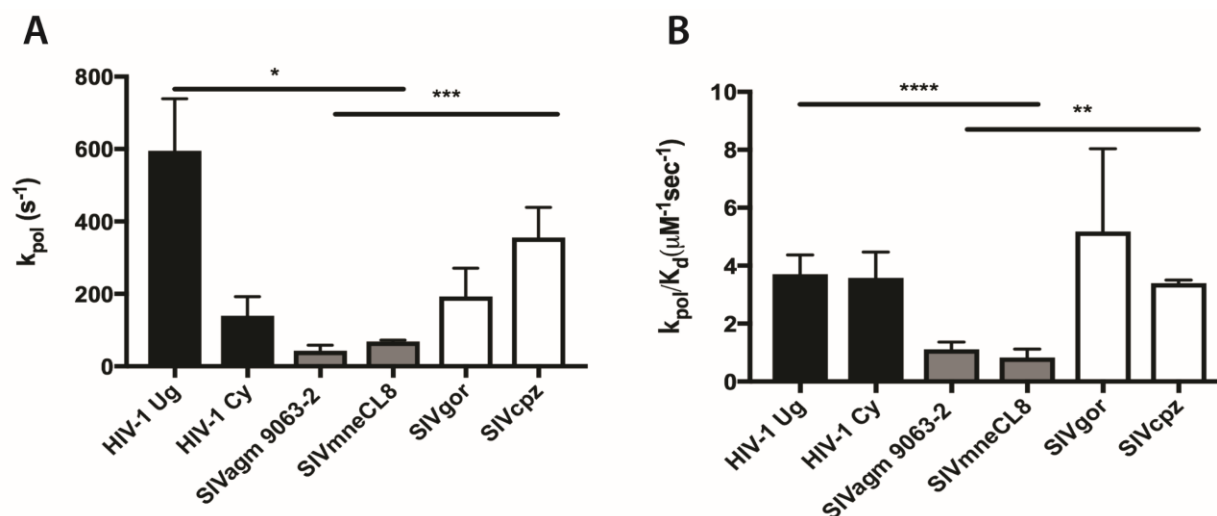


Figure 2.3: Comparison of pre-steady state kinetic values among six lentiviral RT proteins. The pre-steady state kinetic k_{pol} and K_d values of HIV-1 Ug, HIV-1 Cy, SIVagm 9063-2, SIVmne CL8, SIVgor, and SIVcpz RT proteins were determined with dTTP (Table 2.1) as described in Experimental Procedures. Their k_{pol} (A) and k_{pol}/K_d (B) values were compared. The assays were conducted in triplicate. Statistical significance was determined by first grouping the lentiviral RTs into three groups for comparison: HIV-1 (HIV-1 Cy and HIV-1 Ug), SAMHD1-counteracting SIVs (SIVagm 9063-2 and SIVmne CL8), and SAMHD1 non-counteracting SIVs (SIVgor and SIVcpz). Statistical significance from unpaired two-tailed student's t-tests is indicated as: *, $p < 0.05$; **, $p < 0.01$; ***, $p < 0.001$; ****, $p < 0.0001$.

Table 2.1: Pre-steady state kinetic values of six primate lentiviral RT proteins with dTTP. Single turnover pre-steady state kinetic analysis was performed using a dTTP substrate. Experiments were conducted in triplicate. Representative plots from which this data derived can be found in Supplemental Figure 2.3.

dTTP			
RT strains	k_{pol} (s ⁻¹)	K_d (μM)	k_{pol}/K_d (s ⁻¹ * μM ⁻¹)
HIV-1 Ug	594.70±144.00	167.90±69.47	3.71
HIV-1 Cy	139.80±52.40	41.54±21.96	3.58
SIVagm 9063-2	42.92±15.27	40.82±20.63	1.11
SIVmne CL8	68.17±4.46	90.37±37.14	0.83
SIVgor	193.10±77.67	45.21±22.62	5.18
SIVcpz	355.70±83.50	104.50±21.45	3.39

Phosphorothioate elemental effect of RTs from SAMHD1 non-counteracting and counteracting

primate lentiviruses: The k_{pol} step consists of two sequential sub-steps, 1) conformational change (K_{conf}) and 2) chemistry (K_{chem}). Therefore, we next tested which of these two sub-steps RTs of SAMHD1 non-counteracting lentiviruses evolutionarily honed over time in order to gain a faster k_{pol} step. The phosphorothioate elemental effect has been used to determine whether the chemical step of a polymerization reaction is rate-limiting and is evaluated by comparing the rates of incorporation of the natural dNTP substrate versus a dNTP α S substrate (Equation 4, Experimental Procedures)^[46, 50]. The sulfur on the α -phosphate in dNTP α S significantly slows down the K_{chem} rate, while not affecting K_{conf} . Therefore, if the K_{chem} step is rate limiting, then k_{pol} during the incorporation of dNTP α S also becomes slower than that of the natural dNTP substrate (k_{pol} for dNTP α S is 4~11 times smaller than that for natural dNTPs: elemental effect = 4~11)^[45-47]. In contrast, if K_{conf} is the rate limiting and K_{chem} is fast (much smaller than K_{conf} or close to 0), the delayed chemistry step by dNTP α S does not significantly affect the overall k_{pol} step (k_{pol} values for both dNTPs and dNTP α S are similar: elemental effect is less than 4), implying that the k_{pol} rate predominantly represents its pre-catalytic conformational change rate, K_{conf} ($k_{\text{pol}} \approx K_{\text{conf}}$)^[24, 46, 50, 56, 57].

To determine whether an elemental effect was present among the six RTs studied here, single turnover experiments were conducted as described above using a dTTP α S substrate and pre-steady state parameters were calculated and compared to those determined with natural dTTP (Table 2.2; Figure 2.4) for each RT. As shown in Figure 2.4 and Table 2.2, phosphorothioate elemental effects ($k_{\text{pol}}^{\text{dTTP}}/k_{\text{pol}}^{\text{dTTP}\alpha\text{S}}$) of all six RT proteins examined in this study were less than 4. The absence of phosphorothioate elemental effect indicates that the conformational change step of these RTs, not their chemistry step, is rate limiting during their overall k_{pol} step, and their k_{pol} values are predominately represented by their conformational change rates. These findings suggest that the faster k_{pol} rate observed with RTs of SAMHD1 non-counteracting lentiviruses (SIVcpz, SIVgor, and HIV-1 strains) is due to their faster rates of the conformational change that occurs post dNTP binding.

Table 2.2: Pre-steady state kinetic values of six primate lentiviral RT proteins with dTTP α S. Single turnover pre-steady state kinetic analysis was performed using a dTTP α S substrate. Experiments were conducted in triplicate. Representative plots from which this data derived can be found in Supplemental Figure 2.4.

dTTP α S			
RT strains	k_{pol} (s $^{-1}$)	K_d (μ M)	k_{pol}/K_d (s $^{-1}$ * μ M $^{-1}$)
HIV-1 Ug	182.2 \pm 12.22	105.6 \pm 16.43	1.74
HIV-1 Cy	140.3 \pm 36.36	102.5 \pm 66.65	1.69
SIVagm 9063-2	51.11 \pm 9.563	114.1 \pm 33.35	0.46
SIVmne CL8	50.73 \pm 24.43	119.5 \pm 41.73	0.41
SIVgor	265.3 \pm 92.09	141.8 \pm 57.33	1.91
SIVcpz	244.2 \pm 163.5	190.5 \pm 149.3	1.36

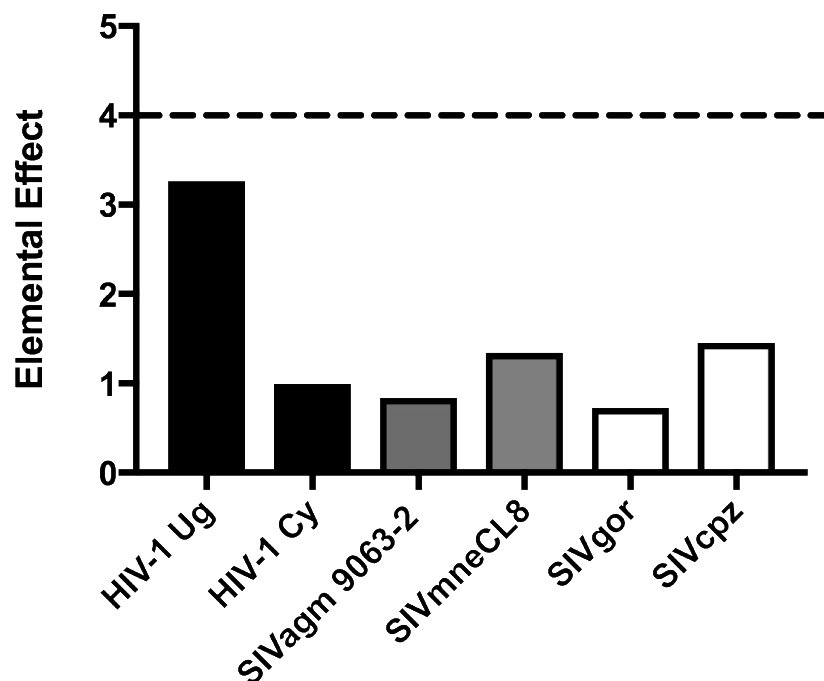
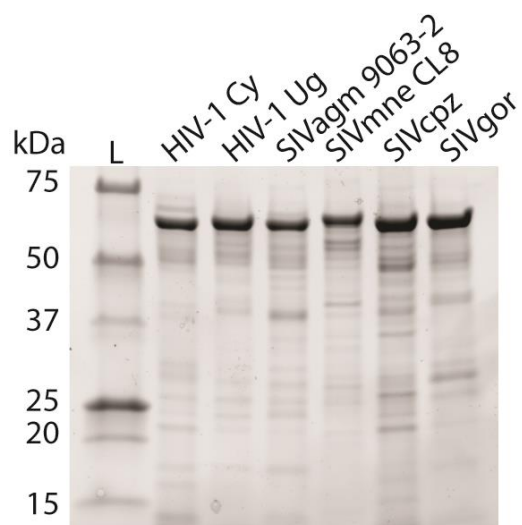


Figure 2.4: Phosphorothioate elemental effect of six lentiviral RT proteins. The K_d and k_{pol} values of the six lentiviral RT proteins with dTTP (Table 2.1) and dTTP α S (Table 2.2) were determined as described in Experimental procedures, and the phosphorothioate elemental effect of these proteins were calculated as the ratios between mean k_{pol} values with natural dTTP and dTTP α S ($k_{pol}^{dTTP}/k_{pol}^{dTTP\alpha S}$) (Equation 4, Experimental Procedures). An elemental effect value of less than 4 (dotted line) indicates that the conformational change sub-step of the k_{pol} step is rate-limiting^[46, 47] and that the pre-catalytic conformational change rate predominantly represents the k_{pol} step in these six RT proteins.

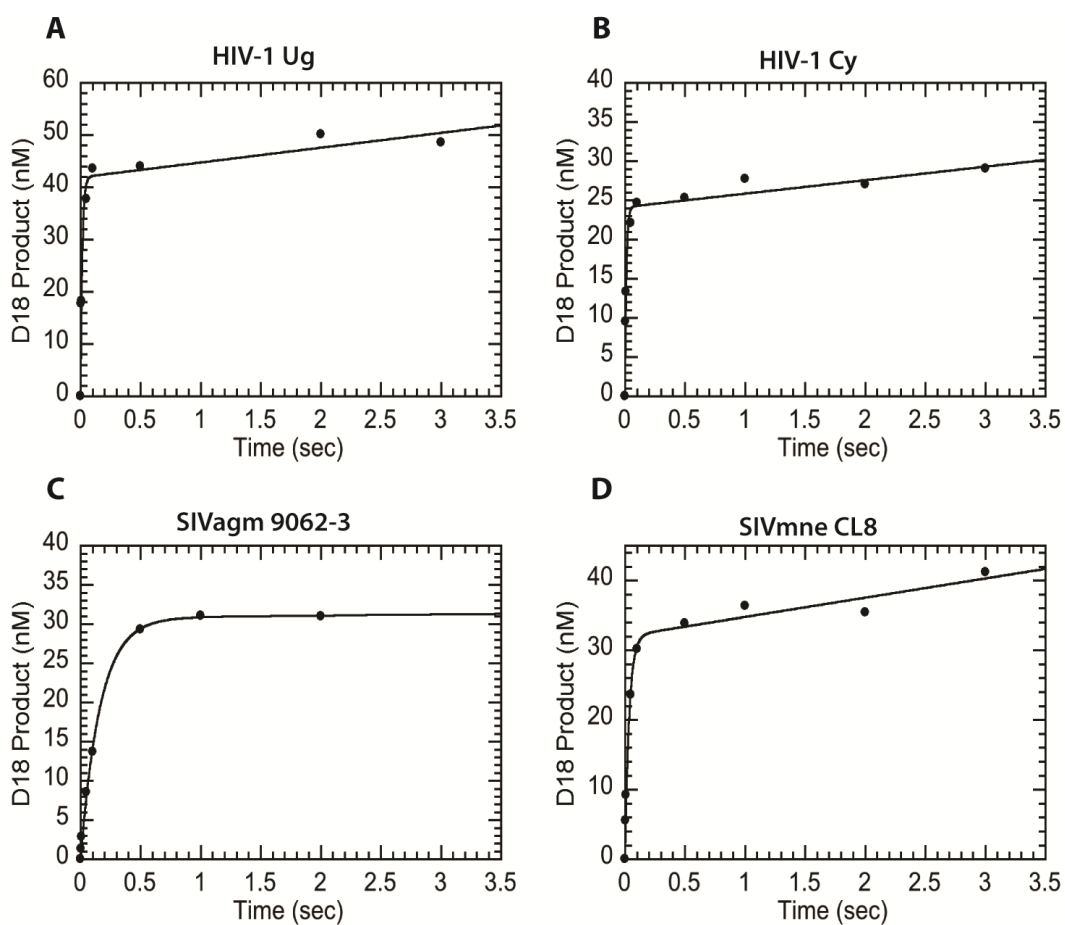
As illustrated in our model (Figure 2.5), while SAMHD1 counteracting lentiviruses (SIVmac239, SIVagm 9063-2, and SIVmne CL8) utilize Vpr/Vpx to counteract SAMHD1 and overcome the kinetic barrier presented in macrophages, our study suggests that SAMHD1 non-counteracting lentiviruses may have evolved over time to harbor RTs that execute a faster conformational change step during nucleotide incorporation, thus enabling the viruses to complete reverse transcription even in the SAMHD1 mediated low dNTP pools of nondividing myeloid cells. In conclusion, while the mechanism employed by SAMHD1 non-counteracting lentiviruses of executing a faster RT conformational change is less effective in overcoming SAMHD1 restriction than the Vpx/Vpr mechanism employed by SAMHD1 counteracting lentiviruses, this RT-based mechanism is sufficient to complete reverse transcription, albeit at slower rates, in the SAMHD1 mediated low dNTP concentrations found in macrophages.

FRET-based measurements have been reported to monitor the post-dNTP binding finger-closing conformational change rate of several DNA polymerases such as DNA polymerase β ^[25] and Klenow fragment of *E. coli* DNA polymerase I^[58]. However, this type of the measurement has not been fully established for any RT protein. It is possible that this FRET-based assay can be applied for directly comparing the pre-catalytic fingers-closing rates between SAMHD1 counteracting lentiviral RTs and SAMHD non-counteracting lentiviral RTs. There are two potential mechanistic pathways to explain the adaption of the more efficient post dNTP binding conformational change displayed by SAMHD1 non-counteracting lentiviral RTs. First, it is possible that the finger-closing conformational change rates of the SAMHD1 non-counteracting lentiviral RTs are simply faster than those of the SAMHD1 counteracting lentiviral RTs. This possibility can be tested by using the FRET-based assay as described for other DNA polymerases. Second, it is possible that the distance of the movement during the finger-closing conformational change is shorter for the RT proteins of the SAMHD1 non-counteracting lentiviruses, compared to the RT proteins of the SAMHD1 counteracting lentiviruses. This possibility can be investigated through the structural comparison of the ternary complexes of the RT proteins from the SAMHD1 non-counteracting lentiviruses and SAMHD1 counteracting lentiviruses.

Overall, these kinetic studies support the idea that SAMHD1 non-counteracting primate lentiviruses such as HIV-1, SIVgor and SIVcpz might have evolved over time to possess RTs that can more efficiently execute the conformational change step, which enables these lentiviruses to circumvent SAMHD1-mediated dNTP depletion and complete proviral DNA synthesis in nondividing myeloid target cell types.



Supplemental Figure 2.1: Purity of the six lentiviral reverse transcriptase enzymes used in pre-steady state studies. Equimolar amounts of the various RTs were loaded to display the purity of each enzyme.



Supplemental Figure 2.2: Representative active site titration curves. Burst kinetic analysis of HIV-1 Ug (A), HIV-1 Cy (B), and SIVagm 9063-2 (C), and SIVmne CL8 (D) reverse transcriptase proteins.

References

1. Jamburuthugoda VK, Chugh P, Kim B. Modification of human immunodeficiency virus type 1 reverse transcriptase to target cells with elevated cellular dNTP concentrations. *J Biol Chem* 2006; 281(19):13388-13395.
2. Diamond TL, Roshal M, Jamburuthugoda VK, Reynolds HM, Merriam AR, Lee KY, et al. Macrophage tropism of HIV-1 depends on efficient cellular dNTP utilization by reverse transcriptase. *J Biol Chem* 2004; 279(49):51545-51553.
3. Weissman D, Rabin RL, Arthos J, Rubbert A, Dybul M, Swofford R, et al. Macrophage-tropic HIV and SIV envelope proteins induce a signal through the CCR5 chemokine receptor. *Nature* 1997; 389(6654):981-985.
4. Swanstrom AE, Del Prete GQ, Deleage C, Elser SE, Lackner AA, Hoxie JA. The SIV Envelope Glycoprotein, Viral Tropism, and Pathogenesis: Novel Insights from Nonhuman Primate Models of AIDS. *Curr HIV Res* 2018; 16(1):29-40.
5. Bejarano D, Puertas M, Börner K, Martinez-Picado J, Müller B, Kräusslich H-G. Detailed Characterization of Early HIV-1 Replication Dynamics in Primary Human Macrophages. *Viruses* 2018; 10(11):620.
6. Williams KC, Hickey WF. Central nervous system damage, monocytes and macrophages, and neurological disorders in AIDS. *Annu Rev Neurosci* 2002; 25:537-562.
7. Amie SM, Noble E, Kim B. Intracellular nucleotide levels and the control of retroviral infections. *Virology* 2013; 436(2):247-254.
8. Goldstone DC, Ennis-Adeniran V, Hedden JJ, Groom HC, Rice GI, Christodoulou E, et al. HIV-1 restriction factor SAMHD1 is a deoxynucleoside triphosphate triphosphohydrolase. *Nature* 2011; 480(7377):379-382.
9. Hrecka K, Hao C, Gierszewska M, Swanson SK, Kesik-Brodacka M, Srivastava S, et al. Vpx relieves inhibition of HIV-1 infection of macrophages mediated by the SAMHD1 protein. *Nature* 2011; 474(7353):658-661.

10. Laguette N, Sobhian B, Casartelli N, Ringeard M, Chable-Bessia C, Segeral E, et al. SAMHD1 is the dendritic- and myeloid-cell-specific HIV-1 restriction factor counteracted by Vpx. *Nature* 2011; 474(7353):654-657.
11. Sharp PM, Bailes E, Stevenson M, Emerman M, Hahn BH. Gene acquisition in HIV and SIV. *Nature* 1996; 383(6601):586-587.
12. Etienne L, Hahn BH, Sharp PM, Matsen FA, Emerman M. Gene loss and adaptation to hominids underlie the ancient origin of HIV-1. *Cell Host Microbe* 2013; 14(1):85-92.
13. Ahn J, Hao C, Yan J, DeLucia M, Mehrens J, Wang C, et al. HIV/simian immunodeficiency virus (SIV) accessory virulence factor Vpx loads the host cell restriction factor SAMHD1 onto the E3 ubiquitin ligase complex CRL4DCAF1. *J Biol Chem* 2012; 287(15):12550-12558.
14. Srivastava S, Swanson SK, Manel N, Florens L, Washburn MP, Skowronski J. Lentiviral Vpx accessory factor targets VprBP/DCAF1 substrate adaptor for cullin 4 E3 ubiquitin ligase to enable macrophage infection. *PLoS Pathog* 2008; 4(5):e1000059.
15. Lahouassa H, Daddacha W, Hofmann H, Ayinde D, Logue EC, Dragin L, et al. SAMHD1 restricts the replication of human immunodeficiency virus type 1 by depleting the intracellular pool of deoxynucleoside triphosphates. *Nat Immunol* 2012; 13(3):223-228.
16. Lim Efrem S, Fregoso Oliver I, McCoy Connor O, Matsen Frederick A, Malik Harmit S, Emerman M. The Ability of Primate Lentiviruses to Degrade the Monocyte Restriction Factor SAMHD1 Preceded the Birth of the Viral Accessory Protein Vpx. *Cell Host & Microbe* 2012; 11(2):194-204.
17. Belzile JP, Duisit G, Rougeau N, Mercier J, Finzi A, Cohen EA. HIV-1 Vpr-mediated G2 arrest involves the DDB1-CUL4AVPRBP E3 ubiquitin ligase. *PLoS Pathog* 2007; 3(7):e85.
18. Hrecka K, Gierszewska M, Srivastava S, Kozackiewicz L, Swanson SK, Florens L, et al. Lentiviral Vpr usurps Cul4-DDB1[VprBP] E3 ubiquitin ligase to modulate cell cycle. *Proc Natl Acad Sci U S A* 2007; 104(28):11778-11783.

19. Fregoso OI, Ahn J, Wang C, Mehrens J, Skowronski J, Emerman M. Evolutionary toggling of Vpx/Vpr specificity results in divergent recognition of the restriction factor SAMHD1. *PLoS Pathog* 2013; 9(7):e1003496.
20. Schwefel D, Groom HC, Boucherit VC, Christodoulou E, Walker PA, Stoye JP, et al. Structural basis of lentiviral subversion of a cellular protein degradation pathway. *Nature* 2014; 505(7482):234-238.
21. Lenzi GM, Domaoal RA, Kim DH, Schinazi RF, Kim B. Kinetic variations between reverse transcriptases of viral protein X coding and noncoding lentiviruses. *Retrovirology* 2014; 11:111.
22. Skasko M, Weiss KK, Reynolds HM, Jamburuthugoda V, Lee K, Kim B. Mechanistic differences in RNA-dependent DNA polymerization and fidelity between murine leukemia virus and HIV-1 reverse transcriptases. *J Biol Chem* 2005; 280(13):12190-12200.
23. Lenzi GM, Domaoal RA, Kim DH, Schinazi RF, Kim B. Mechanistic and Kinetic Differences between Reverse Transcriptases of Vpx Coding and Non-coding Lentiviruses. *J Biol Chem* 2015; 290(50):30078-30086.
24. Mizrahi V HR, Marlier JF, Johnson KA, Benkovic SJ. Rate-limiting steps in the DNA polymerase I reaction pathway. *Biochemistry* 1985; 24(15):4010-4018.
25. Huang J, Alnajjar KS, Mahmoud MM, Eckenroth B, Doublet S, Sweasy JB. The nature of the DNA substrate influences pre-catalytic conformational changes of DNA polymerase beta. *J Biol Chem* 2018; 293(39):15084-15094.
26. Fiala KA, Suo Z. Mechanism of DNA polymerization catalyzed by *Sulfolobus solfataricus* P2 DNA polymerase IV. *Biochemistry* 2004; 43(7):2116-2125.
27. Zahurancik WJ, Klein SJ, Suo Z. Kinetic mechanism of DNA polymerization catalyzed by human DNA polymerase epsilon. *Biochemistry* 2013; 52(40):7041-7049.
28. Hsieh JC ZS, Modrich P. Kinetic mechanism of the DNA-dependent DNA polymerase activity of human immunodeficiency virus reverse transcriptase. *J Biol Chem* 1993; 268(33):24607-24613.

29. Gao F, Robertson DL, Carruthers CD, Morrison SG, Jian B, Chen Y, et al. A comprehensive panel of near-full-length clones and reference sequences for non-subtype B isolates of human immunodeficiency virus type 1. *J Virol* 1998; 72(7):5680-5698.
30. Gao F, Vidal N, Li Y, Trask SA, Chen Y, Kostrikis LG, et al. Evidence of Two Distinct Subsubtypes within the HIV-1 Subtype A Radiation. *AIDS Research and Human Retroviruses* 2001; 17(8):675-688.
31. Takehisa J, Kraus MH, Ayouba A, Bailes E, Van Heuverswyn F, Decker JM, et al. Origin and biology of simian immunodeficiency virus in wild-living western gorillas. *J Virol* 2009; 83(4):1635-1648.
32. Takehisa J, Kraus MH, Decker JM, Li Y, Keele BF, Bibollet-Ruche F, et al. Generation of infectious molecular clones of simian immunodeficiency virus from fecal consensus sequences of wild chimpanzees. *J Virol* 2007; 81(14):7463-7475.
33. Rudensey LM, Kimata JT, Benveniste RE, Overbaugh J. Progression to AIDS in macaques is associated with changes in the replication, tropism, and cytopathic properties of the simian immunodeficiency virus variant population. *Virology* 1995; 207(2):528-542.
34. Hirsch VM, Dapolito G, Johnson PR, Elkins WR, London WT, Montali RJ, et al. Induction of AIDS by simian immunodeficiency virus from an African green monkey: species-specific variation in pathogenicity correlates with the extent of in vivo replication. *J Virol* 1995; 69(2):955-967.
35. Skasko M, Diamond TL, Kim B. Mechanistic variations among reverse transcriptases of simian immunodeficiency virus variants isolated from African green monkeys. *Biochemistry* 2009; 48(23):5389-5395.
36. Bhattacharya A, Wang Z, White T, Buffone C, Nguyen LA, Shepard CN, et al. Effects of T592 phosphomimetic mutations on tetramer stability and dNTPase activity of SAMHD1 can not explain the retroviral restriction defect. *Sci Rep* 2016; 6:31353.
37. Spragg CJ, Emerman M. Antagonism of SAMHD1 is actively maintained in natural infections of simian immunodeficiency virus. *Proc Natl Acad Sci U S A* 2013; 110(52):21136-21141.

38. Berger G, Durand S, Goujon C, Nguyen XN, Cordeil S, Darlix JL, et al. A simple, versatile and efficient method to genetically modify human monocyte-derived dendritic cells with HIV-1-derived lentiviral vectors. *Nat Protoc* 2011; 6(6):806-816.
39. Mangeot PE, Negre D, Dubois B, Winter AJ, Leissner P, Mehtali M, et al. Development of minimal lentivirus vectors derived from simian immunodeficiency virus (SIVmac251) and their use for gene transfer into human dendritic cells. *Journal of Virology* 2000; 74(18):8307-8315.
40. Mereby SA, Maehigashi T, Holler JM, Kim DH, Schinazi RF, Kim B. Interplay of ancestral non-primate lentiviruses with the virus-restricting SAMHD1 proteins of their hosts. *J Biol Chem* 2018; 293(42):16402-16412.
41. Kim B. Genetic selection in *Escherichia coli* for active human immunodeficiency virus reverse transcriptase mutants. *Methods* 1997; 12(4):318-324.
42. Kati WM, Johnson KA, Jerva LF, Anderson KS. Mechanism and fidelity of HIV reverse transcriptase. *J Biol Chem* 1992; 267(36):25988-25997.
43. Reardon JE. Human immunodeficiency virus reverse transcriptase: steady-state and pre-steady-state kinetics of nucleotide incorporation. *Biochemistry* 1992; 31(18):4473-4479.
44. Johnson KA. Rapid quench kinetic analysis of polymerases, adenosinetriphosphatases, and enzyme intermediates. *Methods Enzymol* 1995; 249:38-61.
45. Herschlag D, Piccirilli JA, Cech TR. Ribozyme-catalyzed and nonenzymic reactions of phosphate diesters: rate effects upon substitution of sulfur for a nonbridging phosphoryl oxygen atom. *Biochemistry* 1991; 30(20):4844-4854.
46. Patel SS, Wong I, Johnson KA. Pre-steady-state kinetic analysis of processive DNA replication including complete characterization of an exonuclease-deficient mutant. *Biochemistry* 1991; 30(2):511-525.
47. Wong I, Patel SS, Johnson KA. An induced-fit kinetic mechanism for DNA replication fidelity: direct measurement by single-turnover kinetics. *Biochemistry* 1991; 30(2):526-537.

48. Yu XF YQ, Essex M, Lee TH. The vpx gene of simian immunodeficiency virus facilitates efficient viral replication in fresh lymphocytes and macrophage. *J Virol* 1991; 65(9):5088-5091.
49. Hollenbaugh JA, Montero C, Schinazi RF, Munger J, Kim B. Metabolic profiling during HIV-1 and HIV-2 infection of primary human monocyte-derived macrophages. *Virology* 2016; 491:106-114.
50. Joyce CM. Techniques used to study the DNA polymerase reaction pathway. *Biochim Biophys Acta* 2010; 1804(5):1032-1040.
51. Zhou X, DeLucia M, Hao C, Hrecka K, Monnie C, Skowronski J, et al. HIV-1 Vpr protein directly loads helicase-like transcription factor (HLTF) onto the CRL4-DCAF1 E3 ubiquitin ligase. *J Biol Chem* 2017; 292(51):21117-21127.
52. Sakai Y, Doi N, Miyazaki Y, Adachi A, Nomaguchi M. Phylogenetic Insights into the Functional Relationship between Primate Lentiviral Reverse Transcriptase and Accessory Proteins Vpx/Vpr. *Front Microbiol* 2016; 7:1655.
53. D'Arc M, Ayouba A, Esteban A, Learn GH, Boue V, Liegeois F, et al. Origin of the HIV-1 group O epidemic in western lowland gorillas. *Proc Natl Acad Sci U S A* 2015; 112(11):E1343-1352.
54. Einolf HJ, Guengerich FP. Fidelity of nucleotide insertion at 8-oxo-7,8-dihydroguanine by mammalian DNA polymerase delta. Steady-state and pre-steady-state kinetic analysis. *J Biol Chem* 2001; 276(6):3764-3771.
55. Schermerhorn KM, Gardner AF. Pre-steady-state Kinetic Analysis of a Family D DNA Polymerase from *Thermococcus* sp. 9 degrees N Reveals Mechanisms for Archaeal Genomic Replication and Maintenance. *J Biol Chem* 2015; 290(36):21800-21810.
56. Polesky AH DM, Benkovic SJ, Grindley ND, Joyce CM. Side chains involved in catalysis of the polymerase reaction of DNA polymerase I from *Escherichia coli*. *J Biol Chem* 1992; 267(12):8417-8428.
57. Wong I PS, Johnson KA. An induced-fit kinetic mechanism for DNA replication fidelity: direct measurement by single-turnover kinetics. *Biochemistry* 1991; 30(2):526-537.

58. Santoso Y, Joyce CM, Potapova O, Le Reste L, Hohlbein J, Torella JP, et al. Conformational transitions in DNA polymerase I revealed by single-molecule FRET. *Proc Natl Acad Sci U S A* 2010; 107(2):715-720.

Chapter 3

Enhanced Enzyme Kinetics of Reverse Transcriptase Variants Cloned from Animals Infected with SIVmac239 Lacking Viral Protein X

Coggins SA, Kim DH, Schinazi RF, Desrosiers RC, and Kim B

Si'Ana Coggins cloned and purified the enzymes, performed the experiments, analyzed the data, and
wrote and edited the paper

Dong-Hyun Kim, Raymond Schinazi, and Ronald Desrosiers conceived the experiments

Baek Kim conceived and designed the experiments and wrote the paper

Abstract

While HIV Type 1 (HIV-1) and simian immunodeficiency virus (SIV) share a target cell tropism of dividing CD4⁺ T cells and nondividing myeloid cells, the lentiviruses display differential replication kinetics in macrophages. High expression levels of active host deoxynucleotide triphosphohydrolase (dNTPase) sterile alpha motif (SAM) domain and histidine-aspartate (HD) domain-containing protein 1 (SAMHD1) in macrophages depletes intracellular dNTPs, restricts HIV-1 reverse transcription, and results in a restrictive infection in this myeloid cell type. Some SIVs overcome SAMHD1 restriction using viral protein X (Vpx), a viral accessory protein that induces proteasomal degradation of SAMHD1, increasing cellular dNTP concentrations in macrophages and enabling efficient proviral DNA synthesis. We previously reported that SAMHD1 non-counteracting lentiviruses may have evolved to harbor reverse transcriptase (RT) proteins that efficiently polymerize DNA, even at low dNTP concentrations, to circumvent SAMHD1 restriction in macrophages. Here we investigated whether RTs from SIVmac239 virus lacking a Vpx protein (i.e. Vpx (-) virus) evolve during the course of in vivo infection to more efficiently synthesize DNA at the low dNTP concentrations found in macrophages, much like the RT of SAMHD1 non-counteracting HIV-1. Sequence analysis of RTs cloned from Vpx (+) and Vpx (-) SIVmac239 infected animals revealed that Vpx (-) RTs contained more extensive mutations than Vpx (+) RTs. While the amino acid substitutions were dispersed indiscriminately across the protein, steady state and pre-steady state analysis demonstrated that selected SIVmac239 Vpx (-) RTs are characterized by higher catalytic efficiency and incorporation efficiency values than RTs cloned from SIVmac239 Vpx (+) infections.

Introduction

During the course of their pathogenesis, lentiviruses such as human immunodeficiency virus type 1 (HIV-1), HIV-2, and simian immunodeficiency virus (SIV) infect both dividing CD4⁺ T cells and terminally differentiated/nondividing myeloid cells such as macrophages and microglia^[1-4]. While sharing a selective cellular tropism, cell-dependent replication kinetics differ amongst the viruses, as HIV-1 replication kinetics are delayed in nondividing cell populations^[5]. Slowed replication kinetics in macrophage and microglial populations, particularly in the brain, support the persistent production of HIV-1 at low levels^[6]. This is in stark contrast to the robust replication of HIV-1 in CD4⁺ T cells which leads to rapid cell death. While dividing cells, like activated CD4⁺ T cells, undergo dNTP biosynthesis in S phase, terminally differentiated cells like macrophages have no necessity to support chromosomal DNA replication or mitotic division and are thus characterized by lower dNTP pools^[7, 8]. Indeed, cellular dNTP concentrations in human primary monocyte-derived macrophages (20-40 nM) are 100-250 times lower than those found in activated/dividing CD4⁺ T cells (2-5 μ M)^[8]. Recent studies have revealed that host deoxynucleotide triphosphohydrolase (dNTPase) sterile alpha motif (SAM) domain and histidine-aspartate (HD) domain-containing protein 1 (SAMHD1), which is active and highly expressed in macrophages, is responsible for the depletion of cellular dNTPs within this nondividing target cell type^[9-12]. While macrophages are not refractory to HIV-1 infection, the SAMHD1-mediated limited substrate availability for reverse transcriptase (RT) during viral replication kinetically restricts HIV-1 proviral DNA synthesis in macrophages^[13, 14]. Conversely, HIV-2 and some SIV strains replicate rapidly in this nondividing myeloid cell type through the implementation of a virally encoded accessory protein called viral protein X (Vpx)^[11, 15, 16]. Lentiviral Vpx targets host SAMHD1 for proteasomal degradation through the E3 ubiquitination pathway, robustly reducing SAMHD1 protein levels and increasing intracellular dNTP concentrations in infected macrophages^[17-19]. In the absence of SAMHD1, abundant dNTP substrate accelerates reverse transcription during the viral replication cycle and enables rapid proviral DNA synthesis of SAMHD1 counteracting viruses^[20]. Since Vpx arose from a gene duplication event of accessory protein viral protein R (Vpr)^[21, 22], Vpr proteins of some SIV strains lacking Vpx (e.g. SIVagm677, SIVagm9648, SIVdeb,

SIVmus1) also possess the ability to target SAMHD1 for proteasomal degradation through the same pathway hijacked by Vpx^[23-25]. However, the Vpr proteins of SAMHD1 non-counteracting strains such as HIV-1 and SIVcpz are unable to induce degradation of their host SAMHD1 proteins^[25, 26].

Unlike SAMHD1 counteracting viruses including SIVmac239 and SIVagm677, which replicate under abundant cellular dNTP concentrations even in macrophages^[20], SAMHD1 non-counteracting viruses such as HIV-1 and SIVcpz replicate within limited dNTP pools during the infection of this nondividing target cell type. Interestingly, recent studies have suggested that SAMHD1 non-counteracting lentiviral RTs have been evolutionarily honed to complete proviral DNA synthesis even at the low dNTP concentrations found in macrophages. We previously observed that RTs from SAMHD1 non-counteracting lentiviruses (e.g. HIV-1) were characterized by lower steady state K_m values and displayed faster pre-steady state rates of dNTP incorporation (k_{poi}) when compared to RTs from SAMHD1 counteracting lentiviruses (e.g. SIVmac239)^[27, 28]. Further pre-steady state kinetic analysis revealed that SAMHD1 non-counteracting lentiviruses overcome low dNTP concentrations in macrophages through the use of RT proteins that execute a faster conformational change during the incorporation of an incoming nucleotide substrate^[29]. While less effective than Vpx/Vpr-induced degradation of SAMHD1, this RT-mediated mechanism enables the slow, but complete, reverse transcription of the viral genome during infection of macrophages by SAMHD1 non-counteracting lentiviruses like HIV-1.

Given the influence of Vpx on viral reverse transcription and replication kinetics in macrophages, Westermoreland et al. previously sought to characterize the cellular and tissue targets of a Vpx-deleted mutant of SIVmac239 (Vpx (-)) in infected Rhesus macaques. Apart from the 101-base deletion of the *vpx* gene, Vpx (-) mutant virus was identical to wild type SIVmac239 (Vpx (+)) virus in this study^[30, 31]. While macaques infected with Vpx (-) virus eventually developed AIDS with opportunistic infections and AIDS-defining lesions, Vpx (-)-infected animals (mean survival: 935.4 dpi) lived roughly 2.5 times longer than those infected with Vpx (+) wild type virus (mean survival: 364.3 dpi). Additionally, the group observed that viral replication in myeloid cells was drastically impaired in the absence of Vpx^[32]. Previous studies have shown that HIV-1 disease progression is associated with the appearance of viral variants containing

an array of different coreceptors that enable the virus to infect a wider range of host cell types^[33]. These viral variants are speculated to arise from selective pressure exerted by the host immune system that drives HIV-1 evolution during the course of infection. Similarly, steady and pre-steady state studies of SAMHD1 non-counteracting RTs (HIV-1 RTs) have demonstrated that SAMHD1 non-counteracting primate lentiviruses might have evolved over time to harbor RTs that can more efficiently incorporate nucleotides at the low dNTP concentrations found in macrophages, which allows these lentiviruses to circumvent the anti-viral selective pressure from dNTPase SAMHD1^[27-29].

In this study, we sought to investigate whether SIVmac239 RT, which is kinetically less efficient than RTs from SAMHD1 non-counteracting HIV-1 strains^[27], undergoes enzymatic improvement in the absence of Vpx during the course of pathogenesis in order to circumvent the SAMHD1 restriction in myeloid cells. For this, we biochemically characterized SIVmac239 RT variants cloned from adult rhesus macaques infected with either Vpx (+) or Vpx (-) SIVmac239 virus and observed that Vpx (-) RT variants, encoding frequently identified amino acid mutations, displayed elevated steady state catalytic efficiency (k_{cat}/K_m) and pre-steady state incorporation efficiency (k_{pol}/K_d) values when compared to Vpx (+) RTs. Overall, our sequence and kinetic analyses support the idea that RTs of SAMHD1-noncounteracting lentiviruses may evolve *in vivo* to better support proviral DNA synthesis in the SAMHD1-mediated low dNTP pools of target macrophage cell populations.

Experimental Procedures

Animal Samples: Serum samples originating from two rhesus macaques infected with Vpx-deleted SIVmac239 (animals 1 and 2) were obtained from the Westmoreland et al. study^[32] and PBMCs from two rhesus macaques infected with wild type SIVmac239 (animals 3 and 4) were provided by Dr. Guido Silvestri. Vpx-deleted SIVmac239 samples were collected 3 years post-infection while wild type SIVmac239 samples, animals 3 and 4, were collected 27- and 29-weeks post-infection respectively.

Cloning and Sequencing Vpx+ and Vpx- RTs: RNA was extracted from infected samples using the RNeasy Mini Kit (Qiagen). SIVmac239 RT sequences were amplified by RT-PCR using SuperScript III One-Step RT-PCR System with Platinum Taq DNA Polymerase (Invitrogen) with 5NdeIF (5'-AAAAAACATATGCCCATAGCTAAAGTAGAGCC-3'; resulting amplicon has 5' NdeI site) and 3XhoIR (5'-AAAAAACTCGAGTTATTGACTAACTAG-3; resulting amplicon has 3' XhoI site) for 40 cycles with primer annealing at 45°C for 30 seconds and primer extension at 68°C for 3 minutes. PCR fragments were isolated using the QIAquick PCR Purification Kit (Qiagen) and subsequently cloned directly into the pCR4-TOPO vector (TOPO-RT) using the TOPO TA Cloning Kit (Invitrogen). TOPO-RT vectors were sequenced using M13 Forward (-20) and M13 Reverse primers. Viral RT nucleotide and amino acid sequences were analyzed and compared to parental viral clone SIVmac239 RT^[30-32]. Ultimately, 40 complete RT clones were identified from each infected sample, and alterations in nucleotide and amino acid sequences noted. The first number within the name of the cloned RT signifies the originating animal—animals 1 and 2 are Vpx (-) infected animals while animals 3 and 4 were infected by WT or Vpx (+) SIVmac239 virus. The subsequent letter and number following the animal distinction are in reference to sequencing records.

RT protein expression and purification: N-terminal His-tagged RT proteins were expressed from cloned pET28a-RT expression plasmids in E.coli BL21 Rosetta 2 DE3 (Millipore) and the p66/p66 homodimers were purified as described previously^[34] with the following changes. For large-scale purifications, clear lysate obtained through sonication of 1L cultures was applied to charged His · Bind resin (Millipore)

equilibrated with a binding buffer containing 40mM Tris-HCl pH 7.5, 250mM KCl, 5mM MgCl₂, 20mM imidazole, and 10% glycerol. The column was washed with 15 column volumes binding buffer prior to being eluted in 1 mL fractions by a solution containing 40mM Tris-HCl pH 7.5, 250mM KCl, 5mM MgCl₂, 240mM imidazole, and 10% glycerol. Fractions containing the His tagged-p66/p66 were pooled and dialyzed for 16 hours in a storage buffer containing 50mM Tris-HCl pH 7.5, 150mM KCl, 0.25mM EDTA, 1mM beta-mercaptoethanol, and 20% glycerol. To examine the purity of the proteins, the dialyzed RTs were run on a 4–15% SDS-PAGE gel (BioRad). All RTs were determined to have at least 95% purity and were flash frozen in liquid nitrogen prior to being stored at –80 °C for future use. Small-scale protein preparations used in the steady state multiple nucleotide incorporation kinetic screen were obtained from 250 mL cultures using His SpinTrap (GE Healthcare) columns and the same buffers utilized in large-scale purifications.

Steady state multiple nucleotide incorporation assay: The previously described primer extension assay^{18, 27]} was slightly modified for this study. Briefly, a ³²P-labelled template/primer (T/P) was prepared by annealing a 5'-³²P 17mer DNA primer (17D: 5'-CGCGCCGAATTCCCGCT-3', Integrated DNA Technologies) to a 3-fold excess of 39mer RNA (39R: 5'-AGCUUGGCUGCAGAAUAUUGCUAGCGGGAAUUCGGCGCG-3', Integrated DNA Technologies). Assay mixtures (20 µL) contained 10 nM T/P, RT, and varying dNTP concentrations (50, 25, 10, 5, 1, 0.5, 0.25, 0.1, 0.05, and 0.025 µM). RT activity was normalized for 50% extension at the highest dNTP concentration (50 µM), and with all dNTPs supplied, this reaction allows multiple rounds of primer extension. Reaction mixtures were incubated at 37°C for 5 minutes, quenched with 40 mM EDTA in 99% formamide, and placed at 95°C for 2 minutes to further inactivate RT. Reaction products were separated on a 14% polyacrylamide/8M urea gel, visualized using a PharosFX (Bio-Rad) phosphoimager, and quantified with Image Lab Software (Bio-Rad). Data were fit to a nonlinear regression curve to obtain Michealis-Menten kinetic parameters describing the maximal reaction velocity (V_{max}) and the amount of substrate required to reach half V_{max} (K_m).

Steady state single nucleotide incorporation assay: Single nucleotide incorporation experiments were conducted using a 5'-³²P-labelled 22mer DNA primer (5'- CGCGCCGAATTCCC GC TAGCAA-3', Integrated DNA Technologies) annealed to a 39mer RNA (39R) or DNA (39D: 5'- AGCTTGGCTGCAGAATATTGCTAGCGGGAATTCGGCGCG-3', Integrated DNA Technologies) template using the same methods described above with the following changes. Instead of adding all four dNTPs to the reaction mixture, the incoming nucleotide (dTTP) was supplied in various concentrations ranging from 25 nM to 50 μ M. Reactions were conducted and quantified as previously described. Per Michaelis-Menten kinetics, V_{max} values were converted to catalytic turnover (k_{cat}) values using total enzyme concentrations. Steady state experiments were conducted in triplicate for each RT.

Pre-steady state single-turnover experiments: The pre-steady state kinetic parameters k_{pol} and K_d were determined as previously described^[27, 29, 35]. Briefly, the active site concentrations of WT SIVmac239 RT and Vpx (-) RT clones 2G7, 2N0, and 1M6 were determined using pre-steady state burst experiments conducted with an RFQ-3 rapid quench-flow apparatus (KinTek Corporation) and a 17mer ³²P-labelled DNA primer (17D) annealed to a 39mer DNA template (39D) supplied in 3-fold excess to RT. The reactions were quenched with EDTA at the following timepoints: 0, 0.005, 0.01, 0.05, 0.1, 0.5, 1, 2, and 3 seconds. Active site concentrations were determined by fitting product formation to the burst equation (Eq. 1):

$$\text{Eq. 1: } [Product] = A[1 - \exp(-k_{obs} \times t)] + (k_{ss} \times t)$$

In which A is the amplitude of the burst and reflects the concentration of enzyme that is in an active form, k_{obs} represents the observed first-order burst rate for dNTP incorporation, and k_{ss} is the linear steady state rate constant^[27, 36, 37]. Active site titrations were performed in triplicate for each RT.

RT active site concentrations were used to ensure subsequent single turnover experiments contained 250 nM active RT enzyme, a 5-fold excess to the 50nM T/P (a 5'-³²P-labelled 22mer DNA primer annealed to 39mer DNA template with enables incorporation of a dTTP molecule, i.e. T-T/P) present in the reactions. In single turnover experiments, excess RT pre-bound to T-T/P was rapidly mixed with a solution containing 10 mM MgCl₂ and varying concentrations of dTTP (1.6-100 μ M). The reactions were quenched with EDTA

at various timepoints ranging from 0.01 seconds to 2 seconds and visualized using the same methods as above. The data were then fit to a single exponential equation (Eq. 2) to obtain the observed pre-steady state rate for dNTP incorporation (k_{obs}) at every dTTP substrate concentration tested.

$$\text{Eq. 2: } [Product] = A(1 - e^{-k_{obs}t})$$

In this equation A is the amplitude of product formation, k_{obs} is the observed pre-steady state rate for dNTP incorporation, and t is time.

Next, k_{obs} was plotted as a function of substrate concentration and fit to a nonlinear regression curve (Eq. 3) to obtain kinetic parameters k_{pol} and K_d for each characterized RT.

$$\text{Eq. 3: } k_{obs} = \frac{k_{pol}[dNTP]}{K_d + [dNTP]}$$

In which k_{pol} is the maximum rate of dNTP incorporation and K_d is the equilibrium dissociation constant for the dNTP substrate^[38]. Pre-steady state single turnover experiments were conducted in triplicate for each RT.

Thermostability Shift Assay: Protein mixtures (40 μ L) containing 2.5 μ M purified RT protein and 5 mM MgCl₂ in RT storage buffer (50mM Tris-HCl pH 7.5, 150mM KCl, 0.25mM EDTA, 1mM beta-mercaptoethanol, and 20% glycerol) were added to a 96 well plate (Lightcycler 480 Multiwell Plate 96 white, Roche) in triplicate for each RT. Wells containing either no enzyme or no dye were performed in triplicate as negative controls. Sypro Orange Protein Gel Stain (Sigma-Aldrich) was diluted 1:20 in RT storage buffer and 1 μ L of the dilution added to the protein mixture in each well. Reactions mixtures were heated from 32°C to 99°C at the rate of 0.02°C per second by a real-time PCR device (LightCycler 480 II, Roche) that monitored protein unfolding signified by changes in fluorescence of the Sypro Orange fluorophore. The resulting fluorescence intensities were plotted against temperature for each sample well and fit to the Boltzmann equation using Spyder Software (Anaconda). The midpoint of each transition (T_m), or melting temperature of the enzyme, was calculated for each well and the average T_m of each RT calculated by averaging the results of the triplicate wells.

Results

Isolation and sequencing of SIVmac239 RT variants from Rhesus macaques infected with Vpx (+) wild type and Vpx (-) mutant SIVmac239 viruses: We previously observed that RT of SAMHD1 counteracting SIVmac239 synthesizes DNA with low efficiency at macrophage-like dNTP concentrations, displaying lower steady state catalytic efficiency (k_{cat}/K_m) values when compared RTs of SAMHD1 non-counteracting HIV-1 strains^[27]. We predicted that the lower enzymatic efficiency of RTs originating from SAMHD1 counteracting lentiviruses (e.g. SIVmac239) is an evolutionary consequence of natural viral replication occurring within high cellular dNTP concentrations, even in nondividing myeloid target cells, due to the virus induced SAMHD1 proteasomal degradation. Therefore, here, we reasoned that if Vpx (-) mutant SIVmac239 replicates in animals, the viral RTs may be selectively honed during *in vivo* infections to contain mutations that can improve viral DNA synthesis efficiency, even in the low dNTP pools found in macrophages that result from the presence of dNTPase SAMHD1 and the absence of Vpx, much like HIV-1 RT^[39].

To test this, we utilized samples previously collected from Rhesus macaques infected with either Vpx (+) wild type or Vpx (-) mutant SIVmac239. We chose samples collected upon the development of AIDS characteristics in these infected animals. To begin, we extracted RNAs from two samples originating from animals infected with Vpx (+) wild type virus (27 and 29 weeks post infection) and two samples from animals infected with Vpx (-) mutant virus (both 36 months post infection^[32]). Since these timepoints immediately precede the development of AIDS in the infected animals, the initially inoculated viruses underwent the entirety of *in vivo* evolution and host pathogenesis. In this near-terminal stage, viral titers were considerably elevated^[32]—even in animals infected with Vpx (-) mutant SIVmac239—which was convenient for our collection of the abundant viral RNA samples. Next, we conducted RT-PCR for the full-length reverse transcriptase gene and cloned the resulting amplicons to obtain plasmids containing Vpx (+) and Vpx (-) RT variants. The cloned RT plasmids were sequenced and compared to wild type RT SIVmac239 nucleotide and amino acid sequences (GeneBank: AY588946.1). A few minor RT clones containing premature stop codons or frame shift mutations were discarded, and a total of 40 complete RT

sequences compiled for each animal sample: 80 clones for Vpx (-) infections and 80 clones for Vpx (-) infections. We first observed that nucleotide and amino acid mutations in both Vpx (+) and Vpx (-) RTs are indiscriminately distributed throughout the five RT functional and structural subdomains (i.e. the fingers, palm, thumb, connection, and RNase H domains) (Table 3.1). Interestingly, when analyzing the number of amino acid mutations present per cloned RT, we found that Vpx (-) RTs, on average, harbored about 2.6 times more amino acid mutations than Vpx (+) RTs (Figure 3.1A). In fact, when observing the distribution of the number of amino acid mutations present in each clone, the predominant number of mutations shifts from 1 in Vpx (+) RTs to 3-4 in Vpx (-) RTs (Figure 3.1B). Consistent with this observation, we determined more than 20 out of 80 RT clones remained unmutated (wild type) in the Vpx (+) infected samples while only 3 out of 80 RT clones showed wild type amino acid sequences in the Vpx (-) infected samples (Figure 3.1B). The maximum number of amino acid mutations present in a single clone was 8 for both groups while the maximum number of nucleic acid mutations was 11 and 16 for Vpx (+) and Vpx (-) RTs, respectively. The data shown in Figure 3.1 suggest that more mutations per cloned RT were found in Vpx (-) samples compared to Vpx (+) samples, which may simply result from Vpx (-) infected animals experiencing infection periods approximately 6 times longer of than Vpx (+) infected animals (Vpx (-): 36 months ; Vpx (+): 27-29 weeks).

Interestingly, while amino acid mutations M164L, S211N, and E218D are found in multiple clones from both Vpx (-) animals, a number of mutations, including K394R, A492V, and E522K, are seen in both Vpx (-) and Vpx (+) RT proteins (Table 3.1). Even though a greater redundancy in amino acid mutations is seen in Vpx (-) RTs, there are surprisingly six mutations exclusive to Vpx (+) RTs (Table 3.1). Overall, we found that if RT clones were identical in amino acid mutation profiles, differing mutations were observed at the gene levels (e.g. different codons for the same amino acid) thus supporting that redundancy in amino acid mutations is less likely the result of amplification during RT-PCR. Overall, these data reveal that while mutations are not isolated to one region of the enzyme, Vpx (-) RTs contain more mutations than Vpx (+) RTs at both the nucleic acid and amino acid levels.

Table 3.1: Redundant amino acid mutations found in Vpx (+) and Vpx (-) RTs.

Mutation	RT Subdomains	Number of Clones (out of 40) with Noted Mutation			
		A1 Vpx (-)	A2 Vpx (-)	A3 Vpx (+)	A4 Vpx (+)
I2L	Fingers	2			
V32I	Fingers	1	21		1
V32A	Fingers			2	1
R82K	Fingers	1		1	
L100I	Palm		2		
E122K	Fingers			2	1
I145M	Fingers			1	2
M164L	Palm	1	38		
L196P	Palm			1	1
S211N	Palm	24	9		
I212L	Palm	2			
E218D	Palm	23	2		
Q228R	Palm			1	1
M230I	Palm			1	1
R281K	Thumb	5			
G285E	Thumb		1	1	
G322D	Connection		2		
P324L	Connection		16		
I330V	Connection		15		
V385I	Connection	1		1	
K394R	Connection	2	37		1
E412G	Connection	1		1	
S417P	Connection			1	1
S449T	RNaseH		2		
T486I	RNaseH	2	1		
V465I	RNaseH			1	2
A492V	RNaseH	2		2	
C508R	RNaseH	1		1	1
E522K	RNaseH	1	2	1	
E523K	RNaseH	1	1		
I525S	RNaseH	1	1		

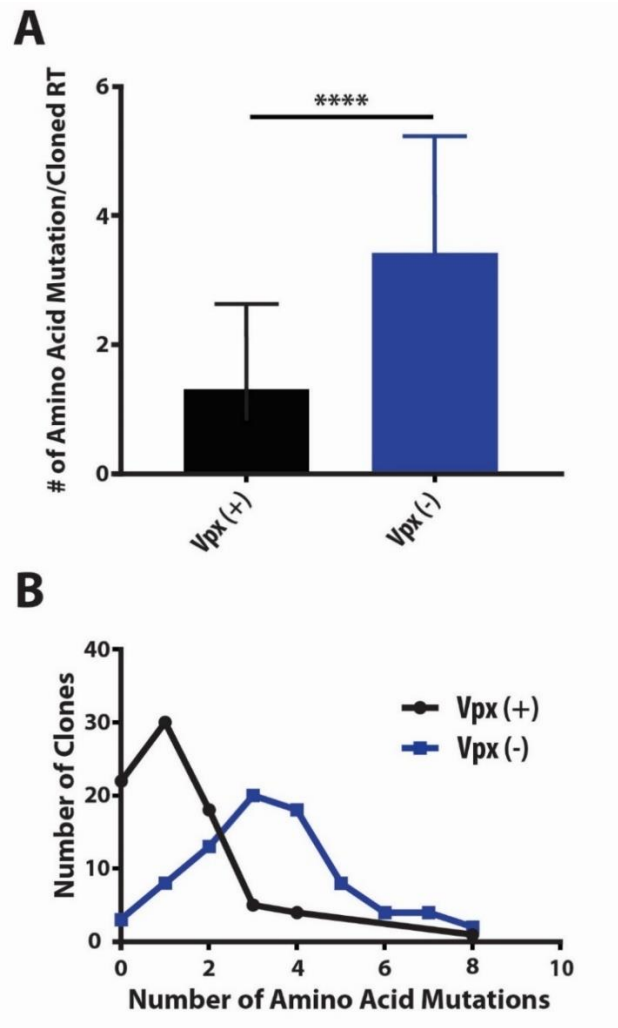


Figure 3.1: Summary of amino acid mutations found in Vpx (+) and Vpx (-) RT variants. (A) The average number of amino acid mutations per cloned RT was plotted for Vpx (+) (black) and Vpx (-) (blue) RTs, with error bars representing standard deviation. Statistical significance from an unpaired two-tailed student's t-test is indicated as ****, $p < 0.0001$. (B) RT clones were grouped by the number of mutations present in the amino acid sequence. The distribution of the number of amino acid mutations present in Vpx (+) and Vpx (-) RTs are shown using black and blue lines respectively.

Steady state kinetic analysis of Vpx (+) and Vpx (-) RTs: Previous studies have shown that there are kinetic variations between RTs originating from lentiviruses with and without the ability to counteract SAMHD1^[27, 28]. To broadly characterize the differential steady state multi-nucleotide incorporation kinetics in Vpx (+) and Vpx (-) infected animals, we conducted a steady state kinetic assay. Starting with the 40 RT clones that were collected and sequenced per animal (Table 3.1), we systematically chose 10 RT clones per animal with commonly identified mutations, proper protein expression in *E. coli*, and close to wild type RT purification yields to conduct multiple nucleotide incorporation kinetic analysis in steady state conditions. Ultimately, 20 Vpx (+) and 20 Vpx (-) RT variant proteins were chosen for enzymatic analysis. To determine the steady state substrate efficiency (V_{max}/K_m) for each RT, we examined the RNA-dependent DNA polymerization activity of these purified RT proteins using a 39mer RNA template annealed to a 5'-³²P-labelled 17mer DNA primer and varying concentrations of dNTPs (25 nM to 50 μ M). RTs displaying substrate efficiency values lower than $0.1 \times 10^{-5} \text{ sec}^{-1}$ were considered dead enzymes and were omitted from final quantifications. As summarized in Figure 3.2, Vpx (-) RTs synthesized DNA from an RNA template with substrate efficiencies approximately two-fold greater than Vpx (+) RTs, indicating that SIVmac239 RT might have improved its steady state kinetic DNA synthesis efficiency during the course of infection in the absence of Vpx.

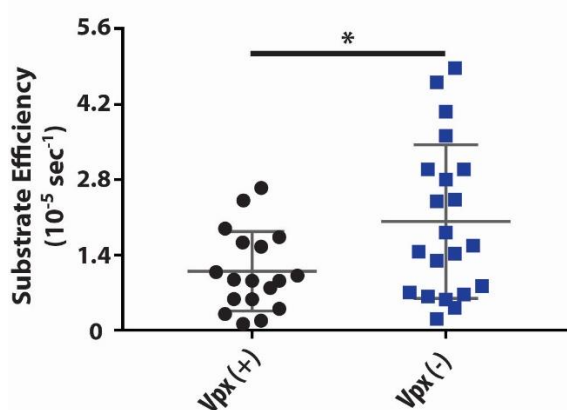


Figure 3.2: Steady state kinetic measurement of Vpx (+) and Vpx (-) RT variants. Substrate efficiency (V_{max}/K_m) for Vpx (+) (black) and Vpx (-) (blue) RTs are represented using scatter dot plots with the grey lines signifying mean and standard deviation values. Statistical significance from an unpaired two-tailed student's t-test is indicated as *, $p=0.0182$.

Steady state single nucleotide incorporation kinetic activity of two Vpx (-) RT variants:

Interestingly, the initial kinetic analysis enabled the identification of two Vpx (-) RT variants with substrate efficiencies much higher than the mean substrate efficiency of Vpx (+) RTs ($1.831 \times 10^{-5} \text{ sec}^{-1}$)—RTs 2G7 ($6.781 \times 10^{-5} \text{ sec}^{-1}$) and 2N0 ($8.135 \times 10^{-5} \text{ sec}^{-1}$). Relative to wild type SIVmac239 RT, 2G7 and 2N0 variants both contain four amino acid mutations—two of which they share (M164L and K394R)—however, they differ in the number of nucleic acid mutations present in their sequences (Table 3.3). Here, we conducted a more extensive kinetic characterization of these two SIVmac239 RT variants identified from Vpx (-) infections. First, considering that these two RTs contain multiple mutations, we tested whether these mutations alter their observed protein thermostability, which is indicative of overall protein stability^[40, 41]. As shown in Table 3.2, both RT variant proteins possess melting temperatures (T_m values) similar to that of wild type SIVmac239 RT protein, indicating that the amino acid mutations present in 2G7 and 2N0 RT variants cause no significant abnormalities in protein folding or structure.

Table 3.2: Melting temperatures (T_m) of various Vpx (+) and Vpx (-) RTs compared to that of wild type SIVmac239 RT.

Clone [†]	T_m (°C)
SIVmac239	54.65
1M6	51.24
2N0	53.78
2G7	54.26

[†] Prefix of 1 or 2 indicate the cloned RT originated from Vpx (-) animals 1 and 2 respectively.

Table 3.3: Amino acid mutations present in Vpx (-) clones 2G7, 2N0, and 1M6.

Clone	NT [†]	AA [‡]	Mut 1	Mut 2	Mut 3	Mut 4	Mut 5	Mut 6	Mut 7	Mut 8
2G7	10	4	V32A	M164L	G322D	K394R				
2N0	8	4	M164L	P324L	I340V	K394R				
1M6	10	8	A158S	S211N	E250K	K357R	A368T	S514N	E522K	E523K

[†] Number of nucleic acid substitutions

[‡] Number of amino acid substitutions

To better understand the kinetic activities of 2G7 and 2N0 RT variants during first and second strand synthesis, we conducted steady state single nucleotide incorporation kinetic analysis to observe their RNA- and DNA-dependent DNA polymerization efficiency. Consistent with previous studies, we found that the K_m associated with dTTP incorporation by wild type SIVmac239 RT from a DNA template (98.15 nM) was two times greater than that observed when using an RNA template (48.08 nM) (Table 3.4)^[42, 43]. This was not the case for 2G7 and 2N0 RT variants which displayed slightly reduced K_m values when polymerizing from a DNA template (2G7: 36.09 nM, 2N0: 33.69 nM) compared to those observed when using an RNA template (2G7: 45.82 nM, 2N0: 47.51 nM). However, RT variants 2G7 and 2N0 were found to turnover substrate faster than WT SIVmac239 RT regardless of template type, as demonstrated by significantly larger k_{cat} values (Table 3.4). As expected, we found that wild type SIVmac239 RT incorporated dTTP using an RNA template (Figure 3.3A, $21902 \text{ sec}^{-1}\mu\text{M}^{-1}$) with almost twice the catalytic efficiency (k_{cat}/K_m) than when polymerizing on a DNA template (Figure 3.3B, $11987 \text{ sec}^{-1}\mu\text{M}^{-1}$). Conversely, 2G7 RT catalyzed dTTP incorporation from RNA- and DNA- templates with similar kinetics, while 2N0 RT more efficiently incorporated dTTP when utilizing a DNA template (Figure 3.3). Despite sharing similar K_m values when polymerizing from an RNA template, the large template-independent k_{cat} values of 2G7 and 2N0 enable the Vpx (-) RTs to be more catalytically efficient than SIVmac239 RT during DNA synthesis from both RNA and DNA templates (Table 3.4, Figure 3.3).

Table 3.4: Steady state dTTP incorporation by WT SIVmac239 RT and Vpx (-) RTs 2G7 and 2N0 from RNA and DNA templates.

Clone	RNA Template	DNA Template
K_m (nM)		
WT	48.08 ± 26.70	98.15 ± 14.98
2G7	45.82 ± 21.61	36.09 ± 5.33
2N0	47.51 ± 5.60	33.69 ± 6.94
k_{cat} (sec ⁻¹)		
WT	$8.96 \times 10^{-4} \pm 0.57 \times 10^{-4}$	$11.65 \times 10^{-4} \pm 1.57 \times 10^{-4}$
2G7	$16.43 \times 10^{-4} \pm 1.40 \times 10^{-4}$	$15.10 \times 10^{-4} \pm 0.56 \times 10^{-4}$
2N0	$23.82 \times 10^{-4} \pm 0.99 \times 10^{-4}$	$32.22 \times 10^{-4} \pm 1.86 \times 10^{-4}$
k_{cat}/K_m (sec ⁻¹ M ⁻¹)		
WT	21902 ± 9137	11897 ± 232.4
2G7	41046 ± 16749	42540 ± 7283
2N0	50464 ± 4550	98030 ± 17571

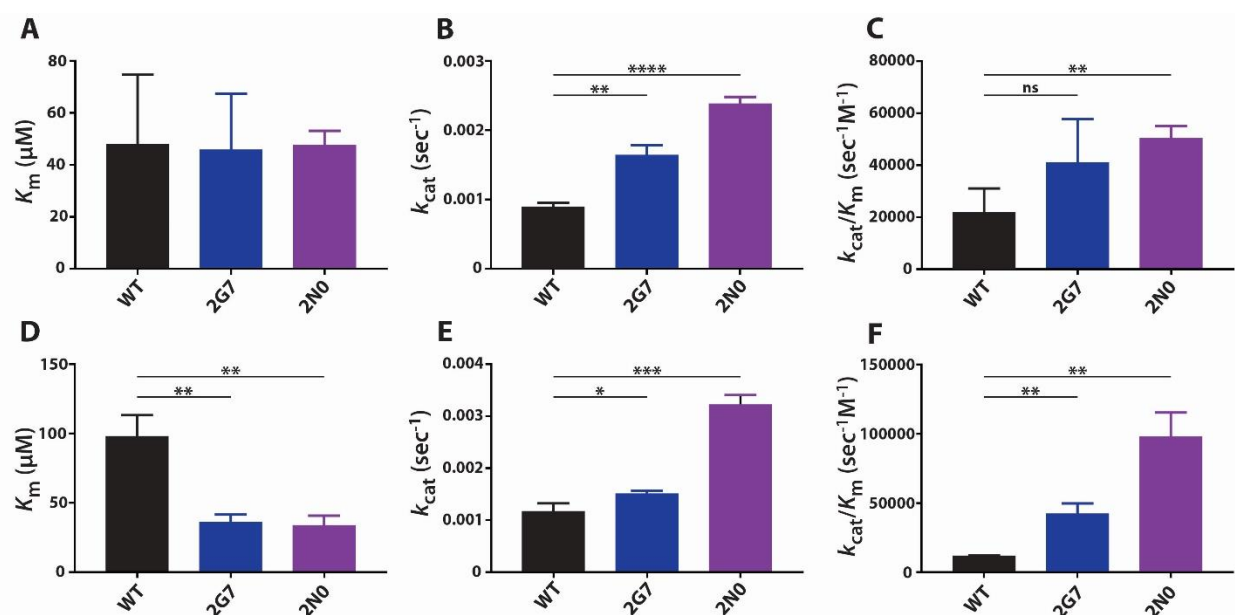


Figure 3.3: Steady state kinetic activity of Vpx (-) 2G7 and 2N0 RT variants compared to that of wild type SIVmac239 RT. Steady state kinetic parameters were determined for WT SIVmac239 RT and Vpx (-) RTs 2G7 and 2N0 with dTTP using RNA (A-C) and DNA (D-F) templates (Table 3.3) as described in Experimental Procedures. The assays were conducted in triplicate before K_m (A, D), k_{cat} (B, E), and catalytic efficiency (k_{cat}/K_m) (C, F) values of Vpx (-) RTs were compared that of wild type RT. Statistical significance from unpaired two-tailed student's t-tests is indicated as: ns, $p < 0.1234$; *, $p < 0.0332$; **, $p < 0.0021$; ***, $p < 0.0002$; ****, $p < 0.0001$.

Pre-steady state kinetic analysis of two Vpx (-) RT variants: Previous studies have detailed the pre-steady state kinetic differences between SAMHD1 counteracting and non-counteracting lentiviral RTs. While characterized by similar dNTP dissociation constants (K_d), SAMHD1 non-counteracting RTs (e.g. HIV-1 RTs) have demonstrated higher rates of polymerization (k_{pol}) and elevated incorporation efficiency values (k_{pol}/K_d) relative to SAMHD1 counteracting lentiviral RTs^[27, 29]. Since it has been shown that SAMHD1 non-counteracting lentiviral RTs can more efficiently incorporate an incoming nucleotide, pre-steady state single turnover experiments were conducted using normalized concentrations of active 2G7, 2N0, and WT SIVmac239 RT proteins in order to assess pre-steady state kinetic activity.

First, we determined the active site concentrations of these purified SIVmac239 RT proteins by conducting pre-steady state burst experiments using a 5'-³²P-labeled 17-mer A primer annealed to a 39mer DNA template (A-T/P). We measured the 18mer product formation resulting from the mixture of a solution containing RT protein (100 nM RT proteins, see below) pre-bound to A-T/P (300 nM, excess T/P) with a solution containing 300 μ M dATP and 10 mM MgCl₂ for various durations of time ranging from 0.05-3 seconds. As shown in Figure 3.4, there was an initial burst of product formation by WT (Figure 3.4A), 2G7 (Figure 3.4B) and 2N0 (Figure 3.4C) RTs due to dATP incorporation onto the pre-bound RT-T/P complex (pre-steady state kinetics), which is followed by a slower, linear phase of product formation corresponding to the steady-state kinetics associated with multiple rounds of DNA polymerization. By fitting these results to the burst equation (Eq.1), we observed that 12-30% the SIVmac239 RT variant proteins are active.

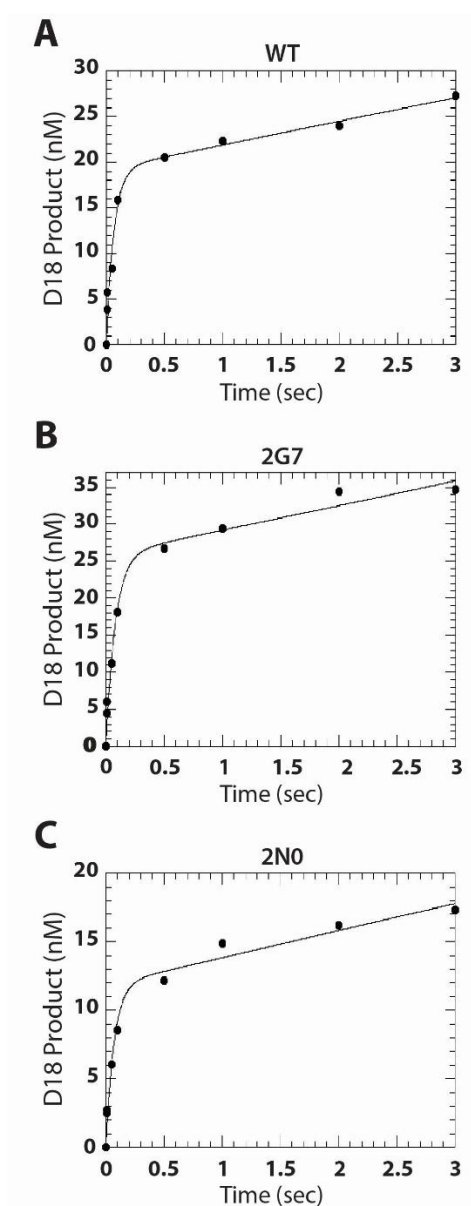


Figure 3.4: Active site determination for wild type SIVmac239 RT and Vpx (-) 2G7 and 2N0 RT variants. Pre-steady state burst kinetics of (A) WT, (B) 2G7, and (C) 2N0 SIVmac239 RTs detailing the incorporation a single dATP molecule onto A-T/P in excess T/P conditions (Experimental Procedures, 3 T/P: 1 active RT) was used to determine the active site concentration of these proteins. The solid line represents the fit of the data to a burst equation (Eq 1). Burst experiments were conducted in triplicate for each enzyme. These RT proteins display 15-30% active enzyme.

Next, using concentrations of dTTP ranging from 1.6-100 μM , 250 nM active RT, and a 5'- ^{32}P -labelled 22mer T primer annealed to the same 39mer DNA template used for the active site determination (T-T/P), we determined the rate of pre-steady state single nucleotide incorporation at each dNTP concentration (Eq. 2). The resulting rates were then plotted as a function of substrate concentration and fit to a non-linear regression curve equation (Eq. 3) to obtain k_{pol} and K_{d} values. As summarized in Table 3.5 and Figure 3.5A, 2G7 displays faster rates of nucleotide incorporation (35.29 sec^{-1}) compared to 2N0 (21.35 sec^{-1}) and WT SIVmac239 RT (20.29 sec^{-1}). While previous studies have shown that SAMHD1 counteracting and non-counteracting lentiviral RTs are characterized by similar K_{d} values [27, 29], both Vpx (-) RTs displayed lower K_{d} values (2G7: $15.99 \mu\text{M}$, 2N0: $17.28 \mu\text{M}$) compared to WT SIVmac239 RT ($33.32 \mu\text{M}$) (Table 3.5, Figure 3.5B). Overall, incorporation efficiency for 2G7 ($2.33 \text{ sec}^{-1}\mu\text{M}^{-1}$) and 2N0 ($1.28 \text{ sec}^{-1}\mu\text{M}^{-1}$) is 2-3 fold greater than that of WT RT ($0.61 \text{ sec}^{-1}\mu\text{M}^{-1}$) (Table 3.5, Figure 3.5C). Since the increased pre-steady state kinetic activity of 2G7 and 2N0 could be due to their shared amino acid mutations, Vpx (-) RT mutant 1M6 was also kinetically assessed. Like 2G7 and 2N0, T_{m} measurements revealed that 1M6 is not significantly less stable than WT SIVmac239 RT, inferring it is not structurally impaired (Table 3.2). 1M6 contains 10 nucleic acid mutations and 8 amino acid mutations, none of which are shared by 2G7 or 2N0 (Table 3.3). Vpx (-) RT 1M6 displayed faster k_{pol} (31.48 sec^{-1}) and lower K_{d} ($22.34 \mu\text{M}$) values than WT SIVmac239 RT, resulting in a significantly larger incorporation efficiency ($1.44 \text{ sec}^{-1}\mu\text{M}^{-1}$) (Table 3.5, Figure 3.5). This result suggests that Vpx (-) RTs can achieve increased enzyme kinetics through numerous differential amino acid mutations.

Table 3.5: Pre-steady state dTTP incorporation by wild type SIVmac239 RT and Vpx (-) RT variants 2G7, 2N0, and 1M6 from DNA template.

RT	K_{d} (μM)	k_{pol} (sec^{-1})	$k_{\text{pol}}/K_{\text{d}}$ ($\text{sec}^{-1}\mu\text{M}^{-1}$)
WT	33.32 ± 2.27	20.29 ± 1.06	0.61 ± 0.01
2G7	15.99 ± 4.86	35.29 ± 0.36	2.33 ± 0.61
2N0	17.28 ± 2.89	21.35 ± 3.24	1.28 ± 0.42
1M6	22.34 ± 4.25	31.48 ± 1.75	1.44 ± 0.28

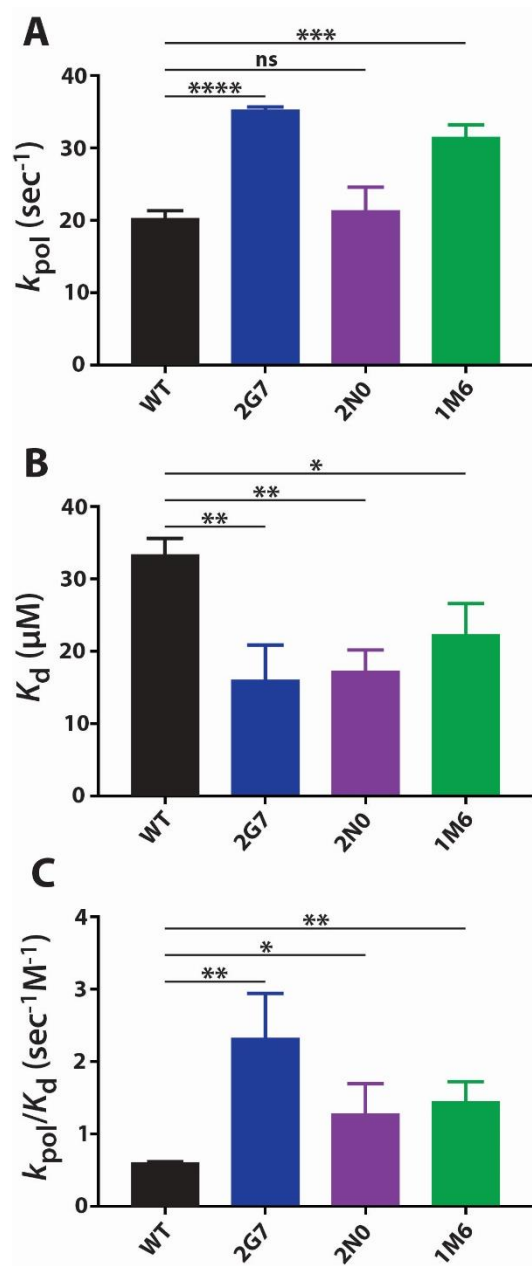


Figure 3.5: Pre-steady state kinetic activity of Vpx (-) 2G7, 2N0 RT, and 1M6 RT variants compared to that of wild type SIVmac239 RT. Pre-steady state kinetic values were determined for WT SIVmac239 RT and Vpx (-) RTs 2G7, 2N0, and 1M6 with dTTP using a DNA template (Table 3.4) as described in Experimental Procedures. The assays were conducted in triplicate before k_{pol} (A), K_d (B), and incorporation efficiency (k_{pol}/K_d) (C) values of Vpx (-) RTs were compared to that of wild type RT. Statistical significance from unpaired two-tailed student's t-tests is indicated as: ns, $p < 0.1234$; *, $p < 0.0332$; **, $p < 0.0021$; ***, $p < 0.002$; ****, $p < 0.0001$.

Discussion

It was previously demonstrated that the limited intracellular dNTP pools found in nondividing myeloid cells restrict lentiviral reverse transcription, and that this limited dNTP availability is a biochemical restriction factor against HIV-1 RT in nondividing myeloid target cells^[8]. Later studies revealed that host dNTPase SAMHD1 is responsible for the low dNTP pools found in these nondividing target cells^[16, 44, 45], and that, for SAMHD1 non-counteracting lentiviruses (beyond and including HIV-1), the SAMHD1-mediated low dNTP pools in macrophages serve as a kinetic hurdle that delays complete reverse transcription and slows proviral DNA synthesis kinetics during the course of viral replication. Indeed, SAMHD1 is a strong myeloid-specific HIV-1 restriction factor that can suppress three distinct intracellular dNTP-dependent steps during a single HIV-1 lifecycle, 1) reverse transcription, 2) DNA gap filling, and 3) endogenous reverse transcription^[46]. Conversely, SAMHD1 counteracting lentiviruses, like SIVmac239, employ viral Vpx proteins to target host dNTPase SAMHD1 for proteasomal degradation, resulting in increased cellular dNTPs and the alleviation of kinetic restriction.

Studies have shown that RTs from lentiviruses without the ability to counteract SAMHD1 have evolved over time to execute a faster enzyme conformational change during dNTP incorporation. This enables SAMHD1 non-counteracting lentiviruses to circumvent SAMHD1 restriction and complete reverse transcription even in the low dNTP concentrations found in nondividing myeloid cells. Since kinetic similarities are seen amongst RTs originating from various lentiviral phylogroups depending on their ability or inability to counteract SAMHD1, the evolution of SAMHD1 non-counteracting lentiviral RTs is presumed to have occurred over many years and by viral passage through many hosts^[47, 48]. In this study, we reasoned that SIVmac239 RT—an enzyme known to synthesize DNA with low efficiency within the limited dNTP pools of the macrophage^[27, 28]—can improve its enzyme kinetics to resemble enzymatically efficient HIV-1 RT when SIVmac239 virus replicates within animals in the absence of Vpx (like HIV-1), an *in vivo* environment likely to create a strong anti-viral selective pressure in myeloid cells due to the presence of host SAMHD1.

SIVmac239 RT proteins assayed in this study originated from single infected animal sources with survival durations of 27-29 weeks and 3 years post-infection for Vpx (+) and Vpx (-) infections respectively. We found that RTs originating from Vpx (-) infections, on average, contained more amino acid mutations and display faster steady state and pre-steady state kinetics than WT SIVmac239 RT and RTs cloned from Vpx (+) infections. However, since Vpx (-) animals lived roughly six times longer than the Vpx (+) animals used in this study, we cannot exclude the possibility that the mutations we observed in Vpx (-) RTs are the result of randomly accumulated viral mutagenesis rather than mutations that have been selected for due to the evolutionary pressure exerted by the absence of Vpx^[49-51]. It is also possible that some of the commonly observed mutations are escape products resulting from certain types of immune selections. Lastly, since *vpx* is the result of a gene duplication event of *vpr*, both proteins have been found to have the potential to counteract SAMHD1, depending on the species origins of the viral Vpx/Vpr and host SAMHD1 proteins. While SIVmac239 Vpr does not possess SAMHD1 counteraction activity, it is possible that Vpx (-) viruses evolved a Vpr protein that can induce the degradation of host dNTPase SAMHD1. Vpx protein was cloned and sequenced from Vpx (-) infected samples in a manner identical to the RTs in this study, revealing truncated *vpx* genes that presumably resulted in no protein product (data not shown). However, neither the anti-SAMHD1 activity of Vpr nor the SAMHD1 protein expression in Vpx (-)-infected cells were verified in this study. Therefore, we cannot negate the possibility that Vpx (-) viruses evolved SAMHD1-counteraction ability through the evolution of Vpr.

As shown in our data, the selected SIVmac239 RT variants from Vpx (-) infections improved their steady state DNA synthesis abilities by having lower K_m values and higher dNTP binding affinity (K_d), compared to wild type SIVmac239 RT. While both 2G7 and 1M6 displayed faster k_{pol} values, 2N0 exhibited no significant difference from WT SIVmac239 RT. These kinetic changes are different from the uniformity we observed between SAMHD1 non-counteracting HIV-1 RTs and SAMHD1 counteracting SIV RTs: HIV-1 RT is characterized by lower steady state K_m values, similar K_d values, and faster pre-steady state k_{pol} values when compared to SIV RT^[27, 28]. To improve their enzyme kinetic efficiency, it appears that the two SIVmac239 RT variants (2G7 and 2N0), originating from a single Vpx (-) infection, employ differential

mechanistic pathways than what has been previously observed for HIV-1 RTs. Multiple-nucleotide incorporation experiments revealed that Vpx (-) RTs, on average, display substrate efficiency values two-fold greater than those observed for Vpx (+) RTs. While a two-fold difference seems minute in number, a two-fold kinetic increase *in vivo* translates into a 6-hour replication period rather than 12 hours, thus drastically decreasing the time required for viral replication. Conversely, a two-fold decrease in kinetics would result in replication taking 24 hours rather than 12 hours—exposing the viral material to cellular defenses for longer durations of time and potentially negatively impacting viral replication.

With no solved structure for the SIV RT heterodimer, a structure of heterodimeric HIV-1 RT bound to nucleic acid (PDB ID: 1RTD) was used to highlight the location of the equivalent residues mutated in Vpx (-) RT clones 2G7 (top panels), 2N0 (middle panels), and 1M6 (bottom panels) (Figure 3.6). This structure of HIV-1 RT shows a large portion of the p66 subunit participating in T/P binding. Interestingly, all three clones contain mutations of residues near the T/P binding cleft, providing possibility that these mutations may impact not only the formation of the binary complex but also polymerase processivity during steady state polymerization. While many mutations are surface exposed (i.e. 3 out of 4 residues in 2G7; 2 out of 4 in 2N0; 4 out of 8 residues in 1M6), residue M164 lies just outside of the active site and is not only substituted in both 2G7 and 2N0 RTs, but has also been adopted by 38 out of the 40 RT variants cloned from one Vpx (-) infected animal (Table 3.1). Additionally, 1M6 contains substitutions of three residues near the heterodimeric interface: A158, K357, and A368. Nevertheless, since Vpx (-) RT variants contain substitutions at residues that are not close to any known residues involved in dNTP binding or catalysis in HIV-1 RT, it is difficult to explain the mechanistic and structural impact made by the various combinations of the observed mutations. Possibly, some, or all, of the mutations found in the three Vpx (-) RTs indirectly coordinate local structural changes to improve dNTP binding affinity in these polymerases.

Finally, these biochemical findings can be further verified through virological investigations that compare the viral infectivity of infectious SIVmac239ΔVpx mutant virus harboring the two Vpx (-) RT variants to that of SIVmac239ΔVpx encoding for wild type RT. These experiments seek to characterize the differential impact of these mutated RTs during single round infection in activated CD4⁺ T cells and

macrophages. Further studies could also identify the specific RT amino acid mutations contributing to the altered enzyme kinetics in Vpx (-) RTs and explore the associated mechanisms. Collectively, these sequencing and kinetic studies support the idea that the absence of Vpx in SIVmac239 infections results in RT enzymes with more numerous amino acid mutations and enhanced kinetics which enable more efficient polymerization from RNA and DNA templates.

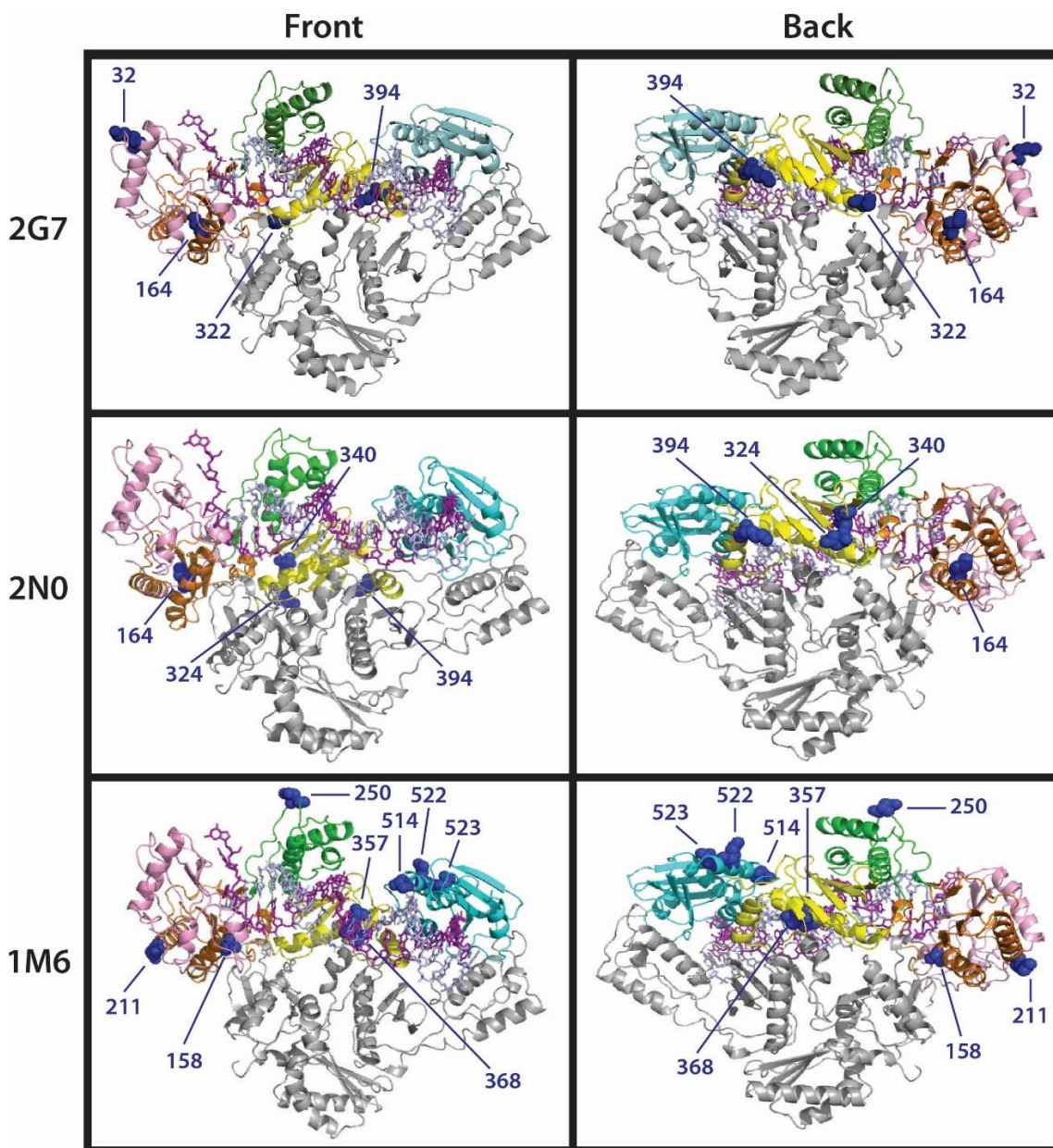


Figure 3.6: Location of mutated residues in 2G7, 2N0, and 1M6 Vpx (-) RT variants. The crystal structure of heterodimeric HIV-1 RT bound to nucleic acid (PDB ID: 1RTD) was used to map the location of the equivalent mutated residues (blue spheres) in 2G7 (first row), 2N0 (second row), and 1M6 (third row) SIVmac239 Vpx (-) RT variants. Front and back views of the polymerase are displayed in the first and second column respectively. The p66 fingers (pink), palm (orange), thumb (green), connection (yellow), and RNaseH (cyan) subdomains and p51 (grey) subunits are color coordinated in agreement with Figure 1.6.

References

1. Mori K, Ringler DJ, Kodama T, Desrosiers RC. Complex determinants of macrophage tropism in env of simian immunodeficiency virus. *J Virol* 1992; 66(4):2067-2075.
2. Jamburuthugoda VK, Chugh P, Kim B. Modification of human immunodeficiency virus type 1 reverse transcriptase to target cells with elevated cellular dNTP concentrations. *J Biol Chem* 2006; 281(19):13388-13395.
3. Weissman D, Rabin RL, Arthos J, Rubbert A, Dybul M, Swofford R, et al. Macrophage-tropic HIV and SIV envelope proteins induce a signal through the CCR5 chemokine receptor. *Nature* 1997; 389(6654):981-985.
4. Swanstrom AE, Del Prete GQ, Deleage C, Elser SE, Lackner AA, Hoxie JA. The SIV Envelope Glycoprotein, Viral Tropism, and Pathogenesis: Novel Insights from Nonhuman Primate Models of AIDS. *Curr HIV Res* 2018; 16(1):29-40.
5. Bejarano DA, Puertas MC, Borner K, Martinez-Picado J, Muller B, Krausslich HG. Detailed Characterization of Early HIV-1 Replication Dynamics in Primary Human Macrophages. *Viruses* 2018; 10(11).
6. Williams KC, Hickey WF. Central nervous system damage, monocytes and macrophages, and neurological disorders in AIDS. *Annu Rev Neurosci* 2002; 25:537-562.
7. Traut TW. Physiological concentrations of purines and pyrimidines. *Mol Cell Biochem* 1994; 140(1):1-22.
8. Diamond TL, Roshal M, Jamburuthugoda VK, Reynolds HM, Merriam AR, Lee KY, et al. Macrophage tropism of HIV-1 depends on efficient cellular dNTP utilization by reverse transcriptase. *J Biol Chem* 2004; 279(49):51545-51553.
9. Schmidt S, Schenkova K, Adam T, Erikson E, Lehmann-Koch J, Sertel S, et al. SAMHD1's protein expression profile in humans. *J Leukoc Biol* 2015; 98(1):5-14.

10. Jin C, Peng X, Liu F, Cheng L, Lu X, Yao H, et al. MicroRNA-181 expression regulates specific post-transcriptional level of SAMHD1 expression in vitro. *Biochem Biophys Res Commun* 2014; 452(3):760-767.
11. Hollenbaugh JA, Tao S, Lenzi GM, Ryu S, Kim DH, Diaz-Griffero F, et al. dNTP pool modulation dynamics by SAMHD1 protein in monocyte-derived macrophages. *Retrovirology* 2014; 11:63.
12. Franzolin E, Pontarin G, Rampazzo C, Miazzi C, Ferraro P, Palumbo E, et al. The deoxynucleotide triphosphohydrolase SAMHD1 is a major regulator of DNA precursor pools in mammalian cells. *Proc Natl Acad Sci U S A* 2013; 110(35):14272-14277.
13. Plitnik T, Sharkey ME, Mahboubi B, Kim B, Stevenson M. Incomplete Suppression of HIV-1 by SAMHD1 Permits Efficient Macrophage Infection. *Pathogens and Immunity* 2018; 3(2):197.
14. Kim B, Nguyen LA, Daddacha W, Hollenbaugh JA. Tight interplay among SAMHD1 protein level, cellular dNTP levels, and HIV-1 proviral DNA synthesis kinetics in human primary monocyte-derived macrophages. *J Biol Chem* 2012; 287(26):21570-21574.
15. Hrecka K, Hao C, Gierszewska M, Swanson SK, Kesik-Brodacka M, Srivastava S, et al. Vpx relieves inhibition of HIV-1 infection of macrophages mediated by the SAMHD1 protein. *Nature* 2011; 474(7353):658-661.
16. Laguette N, Sobhian B, Casartelli N, Ringeard M, Chable-Bessia C, Segéral E, et al. SAMHD1 is the dendritic- and myeloid-cell-specific HIV-1 restriction factor counteracted by Vpx. *Nature* 2011; 474(7353):654-657.
17. Hrecka K, Gierszewska M, Srivastava S, Kozackiewicz L, Swanson SK, Florens L, et al. Lentiviral Vpr usurps Cul4-DDB1[VprBP] E3 ubiquitin ligase to modulate cell cycle. *Proc Natl Acad Sci U S A* 2007; 104(28):11778-11783.
18. Ahn J, Hao C, Yan J, DeLucia M, Mehrens J, Wang C, et al. HIV/simian immunodeficiency virus (SIV) accessory virulence factor Vpx loads the host cell restriction factor SAMHD1 onto the E3 ubiquitin ligase complex CRL4DCAF1. *J Biol Chem* 2012; 287(15):12550-12558.

19. Srivastava S, Swanson SK, Manel N, Florens L, Washburn MP, Skowronski J. Lentiviral Vpx accessory factor targets VprBP/DCAF1 substrate adaptor for cullin 4 E3 ubiquitin ligase to enable macrophage infection. *PLoS Pathog* 2008; 4(5):e1000059.
20. Lahouassa H, Daddacha W, Hofmann H, Ayinde D, Logue EC, Dragin L, et al. SAMHD1 restricts the replication of human immunodeficiency virus type 1 by depleting the intracellular pool of deoxynucleoside triphosphates. *Nat Immunol* 2012; 13(3):223-228.
21. Etienne L, Hahn BH, Sharp PM, Matsen FA, Emerman M. Gene loss and adaptation to hominids underlie the ancient origin of HIV-1. *Cell Host Microbe* 2013; 14(1):85-92.
22. Sharp PM, Bailes E, Stevenson M, Emerman M, Hahn BH. Gene acquisition in HIV and SIV. *Nature* 1996; 383(6601):586-587.
23. Zhou X, DeLucia M, Hao C, Hrecka K, Monnie C, Skowronski J, et al. HIV-1 Vpr protein directly loads helicase-like transcription factor (HLTF) onto the CRL4-DCAF1 E3 ubiquitin ligase. *J Biol Chem* 2017; 292(51):21117-21127.
24. Belzile JP, Duisit G, Rougeau N, Mercier J, Finzi A, Cohen EA. HIV-1 Vpr-mediated G2 arrest involves the DDB1-CUL4AVPRBP E3 ubiquitin ligase. *PLoS Pathog* 2007; 3(7):e85.
25. Lim Efreem S, Fregoso Oliver I, McCoy Connor O, Matsen Frederick A, Malik Harmit S, Emerman M. The Ability of Primate Lentiviruses to Degrade the Monocyte Restriction Factor SAMHD1 Preceded the Birth of the Viral Accessory Protein Vpx. *Cell Host & Microbe* 2012; 11(2):194-204.
26. Fregoso OI, Ahn J, Wang C, Mehrens J, Skowronski J, Emerman M. Evolutionary toggling of Vpx/Vpr specificity results in divergent recognition of the restriction factor SAMHD1. *PLoS Pathog* 2013; 9(7):e1003496.
27. Lenzi GM, Domaoal RA, Kim DH, Schinazi RF, Kim B. Mechanistic and Kinetic Differences between Reverse Transcriptases of Vpx Coding and Non-coding Lentiviruses. *J Biol Chem* 2015; 290(50):30078-30086.
28. Lenzi GM, Domaoal RA, Kim DH, Schinazi RF, Kim B. Kinetic variations between reverse transcriptases of viral protein X coding and noncoding lentiviruses. *Retrovirology* 2014; 11:111.

29. Coggins SA, Holler JM, Kimata JT, Kim DH, Schinazi RF, Kim B. Efficient pre-catalytic conformational change of reverse transcriptases from SAMHD1 non-counteracting primate lentiviruses during dNTP incorporation. *Virology* 2019; 537:36-44.
30. Gibbs JS, Regier DA, Desrosiers RC. Construction and in vitro properties of SIVmac mutants with deletions in "nonessential" genes. *AIDS Res Hum Retroviruses* 1994; 10(4):333-342.
31. Desrosiers RC, Lifson JD, Gibbs JS, Czajak SC, Howe AY, Arthur LO, et al. Identification of highly attenuated mutants of simian immunodeficiency virus. *J Virol* 1998; 72(2):1431-1437.
32. Westmoreland SV, Converse AP, Hrecka K, Hurley M, Knight H, Piatak M, et al. SIV vpx is essential for macrophage infection but not for development of AIDS. *PLoS One* 2014; 9(1):e84463.
33. Connor RI, Sheridan KE, Ceradini D, Choe S, Landau NR. Change in coreceptor use correlates with disease progression in HIV-1--infected individuals. *J Exp Med* 1997; 185(4):621-628.
34. Kim B. Genetic selection in Escherichia coli for active human immunodeficiency virus reverse transcriptase mutants. *Methods* 1997; 12(4):318-324.
35. Skasko M, Weiss KK, Reynolds HM, Jamburuthugoda V, Lee K, Kim B. Mechanistic differences in RNA-dependent DNA polymerization and fidelity between murine leukemia virus and HIV-1 reverse transcriptases. *J Biol Chem* 2005; 280(13):12190-12200.
36. Kati WM, Johnson KA, Jerva LF, Anderson KS. Mechanism and fidelity of HIV reverse transcriptase. *J Biol Chem* 1992; 267(36):25988-25997.
37. Reardon JE. Human immunodeficiency virus reverse transcriptase: steady-state and pre-steady-state kinetics of nucleotide incorporation. *Biochemistry* 1992; 31(18):4473-4479.
38. Johnson KA. Rapid quench kinetic analysis of polymerases, adenosinetriphosphatases, and enzyme intermediates. *Methods Enzymol* 1995; 249:38-61.
39. Hollenbaugh JA, Montero C, Schinazi RF, Munger J, Kim B. Metabolic profiling during HIV-1 and HIV-2 infection of primary human monocyte-derived macrophages. *Virology* 2016; 491:106-114.
40. Yutani K, Ogasahara K, Sugino Y. Effect of amino acid substitutions on conformational stability of a protein. *Adv Biophys* 1985; 20:13-29.

41. Miyazawa S, Jernigan RL. Protein stability for single substitution mutants and the extent of local compactness in the denatured state. *Protein Eng* 1994; 7(10):1209-1220.
42. Parker WB, White EL, Shaddix SC, Ross LJ, Buckheit RW, Germany JM, et al. Mechanism of inhibition of human immunodeficiency virus type 1 reverse transcriptase and human DNA polymerases alpha, beta, and gamma by the 5'-triphosphates of carbovir, 3'-azido-3'-deoxythymidine, 2',3'-dideoxyguanosine and 3'-deoxythymidine. A novel RNA template for the evaluation of antiretroviral drugs. *Journal of Biological Chemistry* 1991; 266(3):1754-1762.
43. Reardon JE, Miller WH. Human immunodeficiency virus reverse transcriptase. Substrate and inhibitor kinetics with thymidine 5'-triphosphate and 3'-azido-3'-deoxythymidine 5'-triphosphate. *Journal of Biological Chemistry* 1990; 265(33):20302-20307.
44. Coggins SA, Mahboubi B, Schinazi RF, Kim B. SAMHD1 Functions and Human Diseases. *Viruses* 2020; 12(4).
45. Goldstone DC, Ennis-Adeniran V, Hedden JJ, Groom HC, Rice GI, Christodoulou E, et al. HIV-1 restriction factor SAMHD1 is a deoxynucleoside triphosphate triphosphohydrolase. *Nature* 2011; 480(7377):379-382.
46. Mahboubi B, Gavegnano C, Kim DH, Schinazi RF, Kim B. Host SAMHD1 protein restricts endogenous reverse transcription of HIV-1 in nondividing macrophages. *Retrovirology* 2018; 15(1):69.
47. Yokoyama S, Chung L, Gojobori T. Molecular evolution of the human immunodeficiency and related viruses. *Mol Biol Evol* 1988; 5(3):237-251.
48. Yokoyama S. Molecular evolution of the human and simian immunodeficiency viruses. *Mol Biol Evol* 1988; 5(6):645-659.
49. Mansky LM. Forward mutation rate of human immunodeficiency virus type 1 in a T lymphoid cell line. *AIDS Res Hum Retroviruses* 1996; 12(4):307-314.
50. Coffin JM. HIV population dynamics in vivo: implications for genetic variation, pathogenesis, and therapy. *Science* 1995; 267(5197):483-489.

51. Mansky LM. Retrovirus mutation rates and their role in genetic variation. *J Gen Virol* 1998; 79 (Pt 6):1337-1345.

Chapter 4: General Discussion

The connection between cell permissivity and viral polymerase kinetics is one that the Kim Lab has been working to characterize for over a decade. While gammaretroviruses like MuLV and FeLV replicate exclusively in dividing cells, the cellular tropism of lentiviruses like HIV and SIV include both dividing and nondividing target cell types^[342, 343]. Development of a sensitive, RT-based dNTP quantification assay revealed a stark distinction between the intracellular environments of dividing and nondividing HIV/SIV target cells: while dividing activated CD4⁺ T cells house 2-5 μM dNTPs, nondividing MDMs contain dNTP concentrations that are 100-250 fold lower (20-40 nM)^[289]. Previous studies have shown that differences in target cell dNTP concentrations are mirrored by viral polymerase kinetics, as lentiviral (e.g. HIV, SIV, and FIV) RTs possess lower K_m and higher K_d values than non-lentiviral (e.g. MuLV and FeLV) RTs^[337, 338]. Interestingly, vectors containing mutant HIV-1 RTs with reduced dNTP binding affinities (i.e. higher K_d) failed to infect macrophages, thus suggesting that the ability of HIV-1 RT to synthesize DNA in cellular environments with limited dNTP substrate enables HIV-1 to infect nondividing macrophage populations.

Disparities in RT enzyme kinetics are not only seen along the basis of lentiviral classification, but also within the *Lentiviridae* genus itself. Kinetic differences between RTs from HIV-1 and HIV-2 viruses were observed as early as 1991: Hizi et al. reported that steady state K_m values for single dNTP incorporation events were significantly lower for HIV-1 RT when compared to HIV-2 RT^[98]. The role of the dNTPase SAMHD1 as a lentiviral restriction factor was exposed in 2011, confirming previous hypotheses that the low dNTP concentrations in macrophages lay at the foundation of the restrictive, rather than permissive, HIV-1 infections of these nondividing myeloid cell types^[344, 345]. Though SAMHD1 was previously known as one of the seven proteins involved in Aicardi–Goutières Syndrome (AGS), a rare genetic encephalopathy that mimics a congenital viral infection^[346], further studies found that selective counteraction of this host restriction factor by lentiviral Vpr or Vpx proteins elevated cellular dNTPs above the K_m of HIV-1 RT and enabled efficient proviral DNA synthesis in an otherwise restrictive intracellular environment^[128, 291, 347]. Indeed, both *in vitro* (cellular) and *in vivo* (animal) studies have demonstrated that

Vpx is essential for HIV-2 and SIVmac replication in nondividing myeloid cells^[348-350]. Interestingly, despite the importance of SAMHD1 counteraction in the replication of some SIV strains and HIV-2, some lentiviruses (e.g. HIV-1) harbor Vpr proteins that lack the ability to induce proteasomal degradation of this host restriction factor. Lim et al. determined the common ancestral SIV of all HIV/SIV lineages likely encoded a single Vpr protein that lacked SAMHD1-counteraction ability^[125]. It is postulated, then, that Vpr adapted the ability to induce SAMHD1 degradation during the split of SIVagm and SIVdeb/mus/mon lineages prior to the birth of Vpx through a gene duplication event. Since Vpr/Vpx directly interacts with SAMHD1 in the pro-degradation complex, studies have identified that viral Vpr/Vpx proteins co-evolve with host SAMHD1, toggling between interactions with the N- and C-terminus of the restriction factor and driving positive selection for SAMHD1 mutations that disrupt the Vpr/Vpx-SAMHD1 interface^[137]. Similar virus-host evolutionary arms races have resulted in the coevolution of viral Vif and host restriction factor APOBEC3G^[351] as well as the adaptation of HIV-1 Vpu when human tetherin proved itself resistant to degradation by Nef^[352].

SAMHD1 counteraction by lentiviral Vpr and Vpx proteins coupled with the known kinetic variations between HIV-1 and HIV-2 RTs presents potential for a fascinating virus-host evolutionary dynamic, whereby restriction of viral replication by host dNTPase SAMHD1 can possibly spur divergent lentiviral evolutionary pathways: kinetic enhancement of viral RT in the case of HIV-1 and elevation of intracellular dNTPs through viral counteraction of SAMHD1 in the case of HIV-2 and some SIVs. The thesis work of Dr. Gina M. Lenzi delved into this divergent evolutionary scenario and assessed the kinetic differences between RTs originating from SAMHD1 counteracting and non-counteracting lentiviruses. RTs from SAMHD1 non-counteracting viruses (e.g. HIV-1) were found to be characterized by lower K_m values and faster rates of polymerization when compared to RTs from SAMHD1 counteracting lentiviruses (e.g. SIVmac239)^[339, 340] (Figure 1.7). Phylogenetic analysis of RT and Vpr/Vpx amino acid sequences from SAMHD1 counteracting and non-counteracting lentiviruses are consistent with this data, displaying similar clustering patterns with respect to viral ability or disability to induce host SAMHD1 degradation^[353].

This thesis expanded upon the culmination of this work: first seeking to identify which polymerization step is accelerated by SAMHD1 non-counteracting lentiviral RTs in order to achieve the observed enhanced enzyme kinetics. In Chapter 2 we found that, relative to SAMHD1 counteracting lentiviral RTs (e.g. SIVagm9063-2 and SIVmne CL8 RTs), SAMHD1 non-counteracting lentiviral RTs (e.g. SIVcpz and HIV-1 Cy RTs) execute a faster conformational change step (i.e. faster K_{conf}) during the incorporation of a dNTP substrate—this enables circumvention of SAMHD1 restriction in nondividing cells, like macrophages, eliminating the need for Vpr/Vpx^[354]. This suggests that the low dNTP pools within nondividing myeloid cells exert selective pressure on viral RT proteins during infection by SAMHD1 non-counteracting lentivirus, evolutionarily honing the enzymes to complete slow proviral DNA synthesis despite the strikingly low substrate availability in these target cells. This evolutionary pressure is absent in SAMHD1 counteracting lentiviral infections since virus induced SAMHD1 degradation results in increased intracellular dNTP concentrations and promotes efficient reverse transcription in nondividing macrophages. This work provides a mechanism detailing how SAMHD1 non-counteracting lentiviral RTs achieve improved enzyme kinetics when compared to SAMHD1 counteracting lentiviral RTs and provides support for the intimate connection between polymerase kinetics and dNTP substrate availability.

Since previous studies observed differences between RTs from SAMHD1 counteracting and non-counteracting lentiviruses that are separated by centuries of evolution, in Chapter 3 we sought to investigate whether SIVmac239 RT underwent similar enzymatic improvement in the absence of Vpx during the course of pathogenesis in a single host. To investigate this question, we cloned RTs from animals that were infected with either wild type SIVmac239 virus (i.e. Vpx (+) virus) or a Vpx-deleted mutant of SIVmac239 virus (i.e. Vpx (-) virus). We selected samples collected upon the development of AIDS characteristics to ensure the studied RT proteins had undergone the entirety of in vivo evolution. While earlier timepoints would have been crucial in mapping the appearance and potential selection for various RT mutations, samples collected at 1- and 2 years post infection contained such low viral load that RT-PCR did not amplify RT sequences for subsequent cloning efforts. Using samples collected upon AIDS diagnoses (3 years post

infection), we found that RTs from Vpx (-) animals are characterized by improved steady state and pre-steady state kinetics when compared to RTs from Vpx (+) infections. In addition, Vpx (-) RT variants contain more numerous amino acid mutations than Vpx (+) RTs, all of which are indiscriminately dispersed throughout the polymerase subdomains. Since Vpx (-) infected animals lived 3-6 times longer than Vpx (+) infected animals, we cannot state with certainty—without data from earlier infection timepoints—whether the observed mutations and improved kinetics of Vpx (-) RTs were the result of evolutionary selection or the byproduct of random viral mutagenesis derived from prolonged pathogenesis within the host.

The kinetic disparities between Vpx (+) and Vpx (-) RT variants are different than those seen between SAMHD1 counteracting and non-counteracting lentiviral RTs. Dr. Lenzi found that while SAMHD1 counteracting and non-counteracting RTs display similar k_{cat} and K_{d} values, SAMHD1 non-counteracting lentiviral RTs are characterized by lower K_{m} and faster k_{pol} values when compared to SAMHD1 counteracting lentiviral RTs^[339, 340]. Conversely, in steady state studies, Vpx (-) variants 2G7 and 2N0 RTs display lower K_{m} values than wild type (WT) RT only when polymerizing from a DNA template (showing no statistical difference in K_{m} values when using an RNA template). Interestingly, while 2N0 has higher a k_{cat} value than WT RT independent of template type, 2G7 only displays a significantly larger k_{cat} value when polymerizing from a DNA template. Pre-steady state studies revealed that all three Vpx (-) RT variants—2G7, 2N0, and 1M6—display lower K_{d} values than WT RT when using a DNA template. However, unlike SAMHD1 non-counteracting lentiviral RTs, the three Vpx (-) RT clones do not reflect uniformly larger k_{pol} values than WT SIVmac239 RT (i.e. SAMHD1 counteracting RT). Instead, only 2G7 and 1M6 are characterized by larger k_{pol} values than WT RT when synthesizing DNA from a DNA template. Collectively, these steady state and pre-steady state data demonstrate that while Vpx (-) RTs display improved enzyme kinetics when compared to Vpx (+) and WT RTs, the mechanisms employed to obtain enhanced enzyme performance appear to be different than those previously observed for SAMHD1 non-counteracting lentiviral RTs. Since the identified mutations in Vpx (-) RTs are not located near residues involved in polymerase catalysis, dNTP substrate binding, or T/P binding, it is difficult to predict the structural or mechanistic impact of each individual mutation. It is possible that some, or all, of the observed

mutations contribute to increased binding affinities, altered polymerase fidelity, improved polymerase processivity, or more efficient structural changes during polymerization.

Further studies can (i) compare the steady state and pre-steady state kinetic activity of Vpx (-) RT variants and SAMHD1 non-counteracting lentiviral RTs like HIV-1 RT, (ii) characterize the processivity of Vpx (+) and Vpx (-) RTs during multiple nucleotide incorporation from DNA and RNA templates of significant length (e.g. > 400 nucleotides to mimic elongation during *in vivo* reverse transcription), (iii) investigate the fidelity and T/P binding activities of Vpx (+) and Vpx (-) RTs compared to WT SIVmac239 RT (iv) identify which amino acid mutations are responsible for the enhanced enzyme kinetics of Vpx (-) RTs, (v) elucidate the mechanisms employed by Vpx (-) RTs to achieve this improved kinetic activity, and (vi) characterize the infectivity of SIVmac239 Vpx (-) viruses containing Vpx (-) RT variants in dividing and nondividing target cell types. Additionally, while recent studies observed viral infectivity after swapping HIV-1 RT for SIV RT^[355], these experiments failed to consider the role of important sequences that lie outside the *pol* gene—namely variable sequences within the LTR regions and the PBS that can influence proviral DNA synthesis and subsequent viral infectivity. Further experiments must take into account these regions of sequence variability in order to properly assess the influence of SAMHD1 non-counteracting lentiviral RTs within an HIV-1 background. Lastly, more in-depth investigations regarding the role and mechanism of pSAMHD1 in HIV-1 restriction could help elucidate a potential dNTPase-independent mechanism of host restriction and possibly expand our understanding of viral SAMHD1 counteraction via Vpr/Vpx proteins past its implications in the modulation of intracellular dNTPs and the resulting evolution of lentiviral RT.

Ultimately, the relationship between viral pathogenicity and the ability to antagonize host restriction factors remains complicated and unclear. Unlike HIV-1, HIV-2 uses viral accessory protein Vpx to counteract host restriction factor SAMHD1 and permissively infect nondividing myeloid target cell populations; however, HIV-1 is known to be highly transmissible, characterized by significantly higher viral loads, and far more likely to progress to AIDS^[356]. Little is known regarding the differences

in pathogenicity between HIV-1 and HIV-2 viral strains—some believe virus-induced cytotoxicity in CD4⁺ T cells is the key to the aggressive pathogenicity of HIV-1 while others suspect additional viral accessory proteins or host restriction factors are at the crux of this distinction. Ultimately, the current confounding literature fails to support a specific hypothesis. SIVmnd1 and SIVmnd2 tell a similar story. While SIVmnd1 only encodes for a single Vpr protein which is inactive against mandrill SAMHD1 (mSAMHD1), SIVmnd2 encodes for both Vpr and Vpx, using the latter of the two to counteract mSAMHD1. Like HIV-1, SIVmnd1 is more pathogenic SIVmnd2^[357]. Interestingly, this dynamic appears to be unique to the viral antagonism of SAMHD1, as the narrative is a bit different when discussing the evolution of HIV-1 Vpu. HIV-1 Group M viruses to harbor Vpu proteins with the ability to not only degrade CD4 but also counteract tetherin; conversely, Group N strains lack the ability to degrade CD4 while Group O viruses are weak tetherin antagonists^[352]. HIV-1 Group M viruses constitute the majority of global HIV/AIDS cases, potentially owing in part to the dual counteraction ability of their Vpu protein.

This thesis has built upon the idea that while HIV-1 (and other SAMHD1 non-counteracting lentiviruses) cannot counteract SAMHD1, this virus has evolved alternative countermeasures that enable sufficient viral replication in target host cells, including the restrictive but slow replication in nondividing macrophages. Since HIV-2 (and other SAMHD1 counteracting lentiviruses) rely solely on SAMHD1 counteraction to infect nondividing cells, this lentivirus never requires selection for alternative mechanisms and is thus evolutionarily stunted. While the absence of Vpx during the course of SIVmac239 viral pathogenesis resulted in significantly enhanced RT enzyme kinetics (Figure 4.1), Vpx (-) virus was still undetectable in *in vivo* macrophage populations^[350]. This suggests that viral evolution within a single host is likely insufficient to overcome SAMHD1 restriction in nondividing myeloid cells. Rather, the evolutionary honing of SAMHD1 non-counteracting lentiviral RTs is the result of hundreds of years of replication within the limited intracellular dNTP environments of many host organisms—a process that has produced a viral polymerase capable of overcoming the SAMHD1-depleted dNTP pools of nondividing myeloid cells, an environment notoriously known to preclude infection by other non-lentiviruses. Collectively, these studies support our hypothesis that (i) cellular dNTP availability, and its modulation by

viral proteins, is mechanistically tethered to the kinetic properties of viral RT and (ii) the absence of SAMHD1 counteraction during lentiviral infection can drive the evolution of viral RT proteins and result in their kinetic improvement.

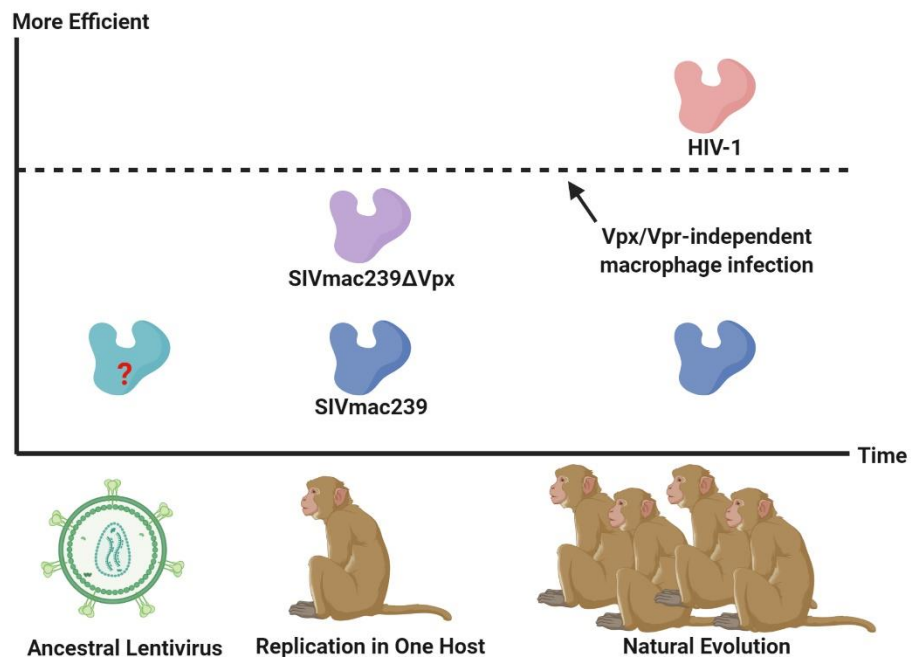


Figure 4.1: Summary of thesis work. HIV and SIV originated from a single ancestral lentivirus (green virion) that harbored common retroviral components, including a reverse transcriptase protein (green RT) with unknown kinetic properties (red question mark). Previous studies have shown that RTs from SAMHD1 non-counteracting lentiviruses, like HIV-1 (red RT), are characterized by elevated enzyme kinetics when compared to SAMHD1 counteracting lentiviral RTs, like SIVmac239 RT (blue RT). With the aid of Vpx during viral replication, SIVmac239 RT sustains no evolutionary pressure, and thus displays no significant kinetic enhancement during replication within a single host or passage through many hosts during natural evolution. Conversely, the absence of SAMHD1 counteraction in HIV-1 infections results in low dNTP pools that apply significant evolutionary pressure on the SAMHD1 non-counteracting RT. Viral replication within the low dNTP pools of many hosts over time created the kinetically honed SAMHD1 non-counteracting lentiviral polymerase that is able to efficiently polymerize proviral DNA even in low dNTP environments. Thus, the enhanced kinetics of HIV-1 RT, enable this virus to achieve Vpx/Vpr-independent

infection of nondividing target cells (dashed line). Similarly, replication of SIVmac239 Δ Vpx virus in one host organism resulted in Vpx (-) RTs (purple RT) with elevated enzyme kinetics when compared to WT SIVmac239 RT and Vpx (+) RTs. However, this increase in RT kinetics is not sufficient to overcome SAMHD1 restriction in nondividing myeloid cells *in vitro* or *in vivo*. This figure was created using Biorender.com.

References

1. Gottlieb MS, Schroff R, Schanker HM, Weisman JD, Fan PT, Wolf RA, et al. Pneumocystis carinii pneumonia and mucosal candidiasis in previously healthy homosexual men: evidence of a new acquired cellular immunodeficiency. *N Engl J Med* 1981; 305(24):1425-1431.
2. CDC. Pneumocystis Pneumonia --- Los Angeles. In: *MMWR Morb Mortal Wkly Rep* 30(21);1-3; 1981.
3. Haverkos HW, Curran JW. The current outbreak of Kaposi's sarcoma and opportunistic infections. *CA Cancer J Clin* 1982; 32(6):330-339.
4. Gerstoft J, Malchow-Moller A, Bygbjerg I, Dickmeiss E, Enk C, Halberg P, et al. Severe acquired immunodeficiency in European homosexual men. *Br Med J (Clin Res Ed)* 1982; 285(6334):17-19.
5. CDC. Opportunistic Infections and Kaposi's Sarcoma among Haitians in the United States. 1982.
6. CDC. Epidemiologic Notes and Reports Persistent, Generalized Lymphadenopathy among Homosexual Males. In: *MMWR Morb Mortal Wkly Rep* 31(19);249-51; 1982.
7. CDC. Epidemiologic Notes and Reports Immunodeficiency among Female Sexual Partners of Males with Acquired Immune Deficiency Syndrome (AIDS) -- New York. In: *MMWR Morb Mortal Wkly Rep* 31(52);697-8; 1983.
8. CDC. Current Trends Update on Acquired Immune Deficiency Syndrome (AIDS) --United States. In: *MMWR Morb Mortal Wkly Rep* 31(37);507-508,513-514; 1982.
9. Gallo RC, Sarin PS, Gelmann EP, Robert-Guroff M, Richardson E, Kalyanaraman VS, et al. Isolation of human T-cell leukemia virus in acquired immune deficiency syndrome (AIDS). *Science* 1983; 220(4599):865-867.
10. Barre-Sinoussi F, Chermann JC, Rey F, Nugeyre MT, Chamaret S, Gruest J, et al. Isolation of a T-lymphotropic retrovirus from a patient at risk for acquired immune deficiency syndrome (AIDS). *Science* 1983; 220(4599):868-871.
11. Popovic M, Sarngadharan MG, Read E, Gallo RC. Detection, isolation, and continuous production of cytopathic retroviruses (HTLV-III) from patients with AIDS and pre-AIDS. *Science* 1984; 224(4648):497-500.

12. Levy JA, Hoffman AD, Kramer SM, Landis JA, Shimabukuro JM, Oshiro LS. Isolation of lymphocytopathic retroviruses from San Francisco patients with AIDS. *Science* 1984; 225(4664):840-842.
13. Schupbach J, Popovic M, Gilden RV, Gonda MA, Sarngadharan MG, Gallo RC. Serological analysis of a subgroup of human T-lymphotropic retroviruses (HTLV-III) associated with AIDS. *Science* 1984; 224(4648):503-505.
14. Brun-Vezinet F, Barre-Sinoussi F, Saimot AG, Christol D, Montagnier L, Rouzioux C, et al. Detection of IgG antibodies to lymphadenopathy-associated virus in patients with AIDS or lymphadenopathy syndrome. *The Lancet* 1984; 323(8389):1253-1256.
15. Hahn BH, Shaw GM, Arya SK, Popovic M, Gallo RC, Wong-Staal F. Molecular cloning and characterization of the HTLV-III virus associated with AIDS. *Nature* 1984; 312(5990):166-169.
16. Luciw PA, Potter SJ, Steimer K, Dina D, Levy JA. Molecular cloning of AIDS-associated retrovirus. *Nature* 1984; 312(5996):760-763.
17. Alizon M, Sonigo P, Barre-Sinoussi F, Chermann JC, Tiollais P, Montagnier L, et al. Molecular cloning of lymphadenopathy-associated virus. *Nature* 1984; 312(5996):757-760.
18. Wain-Hobson S, Sonigo P, Danos O, Cole S, Alizon M. Nucleotide sequence of the AIDS virus, LAV. *Cell* 1985; 40(1):9-17.
19. Sanchez-Pescador R, Power MD, Barr PJ, Steimer KS, Stempien MM, Brown-Shimer SL, et al. Nucleotide sequence and expression of an AIDS-associated retrovirus (ARV-2). *Science* 1985; 227(4686):484-492.
20. Clavel F, Guetard D, Brun-Vezinet F, Chamaret S, Rey MA, Santos-Ferreira MO, et al. Isolation of a new human retrovirus from West African patients with AIDS. *Science* 1986; 233(4761):343-346.
21. Chakrabarti L, Guyader M, Alizon M, Daniel MD, Desrosiers RC, Tiollais P, et al. Sequence of simian immunodeficiency virus from macaque and its relationship to other human and simian retroviruses. *Nature* 1987; 328(6130):543-547.

22. Guyader M, Emerman M, Sonigo P, Clavel F, Montagnier L, Alizon M. Genome organization and transactivation of the human immunodeficiency virus type 2. *Nature* 1987; 326(6114):662-669.
23. CDC. HIV Surveillance Report 2018 (Updated). In; 2020.
24. UNAIDS. Fact Sheet - World AIDS Day 2019. In; 2019.
25. WHO. Progress report on HIV, viral hepatitis and sexually transmitted infections, 2019: Accountability for the global health sector strategies, 2016–2021. In; 2019.
26. Daniel MD, Letvin NL, King NW, Kannagi M, Sehgal PK, Hunt RD, et al. Isolation of T-cell tropic HTLV-III-like retrovirus from macaques. *Science* 1985; 228(4704):1201-1204.
27. Kanki PJ, McLane MF, King NW, Jr., Letvin NL, Hunt RD, Sehgal P, et al. Serologic identification and characterization of a macaque T-lymphotropic retrovirus closely related to HTLV-III. *Science* 1985; 228(4704):1199-1201.
28. Letvin NL, Daniel MD, Sehgal PK, Desrosiers RC, Hunt RD, Waldron LM, et al. Induction of AIDS-like disease in macaque monkeys with T-cell tropic retrovirus STLV-III. *Science* 1985; 230(4721):71-73.
29. Kanki P. Antibodies to Simian T-Lymphotropic Retrovirus Type Iii in African Green Monkeys and Recognition of Stlv-Iii Viral Proteins by Aids and Related Sera. *The Lancet* 1985; 325(8441):1330-1332.
30. Fultz PN, McClure HM, Anderson DC, Swenson RB, Anand R, Srinivasan A. Isolation of a T-lymphotropic retrovirus from naturally infected sooty mangabey monkeys (*Cercocebus atys*). *Proc Natl Acad Sci U S A* 1986; 83(14):5286-5290.
31. Franchini G, Gurgo C, Guo HG, Gallo RC, Collalti E, Fargnoli KA, et al. Sequence of simian immunodeficiency virus and its relationship to the human immunodeficiency viruses. *Nature* 1987; 328(6130):539-543.
32. Tsujimoto H, Cooper RW, Kodama T, Fukasawa M, Miura T, Ohta Y, et al. Isolation and characterization of simian immunodeficiency virus from mandrills in Africa and its relationship to other human and simian immunodeficiency viruses. *Journal of Virology* 1988; 62(11):4044-4050.

33. Georges-Courbot MC, Lu CY, Makuwa M, Telfer P, Onanga R, Dubreuil G, et al. Natural Infection of a Household Pet Red-Capped Mangabey (*Cercocebus torquatus torquatus*) with a New Simian Immunodeficiency Virus. *Journal of Virology* 1998; 72(1):600-608.
34. Boue V, Locatelli S, Boucher F, Ayouba A, Butel C, Esteban A, et al. High Rate of Simian Immunodeficiency Virus (SIV) Infections in Wild Chimpanzees in Northeastern Gabon. *Viruses* 2015; 7(9):4997-5015.
35. Gao F, Bailes E, Robertson DL, Chen Y, Rodenburg CM, Michael SF, et al. Origin of HIV-1 in the chimpanzee *Pan troglodytes troglodytes*. *Nature* 1999; 397(6718):436-441.
36. Gonda MA, Wong-Staal F, Gallo RC, Clements JE, Narayan O, Gildea RV. Sequence homology and morphologic similarity of HTLV-III and visna virus, a pathogenic lentivirus. *Science* 1985; 227(4683):173-177.
37. Wertheim JO, Worobey M. Dating the age of the SIV lineages that gave rise to HIV-1 and HIV-2. *PLoS Comput Biol* 2009; 5(5):e1000377.
38. Korber B, Muldoon M, Theiler J, Gao F, Gupta R, Lapedes A, et al. Timing the ancestor of the HIV-1 pandemic strains. *Science* 2000; 288(5472):1789-1796.
39. Peeters M, Courgnaud V, Abela B, Auzel P, Pourrut X, Bibollet-Ruche F, et al. Risk to human health from a plethora of simian immunodeficiency viruses in primate bushmeat. *Emerg Infect Dis* 2002; 8(5):451-457.
40. Hahn BH, Shaw GM, De Cock KM, Sharp PM. AIDS as a zoonosis: scientific and public health implications. *Science* 2000; 287(5453):607-614.
41. Apetrei C, Lerche NW, Pandrea I, Gormus B, Silvestri G, Kaur A, et al. Kuru experiments triggered the emergence of pathogenic SIVmac. *AIDS* 2006; 20(3):317-321.
42. Hirsch VM, Olmsted RA, Murphey-Corb M, Purcell RH, Johnson PR. An African primate lentivirus (SIVsm) closely related to HIV-2. *Nature* 1989; 339(6223):389-392.
43. Keele BF, Van Heuverswyn F, Li Y, Bailes E, Takehisa J, Santiago ML, et al. Chimpanzee reservoirs of pandemic and nonpandemic HIV-1. *Science* 2006; 313(5786):523-526.

44. Peeters M, Honore C, Huet T, Bedjabaga L, Ossari S, Bussi P, et al. Isolation and partial characterization of an HIV-related virus occurring naturally in chimpanzees in Gabon. *AIDS* 1989; 3(10):625-630.
45. Van Heuverswyn F, Li Y, Neel C, Bailes E, Keele BF, Liu W, et al. Human immunodeficiency viruses: SIV infection in wild gorillas. *Nature* 2006; 444(7116):164.
46. Plantier JC, Leoz M, Dickerson JE, De Oliveira F, Cordonnier F, Lemee V, et al. A new human immunodeficiency virus derived from gorillas. *Nat Med* 2009; 15(8):871-872.
47. Villabona-Arenas CJ, Ayouba A, Esteban A, D'Arc M, Mpoudi Ngole E, Peeters M. Noninvasive western lowland gorilla's health monitoring: A decade of simian immunodeficiency virus surveillance in southern Cameroon. *Ecol Evol* 2018; 8(22):10698-10710.
48. Van Heuverswyn F, Li Y, Bailes E, Neel C, Lafay B, Keele BF, et al. Genetic diversity and phylogeographic clustering of SIVcpzPtt in wild chimpanzees in Cameroon. *Virology* 2007; 368(1):155-171.
49. Sharp PM, Hahn BH. Origins of HIV and the AIDS pandemic. *Cold Spring Harb Perspect Med* 2011; 1(1):a006841.
50. Spira S, Wainberg MA, Loemba H, Turner D, Brenner BG. Impact of clade diversity on HIV-1 virulence, antiretroviral drug sensitivity and drug resistance. *J Antimicrob Chemother* 2003; 51(2):229-240.
51. Buonaguro L, Tornesello ML, Buonaguro FM. Human immunodeficiency virus type 1 subtype distribution in the worldwide epidemic: pathogenetic and therapeutic implications. *J Virol* 2007; 81(19):10209-10219.
52. Berger A, Muenchhoff M, Hourfar K, Kortenbusch M, Ambiel I, Stegmann L, et al. Severe underquantification of HIV-1 group O isolates by major commercial PCR-based assays. *Clin Microbiol Infect* 2020.
53. Peeters M, Gueye A, Mboup S, Bibollet-Ruche F, Ekaza E, Mulanga C, et al. Geographical distribution of HIV-1 group O viruses in Africa. *AIDS* 1997; 11(4):493-498.

54. Mourez T, Simon F, Plantier JC. Non-M variants of human immunodeficiency virus type 1. *Clin Microbiol Rev* 2013; 26(3):448-461.
55. D'Arc M, Ayouba A, Esteban A, Learn GH, Boue V, Liegeois F, et al. Origin of the HIV-1 group O epidemic in western lowland gorillas. *Proc Natl Acad Sci U S A* 2015; 112(11):E1343-1352.
56. Rodgers MA, Vallari AS, Harris B, Yamaguchi J, Holzmayer V, Forberg K, et al. Identification of rare HIV-1 Group N, HBV AE, and HTLV-3 strains in rural South Cameroon. *Virology* 2017; 504:141-151.
57. Vallari A, Bodelle P, Ngansop C, Makamche F, Ndembi N, Mbanya D, et al. Four new HIV-1 group N isolates from Cameroon: Prevalence continues to be low. *AIDS Res Hum Retroviruses* 2010; 26(1):109-115.
58. Vallari A, Holzmayer V, Harris B, Yamaguchi J, Ngansop C, Makamche F, et al. Confirmation of putative HIV-1 group P in Cameroon. *J Virol* 2011; 85(3):1403-1407.
59. Alessandri-Gradt E, De Oliveira F, Leoz M, Lemee V, Robertson DL, Feyertag F, et al. HIV-1 group P infection: towards a dead-end infection? *AIDS* 2018; 32(10):1317-1322.
60. Sakai Y, Miyake A, Doi N, Sasada H, Miyazaki Y, Adachi A, et al. Expression Profiles of Vpx/Vpr Proteins Are Co-related with the Primate Lentiviral Lineage. *Front Microbiol* 2016; 7:1211.
61. Flint SJ, Enquist LW, Racaniello VR, Skalka AM. Principles of Virology: Molecular Biology, Pathogenesis, and Control of Animal Viruses, 2nd Edition. ASM Press; 2004.
62. Muesing M. Regulation of mRNA accumulation by a human immunodeficiency virus trans-activator protein. *Cell* 1987; 48(4):691-701.
63. Gaynor R. Cellular transcription factors involved in the regulation of HIV-1 gene expression. *AIDS* 1992; 6(4):347-363.
64. Rosen CA, Sodroski JG, Haseltine WA. The location of cis-acting regulatory sequences in the human T cell lymphotropic virus type III (HTLV-III/LAV) long terminal repeat. *Cell* 1985; 41(3):813-823.
65. Pereira LA, Bentley K, Peeters A, Churchill MJ, Deacon NJ. A compilation of cellular transcription factor interactions with the HIV-1 LTR promoter. *Nucleic Acids Res* 2000; 28(3):663-668.

66. Pettit SC, Moody MD, Wehbie RS, Kaplan AH, Nantermet PV, Klein CA, et al. The p2 domain of human immunodeficiency virus type 1 Gag regulates sequential proteolytic processing and is required to produce fully infectious virions. *Journal of Virology* 1994; 68(12):8017-8027.
67. Freed EO. HIV-1 gag proteins: diverse functions in the virus life cycle. *Virology* 1998; 251(1):1-15.
68. Bryant M, Ratner L. Myristoylation-dependent replication and assembly of human immunodeficiency virus 1. *Proc Natl Acad Sci U S A* 1990; 87(2):523-527.
69. Ono A, Ablan SD, Lockett SJ, Nagashima K, Freed EO. Phosphatidylinositol (4,5) bisphosphate regulates HIV-1 Gag targeting to the plasma membrane. *Proc Natl Acad Sci U S A* 2004; 101(41):14889-14894.
70. Hill CP, Worthylake D, Bancroft DP, Christensen AM, Sundquist WI. Crystal structures of the trimeric human immunodeficiency virus type 1 matrix protein: implications for membrane association and assembly. *Proc Natl Acad Sci U S A* 1996; 93(7):3099-3104.
71. Freed EO, Martin MA. Virion incorporation of envelope glycoproteins with long but not short cytoplasmic tails is blocked by specific, single amino acid substitutions in the human immunodeficiency virus type 1 matrix. *Journal of Virology* 1995; 69(3):1984-1989.
72. Frankel AD, Young JA. HIV-1: fifteen proteins and an RNA. *Annu Rev Biochem* 1998; 67:1-25.
73. Purohit P, Dupont S, Stevenson M, Green MR. Sequence-specific interaction between HIV-1 matrix protein and viral genomic RNA revealed by in vitro genetic selection. *RNA* 2001; 7(4):576-584.
74. Jayappa K, Ao Z, Yao X. The HIV-1 passage from cytoplasm to nucleus: The process involving a complex exchange between the components of HIV-1 and cellular machinery to access nucleus and successful integration. *International Journal of Biochemistry and Molecular Biology* 2012; 3:70-85.
75. Briggs JA, Simon MN, Gross I, Krausslich HG, Fuller SD, Vogt VM, et al. The stoichiometry of Gag protein in HIV-1. *Nat Struct Mol Biol* 2004; 11(7):672-675.
76. Li S, Hill CP, Sundquist WI, Finch JT. Image reconstructions of helical assemblies of the HIV-1 CA protein. *Nature* 2000; 407(6802):409-413.

77. Welker R, Hohenberg H, Tessmer U, Huckhagel C, Krausslich HG. Biochemical and structural analysis of isolated mature cores of human immunodeficiency virus type 1. *J Virol* 2000; 74(3):1168-1177.
78. Kotov A, Zhou J, Flicker P, Aiken C. Association of Nef with the Human Immunodeficiency Virus Type 1 Core. *Journal of Virology* 1999; 73(10):8824-8830.
79. Lahaye X, Satoh T, Gentili M, Cerboni S, Conrad C, Hurbain I, et al. The capsids of HIV-1 and HIV-2 determine immune detection of the viral cDNA by the innate sensor cGAS in dendritic cells. *Immunity* 2013; 39(6):1132-1142.
80. Rasaiyaah J, Tan CP, Fletcher AJ, Price AJ, Blondeau C, Hilditch L, et al. HIV-1 evades innate immune recognition through specific cofactor recruitment. *Nature* 2013; 503(7476):402-405.
81. Yamashita M, Emerman M. Cellular restriction targeting viral capsids perturbs human immunodeficiency virus type 1 infection of nondividing cells. *J Virol* 2009; 83(19):9835-9843.
82. Clever JL, Parslow TG. Mutant human immunodeficiency virus type 1 genomes with defects in RNA dimerization or encapsidation. *Journal of Virology* 1997; 71(5):3407-3414.
83. Geigenmüller U, Linial ML. Specific binding of human immunodeficiency virus type 1 (HIV-1) Gag-derived proteins to a 5' HIV-1 genomic RNA sequence. *Journal of Virology* 1996; 70(1):667-671.
84. Levin JG, Guo J, Rouzina I, Musier-Forsyth K. Nucleic acid chaperone activity of HIV-1 nucleocapsid protein: critical role in reverse transcription and molecular mechanism. *Prog Nucleic Acid Res Mol Biol* 2005; 80:217-286.
85. Zhu H, Jian H, Zhao LJ. Identification of the 15FRFG domain in HIV-1 Gag p6 essential for Vpr packaging into the virion. *Retrovirology* 2004; 1:26.
86. Yu XF, Matsuda Z, Yu QC, Lee TH, Essex M. Role of the C terminus Gag protein in human immunodeficiency virus type 1 virion assembly and maturation. *J Gen Virol* 1995; 76 (Pt 12):3171-3179.
87. Friedrich M, Setz C, Hahn F, Matthaei A, Fraedrich K, Rauch P, et al. Glutamic Acid Residues in HIV-1 p6 Regulate Virus Budding and Membrane Association of Gag. *Viruses* 2016; 8(4):117.

88. Votteler J, Sundquist WI. Virus budding and the ESCRT pathway. *Cell Host Microbe* 2013; 14(3):232-241.
89. Radestock B, Burk R, Muller B, Krausslich HG. Re-visiting the functional Relevance of the highly conserved Serine 40 Residue within HIV-1 p6(Gag). *Retrovirology* 2014; 11:114.
90. Solbak SM, Reksten TR, Hahn F, Wray V, Henklein P, Henklein P, et al. HIV-1 p6 - a structured to flexible multifunctional membrane-interacting protein. *Biochim Biophys Acta* 2013; 1828(2):816-823.
91. Cassan M, Delaunay N, Vaquero C, Rousset JP. Translational frameshifting at the gag-pol junction of human immunodeficiency virus type 1 is not increased in infected T-lymphoid cells. *Journal of Virology* 1994; 68(3):1501-1508.
92. Jacks T, Power MD, Masiarz FR, Luciw PA, Barr PJ, Varmus HE. Characterization of ribosomal frameshifting in HIV-1 gag-pol expression. *Nature* 1988; 331(6153):280-283.
93. Loeb DD, Swanstrom R, Everitt L, Manchester M, Stamper SE, Hutchison CA, 3rd. Complete mutagenesis of the HIV-1 protease. *Nature* 1989; 340(6232):397-400.
94. Louis JM, Clore GM, Gronenborn AM. Autoprocessing of HIV-1 protease is tightly coupled to protein folding. *Nat Struct Biol* 1999; 6(9):868-875.
95. Huang L, Chen C. Understanding HIV-1 protease autoprocessing for novel therapeutic development. *Future Med Chem* 2013; 5(11):1215-1229.
96. Kohl NE, Emini EA, Schleif WA, Davis LJ, Heimbach JC, Dixon RA, et al. Active human immunodeficiency virus protease is required for viral infectivity. *Proc Natl Acad Sci U S A* 1988; 85(13):4686-4690.
97. Voshavar C. Protease Inhibitors for the Treatment of HIV/AIDS: Recent Advances and Future Challenges. *Curr Top Med Chem* 2019; 19(18):1571-1598.
98. Hizi A, Tal R, Shaharabany M, Loya S. Catalytic properties of the reverse transcriptases of human immunodeficiency viruses type 1 and type 2. *Journal of Biological Chemistry* 1991; 266(10):6230-6239.

99. Lightfoote MM, Coligan JE, Folks TM, Fauci AS, Martin MA, Venkatesan S. Structural characterization of reverse transcriptase and endonuclease polypeptides of the acquired immunodeficiency syndrome retrovirus. *Journal of Virology* 1986; 60(2):771-775.
100. Sarafianos SG, Marchand B, Das K, Himmel DM, Parniak MA, Hughes SH, et al. Structure and function of HIV-1 reverse transcriptase: molecular mechanisms of polymerization and inhibition. *J Mol Biol* 2009; 385(3):693-713.
101. Engelman A, Mizuuchi K, Craigie R. HIV-1 DNA integration: Mechanism of viral DNA cleavage and DNA strand transfer. *Cell* 1991; 67(6):1211-1221.
102. Dyda F, Hickman AB, Jenkins TM, Engelman A, Craigie R, Davies DR. Crystal structure of the catalytic domain of HIV-1 integrase: similarity to other polynucleotidyl transferases. *Science* 1994; 266(5193):1981-1986.
103. Gallay P, Hope T, Chin D, Trono D. HIV-1 infection of nondividing cells through the recognition of integrase by the importin/karyopherin pathway. *Proc Natl Acad Sci U S A* 1997; 94(18):9825-9830.
104. Bukrinsky MI, Haffar OK. HIV-1 nuclear import: in search of a leader. *Front Biosci* 1997; 2:d578-587.
105. Metifiot M, Marchand C, Pommier Y. HIV integrase inhibitors: 20-year landmark and challenges. *Adv Pharmacol* 2013; 67:75-105.
106. Choi E, Mallareddy JR, Lu D, Kolluru S. Recent advances in the discovery of small-molecule inhibitors of HIV-1 integrase. *Future Sci OA* 2018; 4(9):FSO338.
107. Hallenberger S, Bosch V, Angliker H, Shaw E, Klenk HD, Garten W. Inhibition of furin-mediated cleavage activation of HIV-1 glycoprotein gp160. *Nature* 1992; 360(6402):358-361.
108. Endres MJ, Clapham PR, Marsh M, Ahuja M, Turner JD, McKnight A, et al. CD4-Independent Infection by HIV-2 Is Mediated by Fusin/CXCR4. *Cell* 1996; 87(4):745-756.
109. Checkley MA, Luttge BG, Freed EO. HIV-1 envelope glycoprotein biosynthesis, trafficking, and incorporation. *J Mol Biol* 2011; 410(4):582-608.

110. Egan MA, Carruth LM, Rowell JF, Yu X, Siliciano RF. Human immunodeficiency virus type 1 envelope protein endocytosis mediated by a highly conserved intrinsic internalization signal in the cytoplasmic domain of gp41 is suppressed in the presence of the Pr55gag precursor protein. *Journal of Virology* 1996; 70(10):6547-6556.
111. Zhu P, Chertova E, Bess J, Jr., Lifson JD, Arthur LO, Liu J, et al. Electron tomography analysis of envelope glycoprotein trimers on HIV and simian immunodeficiency virus virions. *Proc Natl Acad Sci U S A* 2003; 100(26):15812-15817.
112. Rambaut A, Posada D, Crandall KA, Holmes EC. The causes and consequences of HIV evolution. *Nat Rev Genet* 2004; 5(1):52-61.
113. Joshi VR, Newman RM, Pack ML, Power KA, Munro JB, Okawa K, et al. Gp41-targeted antibodies restore infectivity of a fusion-deficient HIV-1 envelope glycoprotein. *PLoS Pathog* 2020; 16(5):e1008577.
114. Rose KM, Marin M, Kozak SL, Kabat D. The viral infectivity factor (Vif) of HIV-1 unveiled. *Trends Mol Med* 2004; 10(6):291-297.
115. Simon JH, Gaddis NC, Fouchier RA, Malim MH. Evidence for a newly discovered cellular anti-HIV-1 phenotype. *Nat Med* 1998; 4(12):1397-1400.
116. Mariani R, Chen D, Schröfelbauer B, Navarro F, König R, Bollman B, et al. Species-Specific Exclusion of APOBEC3G from HIV-1 Virions by Vif. *Cell* 2003; 114(1):21-31.
117. Yu X, Yu Y, Liu B, Luo K, Kong W, Mao P, et al. Induction of APOBEC3G ubiquitination and degradation by an HIV-1 Vif-Cul5-SCF complex. *Science* 2003; 302(5647):1056-1060.
118. Paxton W, Connor RI, Landau NR. Incorporation of Vpr into human immunodeficiency virus type 1 virions: requirement for the p6 region of gag and mutational analysis. *Journal of Virology* 1993; 67(12):7229-7237.
119. Lu YL, Spearman P, Ratner L. Human immunodeficiency virus type 1 viral protein R localization in infected cells and virions. *J Virol* 1993; 67(11):6542-6550.

120. Popov S, Rexach M, Zybarth G, Reiling N, Lee MA, Ratner L, et al. Viral protein R regulates nuclear import of the HIV-1 pre-integration complex. *EMBO J* 1998; 17(4):909-917.
121. Hattori N, Michaels F, Fargnoli K, Marcon L, Gallo RC, Franchini G. The human immunodeficiency virus type 2 vpr gene is essential for productive infection of human macrophages. *Proc Natl Acad Sci U S A* 1990; 87(20):8080-8084.
122. Iijima S, Nitahara-Kasahara Y, Kimata K, Zhong Zhuang W, Kamata M, Isogai M, et al. Nuclear localization of Vpr is crucial for the efficient replication of HIV-1 in primary CD4+ T cells. *Virology* 2004; 327(2):249-261.
123. Jacquot G, Le Rouzic E, David A, Mazzolini J, Bouchet J, Bouaziz S, et al. Localization of HIV-1 Vpr to the nuclear envelope: impact on Vpr functions and virus replication in macrophages. *Retrovirology* 2007; 4:84.
124. Fletcher TM, 3rd, Brichacek B, Sharova N, Newman MA, Stivahtis G, Sharp PM, et al. Nuclear import and cell cycle arrest functions of the HIV-1 Vpr protein are encoded by two separate genes in HIV-2/SIV(SM). *Embo j* 1996; 15(22):6155-6165.
125. Lim Efrem S, Fregoso Oliver I, McCoy Connor O, Matsen Frederick A, Malik Harmit S, Emerman M. The Ability of Primate Lentiviruses to Degrade the Monocyte Restriction Factor SAMHD1 Preceded the Birth of the Viral Accessory Protein Vpx. *Cell Host & Microbe* 2012; 11(2):194-204.
126. Coggins SA, Mahboubi B, Schinazi RF, Kim B. SAMHD1 Functions and Human Diseases. *Viruses* 2020; 12(4).
127. Wu Y, Zhou X, Barnes CO, DeLucia M, Cohen AE, Gronenborn AM, et al. The DDB1-DCAF1-Vpr-UNG2 crystal structure reveals how HIV-1 Vpr steers human UNG2 toward destruction. *Nat Struct Mol Biol* 2016; 23(10):933-940.
128. Lahouassa H, Daddacha W, Hofmann H, Ayinde D, Logue EC, Dragin L, et al. SAMHD1 restricts the replication of human immunodeficiency virus type 1 by depleting the intracellular pool of deoxynucleoside triphosphates. *Nat Immunol* 2012; 13(3):223-228.

129. Zhou X, DeLucia M, Hao C, Hrecka K, Monnie C, Skowronski J, et al. HIV-1 Vpr protein directly loads helicase-like transcription factor (HLTF) onto the CRL4-DCAF1 E3 ubiquitin ligase. *J Biol Chem* 2017; 292(51):21117-21127.
130. Tristem M, Marshall C, Karpas A, Petrik J, Hill F. Origin of vpx in lentiviruses. *Nature* 1990; 347(6291):341-342.
131. Wu X, Conway JA, Kim J, Kappes JC. Localization of the Vpx packaging signal within the C terminus of the human immunodeficiency virus type 2 Gag precursor protein. *Journal of Virology* 1994; 68(10):6161-6169.
132. Bergamaschi A, Ayinde D, David A, Le Rouzic E, Morel M, Collin G, et al. The human immunodeficiency virus type 2 Vpx protein usurps the CUL4A-DDB1 DCAF1 ubiquitin ligase to overcome a postentry block in macrophage infection. *J Virol* 2009; 83(10):4854-4860.
133. Ahn J, Hao C, Yan J, DeLucia M, Mehrens J, Wang C, et al. HIV/simian immunodeficiency virus (SIV) accessory virulence factor Vpx loads the host cell restriction factor SAMHD1 onto the E3 ubiquitin ligase complex CRL4DCAF1. *J Biol Chem* 2012; 287(15):12550-12558.
134. Guo H, Zhang N, Shen S, Yu XF, Wei W. Determinants of lentiviral Vpx-CRL4 E3 ligase-mediated SAMHD1 degradation in the substrate adaptor protein DCAF1. *Biochem Biophys Res Commun* 2019; 513(4):933-939.
135. Goujon C, Riviere L, Jarrosson-Wuilleme L, Bernaud J, Rigal D, Darlix JL, et al. SIVSM/HIV-2 Vpx proteins promote retroviral escape from a proteasome-dependent restriction pathway present in human dendritic cells. *Retrovirology* 2007; 4:2.
136. Srivastava S, Swanson SK, Manel N, Florens L, Washburn MP, Skowronski J. Lentiviral Vpx accessory factor targets VprBP/DCAF1 substrate adaptor for cullin 4 E3 ubiquitin ligase to enable macrophage infection. *PLoS Pathog* 2008; 4(5):e1000059.
137. Fregoso OI, Ahn J, Wang C, Mehrens J, Skowronski J, Emerman M. Evolutionary toggling of Vpx/Vpr specificity results in divergent recognition of the restriction factor SAMHD1. *PLoS Pathog* 2013; 9(7):e1003496.

138. Schwartz S, Felber BK, Fenyö EM, Pavlakis GN. Env and Vpu proteins of human immunodeficiency virus type 1 are produced from multiple bicistronic mRNAs. *Journal of Virology* 1990; 64(11):5448-5456.
139. Willey RL, Maldarelli F, Martin MA, Strebel K. Human immunodeficiency virus type 1 Vpu protein induces rapid degradation of CD4. *Journal of Virology* 1992; 66(12):7193-7200.
140. Schubert U, Strebel K. Differential activities of the human immunodeficiency virus type 1-encoded Vpu protein are regulated by phosphorylation and occur in different cellular compartments. *Journal of Virology* 1994; 68(4):2260-2271.
141. Willey RL, Maldarelli F, Martin MA, Strebel K. Human immunodeficiency virus type 1 Vpu protein regulates the formation of intracellular gp160-CD4 complexes. *Journal of Virology* 1992; 66(1):226-234.
142. Veillette M, Desormeaux A, Medjahed H, Gharsallah NE, Coutu M, Baalwa J, et al. Interaction with cellular CD4 exposes HIV-1 envelope epitopes targeted by antibody-dependent cell-mediated cytotoxicity. *J Virol* 2014; 88(5):2633-2644.
143. Strebel K, Klimkait T, Maldarelli F, Martin MA. Molecular and biochemical analyses of human immunodeficiency virus type 1 vpu protein. *Journal of Virology* 1989; 63(9):3784-3791.
144. Perez-Caballero D, Zang T, Ebrahimi A, McNatt MW, Gregory DA, Johnson MC, et al. Tetherin inhibits HIV-1 release by directly tethering virions to cells. *Cell* 2009; 139(3):499-511.
145. Iwabu Y, Fujita H, Kinomoto M, Kaneko K, Ishizaka Y, Tanaka Y, et al. HIV-1 accessory protein Vpu internalizes cell-surface BST-2/tetherin through transmembrane interactions leading to lysosomes. *J Biol Chem* 2009; 284(50):35060-35072.
146. Yao W, Yoshida T, Hashimoto S, Takeuchi H, Strebel K, Yamaoka S. Vpu of a Simian Immunodeficiency Virus Isolated from Greater Spot-Nosed Monkey Antagonizes Human BST-2 via Two AxxxxxxxW Motifs. *Journal of Virology* 2020; 94(2):e01669-01619.

147. Pham TN, Lukhele S, Hajjar F, Routy JP, Cohen EA. HIV Nef and Vpu protect HIV-infected CD4+ T cells from antibody-mediated cell lysis through down-modulation of CD4 and BST2. *Retrovirology* 2014; 11:15.
148. Arya SK, Guo C, Josephs SF, Wong-Staal F. Trans-activator gene of human T-lymphotropic virus type III (HTLV-III). *Science* 1985; 229(4708):69-73.
149. Sodroski J, Patarca R, Rosen C, Wong-Staal F, Haseltine W. Location of the trans-activating region on the genome of human T-cell lymphotropic virus type III. *Science* 1985; 229(4708):74-77.
150. Pavlakis GN, Felber BK. Regulation of expression of human immunodeficiency virus. *New Biol* 1990; 2(1):20-31.
151. Chang LJ, Zhang C. Infection and replication of Tat- human immunodeficiency viruses: genetic analyses of LTR and tat mutations in primary and long-term human lymphoid cells. *Virology* 1995; 211(1):157-169.
152. Cujec TP, Okamoto H, Fujinaga K, Meyer J, Chamberlin H, Morgan DO, et al. The HIV transactivator TAT binds to the CDK-activating kinase and activates the phosphorylation of the carboxy-terminal domain of RNA polymerase II. *Genes Dev* 1997; 11(20):2645-2657.
153. Laspias MF, Rice AP, Mathews MB. HIV-1 Tat protein increases transcriptional initiation and stabilizes elongation. *Cell* 1989; 59(2):283-292.
154. Kato H, Sumimoto H, Pognonec P, Chen CH, Rosen CA, Roeder RG. HIV-1 Tat acts as a processivity factor in vitro in conjunction with cellular elongation factors. *Genes Dev* 1992; 6(4):655-666.
155. Rice AP. Roles of CDKs in RNA polymerase II transcription of the HIV-1 genome. *Transcription* 2019; 10(2):111-117.
156. Rayne F, Debaisieux S, Yezid H, Lin YL, Mettling C, Konate K, et al. Phosphatidylinositol-(4,5)-bisphosphate enables efficient secretion of HIV-1 Tat by infected T-cells. *EMBO J* 2010; 29(8):1348-1362.

157. Marino J, Wigdahl B, Nonnemacher MR. Extracellular HIV-1 Tat Mediates Increased Glutamate in the CNS Leading to Onset of Senescence and Progression of HAND. *Front Aging Neurosci* 2020; 12:168.
158. Malim MH, Hauber J, Fenrick R, Cullen BR. Immunodeficiency virus rev trans-activator modulates the expression of the viral regulatory genes. *Nature* 1988; 335(6186):181-183.
159. Fisher AG, Feinberg MB, Josephs SF, Harper ME, Marselle LM, Reyes G, et al. The trans-activator gene of HTLV-III is essential for virus replication. *Nature* 1986; 320(6060):367-371.
160. Zimmel RW, Kelley AC, Karn J, Butler PJ. Flexible regions of RNA structure facilitate co-operative Rev assembly on the Rev-response element. *J Mol Biol* 1996; 258(5):763-777.
161. Van Ryk DI, Venkatesan S. Real-time kinetics of HIV-1 Rev-Rev response element interactions. Definition of minimal binding sites on RNA and protein and stoichiometric analysis. *J Biol Chem* 1999; 274(25):17452-17463.
162. Nalin CM, Purcell RD, Antelman D, Mueller D, Tomchak L, Wegrzynski B, et al. Purification and characterization of recombinant Rev protein of human immunodeficiency virus type 1. *Proc Natl Acad Sci U S A* 1990; 87(19):7593-7597.
163. Vergara-Mendoza M, Gomez-Quiroz LE, Miranda-Labra RU, Fuentes-Romero LL, Romero-Rodriguez DP, Gonzalez-Ruiz J, et al. Regulation of Cas9 by viral proteins Tat and Rev for HIV-1 inactivation. *Antiviral Res* 2020:104856.
164. Bentham M, Mazaleyrat S, Harris M. Role of myristoylation and N-terminal basic residues in membrane association of the human immunodeficiency virus type 1 Nef protein. *J Gen Virol* 2006; 87(Pt 3):563-571.
165. Landi A, Iannucci V, Nuffel AV, Meuwissen P, Verhasselt B. One protein to rule them all: modulation of cell surface receptors and molecules by HIV Nef. *Curr HIV Res* 2011; 9(7):496-504.
166. Levesque K, Finzi A, Binette J, Cohen EA. Role of CD4 receptor down-regulation during HIV-1 infection. *Curr HIV Res* 2004; 2(1):51-59.

167. Schwartz O, Marechal V, Le Gall S, Lemonnier F, Heard JM. Endocytosis of major histocompatibility complex class I molecules is induced by the HIV-1 Nef protein. *Nat Med* 1996; 2(3):338-342.
168. Michel N, Allespach I, Venzke S, Fackler OT, Keppler OT. The Nef protein of human immunodeficiency virus establishes superinfection immunity by a dual strategy to downregulate cell-surface CCR5 and CD4. *Curr Biol* 2005; 15(8):714-723.
169. Collins KL, Chen BK, Kalams SA, Walker BD, Baltimore D. HIV-1 Nef protein protects infected primary cells against killing by cytotoxic T lymphocytes. *Nature* 1998; 391(6665):397-401.
170. Jia B, Serra-Moreno R, Neidermyer W, Rahmberg A, Mackey J, Fofana IB, et al. Species-specific activity of SIV Nef and HIV-1 Vpu in overcoming restriction by tetherin/BST2. *PLoS Pathog* 2009; 5(5):e1000429.
171. Lehmann MH, Lehmann JM, Erfle V. Nef-induced CCL2 Expression Contributes to HIV/SIV Brain Invasion and Neuronal Dysfunction. *Front Immunol* 2019; 10:2447.
172. Ma X, Lu M, Gorman J, Terry DS, Hong X, Zhou Z, et al. HIV-1 Env trimer opens through an asymmetric intermediate in which individual protomers adopt distinct conformations. *Elife* 2018; 7.
173. Dalgleish AG, Beverley PC, Clapham PR, Crawford DH, Greaves MF, Weiss RA. The CD4 (T4) antigen is an essential component of the receptor for the AIDS retrovirus. *Nature* 1984; 312(5996):763-767.
174. Clements GJ, Price-Jones MJ, Stephens PE, Sutton C, Schulz TF, Clapham PR, et al. The V3 loops of the HIV-1 and HIV-2 surface glycoproteins contain proteolytic cleavage sites: a possible function in viral fusion? *AIDS Res Hum Retroviruses* 1991; 7(1):3-16.
175. Sattentau QJ, Moore JP, Vignaux F, Traincard F, Poignard P. Conformational changes induced in the envelope glycoproteins of the human and simian immunodeficiency viruses by soluble receptor binding. *J Virol* 1993; 67(12):7383-7393.
176. Feng Y, Broder CC, Kennedy PE, Berger EA. HIV-1 entry cofactor: functional cDNA cloning of a seven-transmembrane, G protein-coupled receptor. *Science* 1996; 272(5263):872-877.

177. Deng H, Liu R, Ellmeier W, Choe S, Unutmaz D, Burkhart M, et al. Identification of a major co-receptor for primary isolates of HIV-1. *Nature* 1996; 381(6584):661-666.
178. Chan DC, Fass D, Berger JM, Kim PS. Core Structure of gp41 from the HIV Envelope Glycoprotein. *Cell* 1997; 89(2):263-273.
179. Zaitseva E, Zaitsev E, Melikov K, Arakelyan A, Marin M, Villasmil R, et al. Fusion Stage of HIV-1 Entry Depends on Virus-Induced Cell Surface Exposure of Phosphatidylserine. *Cell Host Microbe* 2017; 22(1):99-110 e117.
180. Pante N, Kann M. Nuclear pore complex is able to transport macromolecules with diameters of about 39 nm. *Mol Biol Cell* 2002; 13(2):425-434.
181. Cosnefroy O, Murray PJ, Bishop KN. HIV-1 capsid uncoating initiates after the first strand transfer of reverse transcription. *Retrovirology* 2016; 13(1):58.
182. Dharan A, Bachmann N, Talley S, Zwickelmaier V, Campbell EM. Nuclear pore blockade reveals that HIV-1 completes reverse transcription and uncoating in the nucleus. *Nat Microbiol* 2020.
183. Ingram Z, Taylor M, Okland G, Martin R, Hulme AE. Characterization of HIV-1 uncoating in human microglial cell lines. *Viol J* 2020; 17(1):31.
184. Ambrose Z, Aiken C. HIV-1 uncoating: connection to nuclear entry and regulation by host proteins. *Virology* 2014; 454-455:371-379.
185. Novikova M, Zhang Y, Freed EO, Peng K. Multiple Roles of HIV-1 Capsid during the Virus Replication Cycle. *Viol Sin* 2019; 34(2):119-134.
186. Iordanskiy S, Bukrinsky M. Reverse transcription complex: the key player of the early phase of HIV replication. *Future Virol* 2007; 2(1):49-64.
187. Hu WS, Hughes SH. HIV-1 reverse transcription. *Cold Spring Harb Perspect Med* 2012; 2(10).
188. Javanbakht H, Halwani R, Cen S, Saadatmand J, Musier-Forsyth K, Gottlinger H, et al. The interaction between HIV-1 Gag and human lysyl-tRNA synthetase during viral assembly. *J Biol Chem* 2003; 278(30):27644-27651.

189. Lanchy JM, Keith G, Le Grice SF, Ehresmann B, Ehresmann C, Marquet R. Contacts between reverse transcriptase and the primer strand govern the transition from initiation to elongation of HIV-1 reverse transcription. *J Biol Chem* 1998; 273(38):24425-24432.
190. Huber HE, McCoy JM, Seehra JS, Richardson CC. Human immunodeficiency virus 1 reverse transcriptase. Template binding, processivity, strand displacement synthesis, and template switching. *J Biol Chem* 1989; 264(8):4669-4678.
191. Sarafianos SG, Das K, Tantillo C, Clark AD, Jr., Ding J, Whitcomb JM, et al. Crystal structure of HIV-1 reverse transcriptase in complex with a polypurine tract RNA:DNA. *EMBO J* 2001; 20(6):1449-1461.
192. Charneau P, Alizon M, Clavel F. A second origin of DNA plus-strand synthesis is required for optimal human immunodeficiency virus replication. *Journal of Virology* 1992; 66(5):2814-2820.
193. Smith JS, Roth MJ. Specificity of human immunodeficiency virus-1 reverse transcriptase-associated ribonuclease H in removal of the minus-strand primer, tRNA(Lys3). *J Biol Chem* 1992; 267(21):15071-15079.
194. Tsuchihashi Z, Brown PO. DNA strand exchange and selective DNA annealing promoted by the human immunodeficiency virus type 1 nucleocapsid protein. *J Virol* 1994; 68(9):5863-5870.
195. Farnet CM, Haseltine WA. Circularization of human immunodeficiency virus type 1 DNA in vitro. *J Virol* 1991; 65(12):6942-6952.
196. Sloan RD, Wainberg MA. The role of unintegrated DNA in HIV infection. *Retrovirology* 2011; 8:52.
197. Hamid FB, Kim J, Shin CG. Distribution and fate of HIV-1 unintegrated DNA species: a comprehensive update. *AIDS Res Ther* 2017; 14(1):9.
198. Brussel A, Sonigo P. Evidence for gene expression by unintegrated human immunodeficiency virus type 1 DNA species. *J Virol* 2004; 78(20):11263-11271.

199. Mahboubi B, Gavegnano C, Kim DH, Schinazi RF, Kim B. Host SAMHD1 protein restricts endogenous reverse transcription of HIV-1 in nondividing macrophages. *Retrovirology* 2018; 15(1):69.
200. Ilina T, Labarge K, Sarafianos SG, Ishima R, Parniak MA. Inhibitors of HIV-1 Reverse Transcriptase-Associated Ribonuclease H Activity. *Biology (Basel)* 2012; 1(3):521-541.
201. Cherepanov P, Maertens G, Proost P, Devreese B, Van Beeumen J, Engelborghs Y, et al. HIV-1 integrase forms stable tetramers and associates with LEDGF/p75 protein in human cells. *J Biol Chem* 2003; 278(1):372-381.
202. Ciuffi A, Llano M, Poeschla E, Hoffmann C, Leipzig J, Shinn P, et al. A role for LEDGF/p75 in targeting HIV DNA integration. *Nat Med* 2005; 11(12):1287-1289.
203. Shun MC, Raghavendra NK, Vandegraaff N, Daigle JE, Hughes S, Kellam P, et al. LEDGF/p75 functions downstream from preintegration complex formation to effect gene-specific HIV-1 integration. *Genes Dev* 2007; 21(14):1767-1778.
204. Pollard VW, Malim MH. The HIV-1 Rev protein. *Annu Rev Microbiol* 1998; 52:491-532.
205. Zhou Q, Sharp PA. Tat-SF1: cofactor for stimulation of transcriptional elongation by HIV-1 Tat. *Science* 1996; 274(5287):605-610.
206. Hulver MJ, Trautman JP, Goodwin AP, Roszczenko SK, Fogarty KH, Miller HB. Human Tat-specific factor 1 binds the HIV-1 genome and selectively transports HIV-1 RNAs. *Mol Biol Rep* 2020; 47(3):1759-1772.
207. Tazi J, Bakkour N, Marchand V, Ayadi L, Aboufirassi A, Branlant C. Alternative splicing: regulation of HIV-1 multiplication as a target for therapeutic action. *FEBS J* 2010; 277(4):867-876.
208. Ohlmann T, Mengardi C, Lopez-Lastra M. Translation initiation of the HIV-1 mRNA. *Translation (Austin)* 2014; 2(2):e960242.
209. Freed EO. HIV-1 replication. *Somat Cell Mol Genet* 2001; 26(1-6):13-33.

210. Paillart JC, Skripkin E, Ehresmann B, Ehresmann C, Marquet R. A loop-loop "kissing" complex is the essential part of the dimer linkage of genomic HIV-1 RNA. *Proc Natl Acad Sci U S A* 1996; 93(11):5572-5577.
211. Ott DE. Cellular proteins detected in HIV-1. *Rev Med Virol* 2008; 18(3):159-175.
212. Freed EO. HIV-1 assembly, release and maturation. *Nat Rev Microbiol* 2015; 13(8):484-496.
213. Shaw GM, Hunter E. HIV transmission. *Cold Spring Harb Perspect Med* 2012; 2(11).
214. Wolfs TF, Zwart G, Bakker M, Goudsmit J. HIV-1 genomic RNA diversification following sexual and parenteral virus transmission. *Virology* 1992; 189(1):103-110.
215. Miller CJ, Li Q, Abel K, Kim EY, Ma ZM, Wietgreffe S, et al. Propagation and dissemination of infection after vaginal transmission of simian immunodeficiency virus. *J Virol* 2005; 79(14):9217-9227.
216. Groot F, Welsch S, Sattentau QJ. Efficient HIV-1 transmission from macrophages to T cells across transient virological synapses. *Blood* 2008; 111(9):4660-4663.
217. Whitney JB, Hill AL, Sanisetty S, Penaloza-MacMaster P, Liu J, Shetty M, et al. Rapid seeding of the viral reservoir prior to SIV viraemia in rhesus monkeys. *Nature* 2014; 512(7512):74-77.
218. Wong JK, Hezareh M, Gunthard HF, Havlir DV, Ignacio CC, Spina CA, et al. Recovery of replication-competent HIV despite prolonged suppression of plasma viremia. *Science* 1997; 278(5341):1291-1295.
219. Cooper D, Maclean P, Finlayson R, Michelmore H, Gold J, Donovan B, et al. Acute Aids Retrovirus Infection. *The Lancet* 1985; 325(8428):537-540.
220. Mattapallil JJ, Douek DC, Hill B, Nishimura Y, Martin M, Roederer M. Massive infection and loss of memory CD4+ T cells in multiple tissues during acute SIV infection. *Nature* 2005; 434(7037):1093-1097.
221. Cavert W, Notermans DW, Staskus K, Wietgreffe SW, Zupancic M, Gebhard K, et al. Kinetics of response in lymphoid tissues to antiretroviral therapy of HIV-1 infection. *Science* 1997; 276(5314):960-964.

222. Little SJ, McLean AR, Spina CA, Richman DD, Havlir DV. Viral dynamics of acute HIV-1 infection. *J Exp Med* 1999; 190(6):841-850.
223. Veazey RS, DeMaria M, Chalifoux LV, Shvetz DE, Pauley DR, Knight HL, et al. Gastrointestinal tract as a major site of CD4+ T cell depletion and viral replication in SIV infection. *Science* 1998; 280(5362):427-431.
224. Brenchley JM, Schacker TW, Ruff LE, Price DA, Taylor JH, Beilman GJ, et al. CD4+ T cell depletion during all stages of HIV disease occurs predominantly in the gastrointestinal tract. *J Exp Med* 2004; 200(6):749-759.
225. Mehandru S, Poles MA, Tenner-Racz K, Horowitz A, Hurley A, Hogan C, et al. Primary HIV-1 infection is associated with preferential depletion of CD4+ T lymphocytes from effector sites in the gastrointestinal tract. *J Exp Med* 2004; 200(6):761-770.
226. Claireaux M, Galperin M, Benati D, Nouel A, Mukhopadhyay M, Klingler J, et al. A High Frequency of HIV-Specific Circulating Follicular Helper T Cells Is Associated with Preserved Memory B Cell Responses in HIV Controllers. *mBio* 2018; 9(3).
227. Blackbourn DJ, Chuang LF, Killam KF, Jr., Chuang RY. Inhibition of simian immunodeficiency virus (SIV) replication by CD8+ cells of SIV-infected rhesus macaques: implications for immunopathogenesis. *J Med Primatol* 1994; 23(6):343-354.
228. Lane HC, Masur H, Edgar LC, Whalen G, Rook AH, Fauci AS. Abnormalities of B-cell activation and immunoregulation in patients with the acquired immunodeficiency syndrome. *N Engl J Med* 1983; 309(8):453-458.
229. Deng K, Perteau M, Rongvaux A, Wang L, Durand CM, Ghiaur G, et al. Broad CTL response is required to clear latent HIV-1 due to dominance of escape mutations. *Nature* 2015; 517(7534):381-385.
230. Deeks SG, Overbaugh J, Phillips A, Buchbinder S. HIV infection. *Nat Rev Dis Primers* 2015; 1:15035.

231. Perelson AS, Neumann AU, Markowitz M, Leonard JM, Ho DD. HIV-1 dynamics in vivo: virion clearance rate, infected cell life-span, and viral generation time. *Science* 1996; 271(5255):1582-1586.
232. Boutwell CL, Rolland MM, Herbeck JT, Mullins JI, Allen TM. Viral evolution and escape during acute HIV-1 infection. *J Infect Dis* 2010; 202 Suppl 2:S309-314.
233. Stevenson M. HIV-1 pathogenesis. *Nat Med* 2003; 9(7):853-860.
234. Finzi D, Hermankova M, Pierson T, Carruth LM, Buck C, Chaisson RE, et al. Identification of a reservoir for HIV-1 in patients on highly active antiretroviral therapy. *Science* 1997; 278(5341):1295-1300.
235. Day CL, Kaufmann DE, Kiepiela P, Brown JA, Moodley ES, Reddy S, et al. PD-1 expression on HIV-specific T cells is associated with T-cell exhaustion and disease progression. *Nature* 2006; 443(7109):350-354.
236. Trautmann L, Janbazian L, Chomont N, Said EA, Gimmig S, Bessette B, et al. Upregulation of PD-1 expression on HIV-specific CD8+ T cells leads to reversible immune dysfunction. *Nat Med* 2006; 12(10):1198-1202.
237. Schneider E, Whitmore S, Glynn KM, Dominguez K, Mitsch A, McKenna MT, et al. Revised surveillance case definitions for HIV infection among adults, adolescents, and children aged <18 months and for HIV infection and AIDS among children aged 18 months to <13 years--United States, 2008. *MMWR Recomm Rep* 2008; 57(RR-10):1-12.
238. Betts MR, Nason MC, West SM, De Rosa SC, Migueles SA, Abraham J, et al. HIV nonprogressors preferentially maintain highly functional HIV-specific CD8+ T cells. *Blood* 2006; 107(12):4781-4789.
239. Migueles SA, Sabbaghian MS, Shupert WL, Bettinotti MP, Marincola FM, Martino L, et al. HLA B*5701 is highly associated with restriction of virus replication in a subgroup of HIV-infected long term nonprogressors. *Proc Natl Acad Sci U S A* 2000; 97(6):2709-2714.
240. Martin MP, Qi Y, Gao X, Yamada E, Martin JN, Pereyra F, et al. Innate partnership of HLA-B and KIR3DL1 subtypes against HIV-1. *Nat Genet* 2007; 39(6):733-740.

241. Saez-Cirion A, Lacabaratz C, Lambotte O, Versmisse P, Urrutia A, Boufassa F, et al. HIV controllers exhibit potent CD8 T cell capacity to suppress HIV infection ex vivo and peculiar cytotoxic T lymphocyte activation phenotype. *Proc Natl Acad Sci U S A* 2007; 104(16):6776-6781.
242. Schim van der Loeff MF, Jaffar S, Aveika AA, Sabally S, Corrah T, Harding E, et al. Mortality of HIV-1, HIV-2 and HIV-1/HIV-2 dually infected patients in a clinic-based cohort in The Gambia. *AIDS* 2002; 16(13):1775-1783.
243. Camacho RJ. Special aspects of the treatment of HIV-2-infected patients. *Intervirology* 2012; 55(2):179-183.
244. Pantaleo G, Graziosi C, Fauci AS. The immunopathogenesis of human immunodeficiency virus infection. *N Engl J Med* 1993; 328(5):327-335.
245. Sekaly RP, Rooke R. CD4. In: *Encyclopedia of Immunology (Second Edition)*. Delves PJ (editor). Oxford: Elsevier; 1998. pp. 468-472.
246. Fagerberg L, Hallstrom BM, Oksvold P, Kampf C, Djureinovic D, Odeberg J, et al. Analysis of the human tissue-specific expression by genome-wide integration of transcriptomics and antibody-based proteomics. *Mol Cell Proteomics* 2014; 13(2):397-406.
247. Joseph SB, Arrildt KT, Swanstrom AE, Schnell G, Lee B, Hoxie JA, et al. Quantification of entry phenotypes of macrophage-tropic HIV-1 across a wide range of CD4 densities. *J Virol* 2014; 88(4):1858-1869.
248. Glatzova D, Cebecauer M. Dual Role of CD4 in Peripheral T Lymphocytes. *Front Immunol* 2019; 10:618.
249. Klatzmann D, Champagne E, Chamaret S, Gruest J, Guetard D, Hercend T, et al. T-lymphocyte T4 molecule behaves as the receptor for human retrovirus LAV. *Nature* 1984; 312(5996):767-768.
250. Maddon PJ, Dagleish AG, McDougal JS, Clapham PR, Weiss RA, Axel R. The T4 gene encodes the AIDS virus receptor and is expressed in the immune system and the brain. *Cell* 1986; 47(3):333-348.
251. Clapham PR, McKnight A. HIV-1 receptors and cell tropism. *Br Med Bull* 2001; 58:43-59.

252. Zamarchi R, Allavena P, Borsetti A, Stievano L, Tosello V, Marcato N, et al. Expression and functional activity of CXCR-4 and CCR-5 chemokine receptors in human thymocytes. *Clin Exp Immunol* 2002; 127(2):321-330.
253. Lee B, Sharron M, Montaner LJ, Weissman D, Doms RW. Quantification of CD4, CCR5, and CXCR4 levels on lymphocyte subsets, dendritic cells, and differentially conditioned monocyte-derived macrophages. *Proc Natl Acad Sci U S A* 1999; 96(9):5215-5220.
254. Keele BF, Giorgi EE, Salazar-Gonzalez JF, Decker JM, Pham KT, Salazar MG, et al. Identification and characterization of transmitted and early founder virus envelopes in primary HIV-1 infection. *Proc Natl Acad Sci U S A* 2008; 105(21):7552-7557.
255. Connor RI, Sheridan KE, Ceradini D, Choe S, Landau NR. Change in Coreceptor Use Correlates with Disease Progression in HIV-1–Infected Individuals. *The Journal of Experimental Medicine* 1997; 185(4):621-628.
256. Schuitemaker H, Koot M, Kootstra NA, Dercksen MW, de Goede RE, van Steenwijk RP, et al. Biological phenotype of human immunodeficiency virus type 1 clones at different stages of infection: progression of disease is associated with a shift from monocyctotropic to T-cell-tropic virus population. *J Virol* 1992; 66(3):1354-1360.
257. Tersmette M, de Goede RE, Al BJ, Winkel IN, Gruters RA, Cuypers HT, et al. Differential syncytium-inducing capacity of human immunodeficiency virus isolates: frequent detection of syncytium-inducing isolates in patients with acquired immunodeficiency syndrome (AIDS) and AIDS-related complex. *J Virol* 1988; 62(6):2026-2032.
258. Doranz BJ, Rucker J, Yi Y, Smyth RJ, Samson M, Peiper SC, et al. A Dual-Tropic Primary HIV-1 Isolate That Uses Fusin and the β -Chemokine Receptors CKR-5, CKR-3, and CKR-2b as Fusion Cofactors. *Cell* 1996; 85(7):1149-1158.
259. Naif HM, Li S, Alali M, Sloane A, Wu L, Kelly M, et al. CCR5 expression correlates with susceptibility of maturing monocytes to human immunodeficiency virus type 1 infection. *J Virol* 1998; 72(1):830-836.

260. Joseph SB, Swanstrom R. The evolution of HIV-1 entry phenotypes as a guide to changing target cells. *J Leukoc Biol* 2018; 103(3):421-431.
261. Parrish NF, Wilen CB, Banks LB, Iyer SS, Pfaff JM, Salazar-Gonzalez JF, et al. Transmitted/founder and chronic subtype C HIV-1 use CD4 and CCR5 receptors with equal efficiency and are not inhibited by blocking the integrin alpha4beta7. *PLoS Pathog* 2012; 8(5):e1002686.
262. Montagna C, De Crignis E, Bon I, Re MC, Mezzaroma I, Turriziani O, et al. V3 net charge: additional tool in HIV-1 tropism prediction. *AIDS Res Hum Retroviruses* 2014; 30(12):1203-1212.
263. Dufour C, Gantner P, Fromentin R, Chomont N. The multifaceted nature of HIV latency. *J Clin Invest* 2020; 130(7):3381-3390.
264. Igarashi T, Brown CR, Endo Y, Buckler-White A, Plishka R, Bischofberger N, et al. Macrophage are the principal reservoir and sustain high virus loads in rhesus macaques after the depletion of CD4+ T cells by a highly pathogenic simian immunodeficiency virus/HIV type 1 chimera (SHIV): Implications for HIV-1 infections of humans. *Proc Natl Acad Sci U S A* 2001; 98(2):658-663.
265. Chun TW, Carruth L, Finzi D, Shen X, DiGiuseppe JA, Taylor H, et al. Quantification of latent tissue reservoirs and total body viral load in HIV-1 infection. *Nature* 1997; 387(6629):183-188.
266. Chomont N, El-Far M, Ancuta P, Trautmann L, Procopio FA, Yassine-Diab B, et al. HIV reservoir size and persistence are driven by T cell survival and homeostatic proliferation. *Nat Med* 2009; 15(8):893-900.
267. Graziano F, Aimola G, Forlani G, Turrini F, Accolla RS, Vicenzi E, et al. Reversible Human Immunodeficiency Virus Type-1 Latency in Primary Human Monocyte-Derived Macrophages Induced by Sustained M1 Polarization. *Sci Rep* 2018; 8(1):14249.
268. Kulpa DA, Talla A, Brehm JH, Ribeiro SP, Yuan S, Bebin-Blackwell AG, et al. Differentiation into an Effector Memory Phenotype Potentiates HIV-1 Latency Reversal in CD4(+) T Cells. *J Virol* 2019; 93(24).

269. Munch-Petersen B. Enzymatic regulation of cytosolic thymidine kinase 1 and mitochondrial thymidine kinase 2: a mini review. *Nucleosides Nucleotides Nucleic Acids* 2010; 29(4-6):363-369.
270. Wintersberger E. Regulation and biological function of thymidine kinase. *Biochem Soc Trans* 1997; 25(1):303-308.
271. Reichard P. Ribonucleotide reductase and deoxyribonucleotide pools. *Basic Life Sci* 1985; 31:33-45.
272. Reichard P. Interactions between deoxyribonucleotide and DNA synthesis. *Annu Rev Biochem* 1988; 57:349-374.
273. Abbotts J, Bebenek K, Kunkel TA, Wilson SH. Mechanism of HIV-1 reverse transcriptase. Termination of processive synthesis on a natural DNA template is influenced by the sequence of the template-primer stem. *Journal of Biological Chemistry* 1993; 268(14):10312-10323.
274. Coppock DL, Pardee AB. Control of thymidine kinase mRNA during the cell cycle. *Mol Cell Biol* 1987; 7(8):2925-2932.
275. Engstrom Y, Eriksson S, Jildevik I, Skog S, Thelander L, Tribukait B. Cell cycle-dependent expression of mammalian ribonucleotide reductase. Differential regulation of the two subunits. *J Biol Chem* 1985; 260(16):9114-9116.
276. Franzolin E, Pontarin G, Rampazzo C, Miazzi C, Ferraro P, Palumbo E, et al. The deoxynucleotide triphosphohydrolase SAMHD1 is a major regulator of DNA precursor pools in mammalian cells. *Proc Natl Acad Sci U S A* 2013; 110(35):14272-14277.
277. Morris ER, Caswell SJ, Kunzelmann S, Arnold LH, Purkiss AG, Kelly G, et al. Crystal structures of SAMHD1 inhibitor complexes reveal the mechanism of water-mediated dNTP hydrolysis. *Nat Commun* 2020; 11(1):3165.
278. St Gelais C, de Silva S, Hach JC, White TE, Diaz-Griffero F, Yount JS, et al. Identification of cellular proteins interacting with the retroviral restriction factor SAMHD1. *J Virol* 2014; 88(10):5834-5844.

279. Schott K, Fuchs NV, Derua R, Mahboubi B, Schnellbacher E, Seifried J, et al. Dephosphorylation of the HIV-1 restriction factor SAMHD1 is mediated by PP2A-B55alpha holoenzymes during mitotic exit. *Nat Commun* 2018; 9(1):2227.
280. Tang C, Ji X, Wu L, Xiong Y. Impaired dNTPase activity of SAMHD1 by phosphomimetic mutation of Thr-592. *J Biol Chem* 2015; 290(44):26352-26359.
281. Patra KK, Bhattacharya A, Bhattacharya S. Uncovering allostery and regulation in SAMHD1 through molecular dynamics simulations. *Proteins* 2017; 85(7):1266-1275.
282. Bhattacharya A, Wang Z, White T, Buffone C, Nguyen LA, Shepard CN, et al. Effects of T592 phosphomimetic mutations on tetramer stability and dNTPase activity of SAMHD1 can not explain the retroviral restriction defect. *Sci Rep* 2016; 6:31353.
283. Welbourn S, Strebel K. Low dNTP levels are necessary but may not be sufficient for lentiviral restriction by SAMHD1. *Virology* 2016; 488:271-277.
284. Ruffin N, Brezar V, Ayinde D, Lefebvre C, Schulze Zur Wiesch J, van Lunzen J, et al. Low SAMHD1 expression following T-cell activation and proliferation renders CD4+ T cells susceptible to HIV-1. *AIDS* 2015; 29(5):519-530.
285. Schmidt S, Schenkova K, Adam T, Erikson E, Lehmann-Koch J, Sertel S, et al. SAMHD1's protein expression profile in humans. *J Leukoc Biol* 2015; 98(1):5-14.
286. de Silva S, Hoy H, Hake TS, Wong HK, Porcu P, Wu L. Promoter methylation regulates SAMHD1 gene expression in human CD4+ T cells. *J Biol Chem* 2013; 288(13):9284-9292.
287. Kohnken R, Kodigepalli KM, Mishra A, Porcu P, Wu L. MicroRNA-181 contributes to downregulation of SAMHD1 expression in CD4+ T-cells derived from Sezary syndrome patients. *Leuk Res* 2017; 52:58-66.
288. Jin C, Peng X, Liu F, Cheng L, Lu X, Yao H, et al. MicroRNA-181 expression regulates specific post-transcriptional level of SAMHD1 expression in vitro. *Biochem Biophys Res Commun* 2014; 452(3):760-767.

289. Diamond TL, Roshal M, Jamburuthugoda VK, Reynolds HM, Merriam AR, Lee KY, et al. Macrophage tropism of HIV-1 depends on efficient cellular dNTP utilization by reverse transcriptase. *J Biol Chem* 2004; 279(49):51545-51553.
290. Baldauf HM, Pan X, Erikson E, Schmidt S, Daddacha W, Burggraf M, et al. SAMHD1 restricts HIV-1 infection in resting CD4(+) T cells. *Nat Med* 2012; 18(11):1682-1687.
291. Hrecka K, Hao C, Gierszewska M, Swanson SK, Kesik-Brodacka M, Srivastava S, et al. Vpx relieves inhibition of HIV-1 infection of macrophages mediated by the SAMHD1 protein. *Nature* 2011; 474(7353):658-661.
292. Jauregui P, Logue EC, Schultz ML, Fung S, Landau NR. Degradation of SAMHD1 by Vpx Is Independent of Uncoating. *J Virol* 2015; 89(10):5701-5713.
293. Kim B, Nguyen LA, Daddacha W, Hollenbaugh JA. Tight interplay among SAMHD1 protein level, cellular dNTP levels, and HIV-1 proviral DNA synthesis kinetics in human primary monocyte-derived macrophages. *J Biol Chem* 2012; 287(26):21570-21574.
294. Hollenbaugh JA, Gee P, Baker J, Daly MB, Amie SM, Tate J, et al. Host factor SAMHD1 restricts DNA viruses in non-dividing myeloid cells. *PLoS Pathog* 2013; 9(6):e1003481.
295. Baldauf HM, Stegmann L, Schwarz SM, Ambiel I, Trotard M, Martin M, et al. Vpx overcomes a SAMHD1-independent block to HIV reverse transcription that is specific to resting CD4 T cells. *Proc Natl Acad Sci U S A* 2017; 114(10):2729-2734.
296. Cribier A, Descours B, Valadao AL, Laguette N, Benkirane M. Phosphorylation of SAMHD1 by cyclin A2/CDK1 regulates its restriction activity toward HIV-1. *Cell Rep* 2013; 3(4):1036-1043.
297. White TE, Brandariz-Nunez A, Valle-Casuso JC, Amie S, Nguyen LA, Kim B, et al. The retroviral restriction ability of SAMHD1, but not its deoxynucleotide triphosphohydrolase activity, is regulated by phosphorylation. *Cell Host Microbe* 2013; 13(4):441-451.
298. Ji X, Xiong Y. Two tales (tails) of SAMHD1 destruction by Vpx. *Cell Host Microbe* 2015; 17(4):425-427.

299. Schwefel D, Boucherit VC, Christodoulou E, Walker PA, Stoye JP, Bishop KN, et al. Molecular determinants for recognition of divergent SAMHD1 proteins by the lentiviral accessory protein Vpx. *Cell Host Microbe* 2015; 17(4):489-499.
300. Baltimore D. RNA-dependent DNA polymerase in virions of RNA tumour viruses. *Nature* 1970; 226(5252):1209-1211.
301. Temin HM, Mizutani S. RNA-dependent DNA polymerase in virions of Rous sarcoma virus. *Nature* 1970; 226(5252):1211-1213.
302. Zheng X, Perera L, Mueller GA, DeRose EF, London RE. Asymmetric conformational maturation of HIV-1 reverse transcriptase. *Elife* 2015; 4.
303. Jacobo-Molina A, Ding J, Nanni RG, Clark AD, Jr., Lu X, Tantillo C, et al. Crystal structure of human immunodeficiency virus type 1 reverse transcriptase complexed with double-stranded DNA at 3.0 Å resolution shows bent DNA. *Proc Natl Acad Sci U S A* 1993; 90(13):6320-6324.
304. Kohlstaedt LA, Wang J, Friedman JM, Rice PA, Steitz TA. Crystal structure at 3.5 Å resolution of HIV-1 reverse transcriptase complexed with an inhibitor. *Science* 1992; 256(5065):1783-1790.
305. Ghosh M, Jacques PS, Rodgers DW, Ottman M, Darlix JL, Le Grice SF. Alterations to the primer grip of p66 HIV-1 reverse transcriptase and their consequences for template-primer utilization. *Biochemistry* 1996; 35(26):8553-8562.
306. Powell MD, Ghosh M, Jacques PS, Howard KJ, Le Grice SF, Levin JG. Alanine-scanning mutations in the "primer grip" of p66 HIV-1 reverse transcriptase result in selective loss of RNA priming activity. *J Biol Chem* 1997; 272(20):13262-13269.
307. Larder BA, Purifoy DJ, Powell KL, Darby G. Site-specific mutagenesis of AIDS virus reverse transcriptase. *Nature* 1987; 327(6124):716-717.
308. Poch O, Sauvaget I, Delarue M, Tordo N. Identification of four conserved motifs among the RNA-dependent polymerase encoding elements. *Embo j* 1989; 8(12):3867-3874.
309. Huang H, Chopra R, Verdine GL, Harrison SC. Structure of a covalently trapped catalytic complex of HIV-1 reverse transcriptase: implications for drug resistance. *Science* 1998; 282(5394):1669-1675.

310. Cases-Gonzalez CE, Gutierrez-Rivas M, Menendez-Arias L. Coupling ribose selection to fidelity of DNA synthesis. The role of Tyr-115 of human immunodeficiency virus type 1 reverse transcriptase. *J Biol Chem* 2000; 275(26):19759-19767.
311. Boyer PL, Sarafianos SG, Arnold E, Hughes SH. Analysis of mutations at positions 115 and 116 in the dNTP binding site of HIV-1 reverse transcriptase. *Proc Natl Acad Sci U S A* 2000; 97(7):3056-3061.
312. Reardon JE. Human immunodeficiency virus reverse transcriptase: steady-state and pre-steady-state kinetics of nucleotide incorporation. *Biochemistry* 1992; 31(18):4473-4479.
313. Kati WM, Johnson KA, Jerva LF, Anderson KS. Mechanism and fidelity of HIV reverse transcriptase. *J Biol Chem* 1992; 267(36):25988-25997.
314. Canard B, Sarfati R, Richardson CC. Binding of RNA template to a complex of HIV-1 reverse transcriptase/primer/template. *Proc Natl Acad Sci U S A* 1997; 94(21):11279-11284.
315. Ding J, Das K, Hsiou Y, Sarafianos SG, Clark AD, Jr., Jacobo-Molina A, et al. Structure and functional implications of the polymerase active site region in a complex of HIV-1 RT with a double-stranded DNA template-primer and an antibody Fab fragment at 2.8 Å resolution. *J Mol Biol* 1998; 284(4):1095-1111.
316. Reardon JE, Miller WH. Human immunodeficiency virus reverse transcriptase. Substrate and inhibitor kinetics with thymidine 5'-triphosphate and 3'-azido-3'-deoxythymidine 5'-triphosphate. *Journal of Biological Chemistry* 1990; 265(33):20302-20307.
317. Parker WB, White EL, Shaddix SC, Ross LJ, Buckheit RW, Germany JM, et al. Mechanism of inhibition of human immunodeficiency virus type 1 reverse transcriptase and human DNA polymerases alpha, beta, and gamma by the 5'-triphosphates of carbovir, 3'-azido-3'-deoxythymidine, 2',3'-dideoxyguanosine and 3'-deoxythymidine. A novel RNA template for the evaluation of antiretroviral drugs. *Journal of Biological Chemistry* 1991; 266(3):1754-1762.

318. Marko RA, Liu HW, Ablenas CJ, Ehteshami M, Gotte M, Cosa G. Binding kinetics and affinities of heterodimeric versus homodimeric HIV-1 reverse transcriptase on DNA-DNA substrates at the single-molecule level. *J Phys Chem B* 2013; 117(16):4560-4567.
319. Evans DB, Fan N, Swaney SM, Tarpley WG, Sharma SK. An active recombinant p15 RNase H domain is functionally distinct from the RNase H domain associated with human immunodeficiency virus type 1 reverse transcriptase. *J Biol Chem* 1994; 269(34):21741-21747.
320. Restle T, Müller B, Goody RS. Dimerization of human immunodeficiency virus type 1 reverse transcriptase. A target for chemotherapeutic intervention. *J Biol Chem* 1990; 265(16):8986-8988.
321. Hansen J, Schulze T, Mellert W, Moelling K. Identification and characterization of HIV-specific RNase H by monoclonal antibody. *Embo j* 1988; 7(1):239-243.
322. AIDSinfo. FDA-Approved HIV Medicines. In: *HIV Treatment*: U.S. Department of Health and Human Services; 2020.
323. Tu X, Das K, Han Q, Bauman JD, Clark AD, Jr., Hou X, et al. Structural basis of HIV-1 resistance to AZT by excision. *Nat Struct Mol Biol* 2010; 17(10):1202-1209.
324. Gao HQ, Boyer PL, Sarafianos SG, Arnold E, Hughes SH. The role of steric hindrance in 3TC resistance of human immunodeficiency virus type-1 reverse transcriptase. *J Mol Biol* 2000; 300(2):403-418.
325. Joyce CM. Techniques used to study the DNA polymerase reaction pathway. *Biochim Biophys Acta* 2010; 1804(5):1032-1040.
326. Astatke M, Grindley ND, Joyce CM. How E. coli DNA polymerase I (Klenow fragment) distinguishes between deoxy- and dideoxynucleotides. *J Mol Biol* 1998; 278(1):147-165.
327. Patel SS, Wong I, Johnson KA. Pre-steady-state kinetic analysis of processive DNA replication including complete characterization of an exonuclease-deficient mutant. *Biochemistry* 1991; 30(2):511-525.
328. Wong I, Patel SS, Johnson KA. An induced-fit kinetic mechanism for DNA replication fidelity: direct measurement by single-turnover kinetics. *Biochemistry* 1991; 30(2):526-537.

329. Su Y, Peter Guengerich F. Pre-Steady-State Kinetic Analysis of Single-Nucleotide Incorporation by DNA Polymerases. *Curr Protoc Nucleic Acid Chem* 2016; 65:7 23 21-27 23 10.
330. Einolf HJ, Guengerich FP. Kinetic analysis of nucleotide incorporation by mammalian DNA polymerase delta. *J Biol Chem* 2000; 275(21):16316-16322.
331. Wang CX, Zakharova E, Li J, Joyce CM, Wang J, Konigsberg W. Pre-steady-state kinetics of RB69 DNA polymerase and its exo domain mutants: effect of pH and thiophosphoryl linkages on 3'-5' exonuclease activity. *Biochemistry* 2004; 43(13):3853-3861.
332. Chaudhuri M, Song L, Parris DS. The herpes simplex virus type 1 DNA polymerase processivity factor increases fidelity without altering pre-steady-state rate constants for polymerization or excision. *J Biol Chem* 2003; 278(11):8996-9004.
333. Ndongwe TP, Adedeji AO, Michailidis E, Ong YT, Hachiya A, Marchand B, et al. Biochemical, inhibition and inhibitor resistance studies of xenotropic murine leukemia virus-related virus reverse transcriptase. *Nucleic Acids Res* 2012; 40(1):345-359.
334. Skasko M, Diamond TL, Kim B. Mechanistic variations among reverse transcriptases of simian immunodeficiency virus variants isolated from African green monkeys. *Biochemistry* 2009; 48(23):5389-5395.
335. Risser R, Horowitz JM, McCubrey J. Endogenous mouse leukemia viruses. *Annu Rev Genet* 1983; 17:85-121.
336. Weiss RA. Retroviruses and human disease. *Journal of Clinical Pathology* 1987; 40(9):1064-1069.
337. Operario DJ, Reynolds HM, Kim B. Comparison of DNA polymerase activities between recombinant feline immunodeficiency and leukemia virus reverse transcriptases. *Virology* 2005; 335(1):106-121.
338. Skasko M, Weiss KK, Reynolds HM, Jamburuthugoda V, Lee K, Kim B. Mechanistic differences in RNA-dependent DNA polymerization and fidelity between murine leukemia virus and HIV-1 reverse transcriptases. *J Biol Chem* 2005; 280(13):12190-12200.

339. Lenzi GM, Domaoal RA, Kim DH, Schinazi RF, Kim B. Mechanistic and Kinetic Differences between Reverse Transcriptases of Vpx Coding and Non-coding Lentiviruses. *J Biol Chem* 2015; 290(50):30078-30086.
340. Lenzi GM, Domaoal RA, Kim DH, Schinazi RF, Kim B. Kinetic variations between reverse transcriptases of viral protein X coding and noncoding lentiviruses. *Retrovirology* 2014; 11:111.
341. St Gelais C, Wu L. SAMHD1: a new insight into HIV-1 restriction in myeloid cells. *Retrovirology* 2011; 8:55.
342. Lewis P, Hensel M, Emerman M. Human immunodeficiency virus infection of cells arrested in the cell cycle. *EMBO J* 1992; 11(8):3053-3058.
343. Lewis PF, Emerman M. Passage through mitosis is required for oncoretroviruses but not for the human immunodeficiency virus. *J Virol* 1994; 68(1):510-516.
344. Goldstone DC, Ennis-Adeniran V, Hedden JJ, Groom HC, Rice GI, Christodoulou E, et al. HIV-1 restriction factor SAMHD1 is a deoxynucleoside triphosphate triphosphohydrolase. *Nature* 2011; 480(7377):379-382.
345. Sharova N, Wu Y, Zhu X, Stranska R, Kaushik R, Sharkey M, et al. Primate lentiviral Vpx commandeers DDB1 to counteract a macrophage restriction. *PLoS Pathog* 2008; 4(5):e1000057.
346. Rice GI, Bond J, Asipu A, Brunette RL, Manfield IW, Carr IM, et al. Mutations involved in Aicardi-Goutieres syndrome implicate SAMHD1 as regulator of the innate immune response. *Nat Genet* 2009; 41(7):829-832.
347. Laguette N, Sobhian B, Casartelli N, Ringeard M, Chable-Bessia C, Segeral E, et al. SAMHD1 is the dendritic- and myeloid-cell-specific HIV-1 restriction factor counteracted by Vpx. *Nature* 2011; 474(7353):654-657.
348. Ueno F. Vpx and Vpr proteins of HIV-2 up-regulate the viral infectivity by a distinct mechanism in lymphocytic cells. *Microbes and Infection* 2003; 5(5):387-395.
349. Gibbs JS, Regier DA, Desrosiers RC. Construction and in vitro properties of SIVmac mutants with deletions in "nonessential" genes. *AIDS Res Hum Retroviruses* 1994; 10(4):333-342.

350. Westmoreland SV, Converse AP, Hrecka K, Hurley M, Knight H, Piatak M, et al. SIV vpx is essential for macrophage infection but not for development of AIDS. *PLoS One* 2014; 9(1):e84463.
351. Compton AA, Hirsch VM, Emerman M. The host restriction factor APOBEC3G and retroviral Vif protein coevolve due to ongoing genetic conflict. *Cell Host Microbe* 2012; 11(1):91-98.
352. Sauter D, Schindler M, Specht A, Landford WN, Munch J, Kim KA, et al. Tetherin-driven adaptation of Vpu and Nef function and the evolution of pandemic and nonpandemic HIV-1 strains. *Cell Host Microbe* 2009; 6(5):409-421.
353. Sakai Y, Doi N, Miyazaki Y, Adachi A, Nomaguchi M. Phylogenetic Insights into the Functional Relationship between Primate Lentiviral Reverse Transcriptase and Accessory Proteins Vpx/Vpr. *Front Microbiol* 2016; 7:1655.
354. Coggins SA, Holler JM, Kimata JT, Kim DH, Schinazi RF, Kim B. Efficient pre-catalytic conformational change of reverse transcriptases from SAMHD1 non-counteracting primate lentiviruses during dNTP incorporation. *Virology* 2019; 537:36-44.
355. Plitnik T, Sharkey ME, Mahboubi B, Kim B, Stevenson M. Incomplete Suppression of HIV-1 by SAMHD1 Permits Efficient Macrophage Infection. *Pathogens and Immunity* 2018; 3(2):197.
356. Nyamweya S, Hegedus A, Jaye A, Rowland-Jones S, Flanagan KL, Macallan DC. Comparing HIV-1 and HIV-2 infection: Lessons for viral immunopathogenesis. *Rev Med Virol* 2013; 23(4):221-240.
357. Souquiere S, Onanga R, Makuwa M, Pandrea I, Ngari P, Rouquet P, et al. Simian immunodeficiency virus types 1 and 2 (SIV mnd 1 and 2) have different pathogenic potentials in rhesus macaques upon experimental cross-species transmission. *J Gen Virol* 2009; 90(Pt 2):488-499.